

Physico-chemical properties and intestinal epithelial permeation of baclofen solid-state forms

S Eicker

 **orcid.org 0000-0002-7302-7517**

Dissertation submitted in partial fulfilment of the requirements for the degree *Master of Science* in *Pharmaceutics* at the North-West University

Supervisor:	Prof JC Wessels
Co-supervisor:	Prof JH Hamman
Co-supervisor:	Dr ME Aucamp

Graduation: October 2018

Student number: 24085294

TABLE OF CONTENTS

Acknowledgements	xii
Abstract	xiii
Research problem	xv
Aim and objectives	xv

CHAPTER 1

SOLID-STATE PROPERTIES OF DRUGS

1.1	Introduction	1
1.2	Classification of different solid-state forms	1
1.2.1	Crystalline	1
a	Polymorphism	3
b	Hydrates	5
c	Solvates	6
d	Co-crystal	8
e	Salts	8
1.2.2	Amorphous	9
1.3	Physico-chemical properties of different solid-state forms	10
1.3.1	Polymorphism	11
1.3.2	Hydrates	11
1.3.3	Solvates	12
1.3.4	Co-crystals	12
1.3.5	Salts	13
1.3.6	Amorphous solids	14
1.4	Solid-state transformations	15
1.4.1	Solid-solid transformations	17
1.4.2	Solvent-mediated transformations	17
1.4.3	Solution-mediated transformations	17
1.5	Biopharmaceutics classification system/Drug like properties	19
1.5.1	Solubility	22
1.5.2	Permeability	22
1.6	<i>In vitro</i> models for screening of membrane permeability properties	24
1.6.1	Cell culture models	25
1.6.1.1	Caco-2 cell line	25
1.7	Conclusion	27
	References	29

Figures & tables

Figure 1.1	Representation of a basic unit cell	2
------------	-------------------------------------	---

Figure 1.2	Classification of the different solid-state forms in which pharmaceutical compounds can exist	3
Figure 1.3	Diagram illustrating the transitions in monotropic and enantiotropic polymorphism	4
Figure 1.4	Stages of a typical caking process	14
Figure 1.5	Steps of solution-mediated transition	18
Figure 1.6	A schematic representation of a cultured monolayer of Caco-2 cells on a microporous membrane in a Transwell plate	26
Table 1.1	Class 3 solvents	7
Table 1.2	BCS classification of drug substances	20
Table 1.3	Solubility terms	22
Table 1.4	Physico-chemical and molecular property requirements for permeability and solubility	24
Table 1.5	The cell culture models that are most commonly used to estimate intestinal transcellular transport	25

CHAPTER 2

BACLOFEN

2.1	Introduction	35
2.2	Synthesis of baclofen	35
2.3	Enantiomers of baclofen	37
2.4	Indications and pharmacological properties of baclofen	38
2.5	The physico-chemical properties of baclofen	39
2.6	Dose and baclofen products	40
2.7	Conclusion	41
	References	42

Figures & tables

Figure 2.1	Synthesis of baclofen	36
Figure 2.2	Synthesis of baclofen	37
Figure 2.3	Enantiomers of baclofen	38
Figure 2.4	Site of action for the pre-synaptic GABA _B receptors	39
Figure 2.5	Zwitterionic properties of baclofen	40

CHAPTER 3

RESEARCH METHODOLOGY

3.1	Introduction	46
3.2	Materials	46
3.3	Methods	47
3.3.1	Solid-state form screening of baclofen	47
3.3.2	Physico-chemical characterisation	48

3.3.2.1	Differential scanning calorimetry (DSC)	48
3.3.2.2	Thermogravimetric analysis (TGA)	48
3.3.2.3	Thermal microscopy (TM)	49
3.3.2.4	Scanning electron microscopy (SEM)	49
3.3.2.5	Fourier-Transform infrared spectroscopy (FT-IR)	50
3.3.2.6	X-ray powder diffraction (XRPD)	50
3.3.2.7	Vapour sorption	5
3.3.2.8	High performance liquid performance (HPLC)	51
3.3.2.9	Equilibrium solubility	51
3.3.2.10	Powder dissolution studies	52
3.3.2.11	Permeability	52
3.3.3	Conclusion	55
	References	56

Figures & tables

Table 3.1	Materials used during permeability studies	46
-----------	--	----

CHAPTER 4

PHYSICO-CHEMICAL PROPERTIES OF BACLOFEN

4.1	Introduction	58
4.2	High performance liquid chromatography (HPLC) method verification	58
4.3	Solid-state screening	61
4.3.1	Basic physico-chemical characterisation of purchased baclofen bulk material	62
4.3.1.1	Differential scanning calorimetry (DSC)	62
4.3.1.2	Thermo-gravimetric analysis (TGA)	63
4.3.1.3	Hot-stage microscopy (HSM)	64
4.3.1.4	Scanning electron microscopy (SEM)	65
4.3.1.5	Fourier-Transform infrared spectroscopy (FT-IR)	66
4.3.1.6	X-Ray powder diffraction (XRPD)	68
4.3.1.7	Vapour sorption of baclofen anhydrate	69
4.3.1.8	Conclusion	70
4.4	Screening for different solid-state forms after recrystallisation	70
4.4.1	Recrystallisation using distilled water	70
4.4.1.1	Differential scanning calorimetry (DSC)	71
4.4.1.2	Thermo-gravimetric analysis (TGA)	71
4.4.1.3	Hot-stage microscopy (HSM)	72
4.4.1.4	Scanning electron microscopy (SEM)	73
4.4.1.5	Fourier-transform infrared spectroscopy (FT-IR)	74
4.4.1.6	X-Ray powder diffraction (XRPD)	75

4.4.1.7	Conclusion	80
4.4.2	Behaviour of baclofen anhydrate in various organic solvents	80
4.5	Equilibrium solubility in solvents	81
4.5.1	Acetone	81
4.5.2	1-Butanol	83
4.5.3	2-Butanol	86
4.5.4	Ethanol	88
4.5.5	Methanol	91
4.5.6	1-Propanol	93
4.5.7	2-Propanol	95
4.5.9	Conclusion	97
4.6	Quench cooling	98
4.6.1	Hot-state microscopy (HSM)	98
4.6.2	Fourier-Transform infrared spectroscopy (FT-IR)	99
4.6.3	X-Ray powder diffraction (XRPD)	100
4.6.4	Conclusion	102
	References	103

Figures & tables

Figure 4.1	Linearity of baclofen obtained using a concentration range of 0.25 µg/ml – 500 µg/ml	59
Figure 4.2	Chromatogram obtained for baclofen solution at a concentration of 2.5 µg/ml	60
Figure 4.3	Chromatogram obtained for baclofen solution at a concentration of 0.25 µg/ml	61
Figure 4.4	Chromatogram obtained for baclofen solution at a concentration of 0.025 µg/ml	61
Figure 4.5	DSC thermogram obtained for baclofen purchased bulk material at a heating rate of 10°C/min	63
Figure 4.6	TGA thermogram obtained for baclofen purchased bulk material (i.e. anhydrate), using a heating rate of 10°C/min, heating from ambient to 300°C	64
Figure 4.7	HSM micrographs obtained for (a) baclofen purchased bulk material (i.e. anhydrate) at ambient temperature (25°C ± 1°C), (b) formation of what seemed to be moisture on the surface of the cover slip at 215°C, (c) complete melting of baclofen anhydrate at 223°C and (d) clear observation of the start of sublimation of baclofen anhydrate at approximately 210°C	65

Figure 4.8	SEM micrographs obtained for baclofen purchased bulk material (i.e. anhydrate) with (a) captured at a 50 μm scale, (b) captured at a larger magnification of 10 μm scale and (c) captured at 2 μm scale	66
Figure 4.9	FT-IR spectrum obtained for baclofen purchased bulk material (i.e. anhydrate)	67
Figure 4.10	XRPD diffractograms obtained for baclofen purchased bulk material (i.e. anhydrate) at ambient temperature	68
Figure 4.11	Vapour sorption isotherm obtained for baclofen purchased bulk material (i.e. anhydrate). The isotherms were obtained at $25 \pm 0.5^\circ\text{C}$ with humidity variation of 0 - 95% (Adsorption 1), 95 - 5% (Desorption 1) and 5 - 95% RH (Adsorption 2)	70
Figure 4.12	DSC thermogram obtained for baclofen recrystallised in water at heating rate of $10^\circ\text{C}/\text{min}$	71
Figure 4.13	TGA thermogram obtained for baclofen recrystallised in water, using a heating rate of $10^\circ\text{C}/\text{min}$, heating from ambient temperature to 300°C	72
Figure 4.14	Photomicrographs obtained for baclofen recrystallised from water at 20°C (a), development of water bubbles (b) and the sublimate of the recrystallised at 20°C (c)	73
Figure 4.15	SEM micrographs obtained for baclofen recrystallised in water with (a) captured at a 50 μm scale, (b) captured at a larger magnification of 10 μm scale and (c) captured at 5 μm scale	74
Figure 4.16	An overlay of the FT-IR spectra obtained for baclofen anhydrate (red) and recrystallised with distilled water baclofen (blue)	75
Figure 4.17	XRPD diffractograms obtained for baclofen anhydrate (blue) and recrystallised baclofen (red)	76

- Figure 4.18 XRPD continuous scan diffractograms obtained during the investigation of the crystallisation of the monohydrate when baclofen anhydrate is exposed to sufficient water to create a thick slurry. Where (a) is the initial scan of baclofen anhydrate immediately after the distilled water was added, (b) is the diffraction pattern obtained after 72 minutes, (c) diffraction pattern of baclofen anhydrate and (d) diffraction pattern for baclofen monohydrate
- Figure 4.19 Graph plotted using the calculated relative intensity of the diffraction peak at $16.2^{\circ}2\theta$ for baclofen monohydrate over a period of 80 minutes. The sample temperature was maintained at ambient conditions during the collection of data and diffraction data was collected every 5 minutes
- Figure 4.20 Photomicrographs obtained for baclofen recrystallised from water at 25°C (a), development of water bubbles 50°C (b) the continuation of water bubbles forming at 60°C (c) and (d) complete dehydration of the sample at 90°C
- Figure 4.21 The solubility profile obtained for baclofen anhydrate in acetone over a period of 24 h at $37^{\circ}\text{C} \pm 0.5^{\circ}\text{C}$
- Figure 4.22 An overlay of the DSC thermogram obtained for baclofen in acetone at 1 h (blue), 4 h (green) and 24 h (red) at heating rate $10^{\circ}\text{C}/\text{min}$
- Figure 4.23 XRPD diffractograms obtained for baclofen in acetone at 1h (red), 4 h (blue), 24 h (green) and baclofen anhydrate (grey)
- Figure 4.24 The solubility profile obtained for baclofen anhydrate 1-butanol over a period of 24 h at $37^{\circ}\text{C} \pm 0.5^{\circ}\text{C}$
- Figure 4.25 An overlay of the DSC thermogram obtained for baclofen in 1-butanol at 1 h (blue) and 24 h (red) at heating rate $10^{\circ}\text{C}/\text{min}$
- Figure 4.26 XRPD diffractograms obtained for baclofen in 1-butanol at 1 h (red), 4 h (blue) and baclofen anhydrate (green)
- Figure 4.27 The solubility profile obtained for baclofen anhydrate in 2-butanol over a period of 24 h at $37^{\circ}\text{C} \pm 0.5^{\circ}\text{C}$
- Figure 4.28 An overlay of the DSC thermogram obtained for baclofen in 2-butanol at 1 h (blue) and 24 h (red) at heating rate $10^{\circ}\text{C}/\text{min}$
- Figure 4.29 XRPD diffractograms obtained for baclofen in 2-butanol at 1 h (red), 4 h (blue) and baclofen anhydrate (green)
- Figure 4.30 The solubility profile obtained for baclofen anhydrate in ethanol over a period of 24 h at $37^{\circ}\text{C} \pm 0.5^{\circ}\text{C}$
- Figure 4.31 An overlay of the DSC thermogram obtained for baclofen in ethanol at 1 h (blue) and 24 h (red) at heating rate $10^{\circ}\text{C}/\text{min}$

Figure 4.32	XRPD diffractograms obtained for baclofen in ethanol at 1 h (red), 4 h (blue) and baclofen anhydrate (green)	90
Figure 4.33	The solubility profile obtained for baclofen anhydrate methanol over a period of 24 h at 37°C ± 0.5°C	91
Figure 4.34	An overlay of the DSC thermogram obtained for baclofen in methanol at 1 h (blue) and 24 h (red) at heating rate 10°C/min	91
Figure 4.35	XRPD diffractograms obtained for baclofen in methanol at 1 h (red), 4 h (blue) and baclofen anhydrate (green)	92
Figure 4.36	The solubility profile obtained for baclofen anhydrate in 1-propanol over a period of 24 h at 37°C ± 0.5°C	93
Figure 4.37	An overlay of the DSC thermogram obtained for baclofen in 1-propanol at 1 h (blue) and 24 h (red) at heating rate 10°C/min	93
Figure 4.38	XRPD diffractograms obtained for baclofen in 1-propanol at 1h (red), 4 h (blue) and baclofen anhydrate (green)	94
Figure 4.39	The solubility profile obtained for baclofen anhydrate in 2-propanol over a period of 24 h at 37°C	95
Figure 4.40	An overlay of the DSC thermogram obtained for baclofen in 2-propanol at 1 h (blue) and 24 h (red) at heating rate 10°C/min	95
Figure 4.41	XRPD diffractograms obtained for baclofen in 2-propanol at 1 h (red), 4 h (blue) and baclofen anhydrate (green)	96
Figure 4.42	Summary of solubilities of baclofen in the different organic solvents	97
Figure 4.43	Photomicrographs obtained for recrystallised baclofen obtained after quench cooling of molten baclofen at 20.5°C (a), the recrystallised baclofen melted at 122°C (b) and the recrystallisation of the melt upon subsequent cooling 20.5°C (c)	98
Figure 4.44	An overlay of the FT-IR spectra obtained for baclofen anhydrate (red), monohydrate (blue) and melt recrystallised baclofen (green)	99
Figure 4.45	XRPD diffractograms obtained for baclofen anhydrate and melt recrystallised baclofen	100
Figure 4.46	Chromatogram obtained for melt recrystallised baclofen	102
Table 4.1	Retention time of baclofen in different solvents	59
Table 4.2	FT-IR peak listing reported for baclofen purchased bulk material (i.e. anhydrate)	67
Table 4.3	XRPD peak listing reported for baclofen anhydrate	68
Table 4.4	FT-IR peak listing reported for baclofen recrystallised with distilled water	75
Table 4.5	XRPD peak listing reported for baclofen anhydrate and recrystallised baclofen	76

Table 4.6	FT-IR peak listing reported for baclofen in acetone	82
Table 4.7	FT-IR peak listing reported for baclofen in 1-butanol	85
Table 4.8	FT-IR peak listing reported for baclofen in 2-butanol	87
Table 4.9	FT-IR peak listing reported for baclofen in ethanol	90
Table 4.10	FT-IR peak listing reported for baclofen in methanol	92
Table 4.11	FT-IR peak listing reported for baclofen in 1-propanol	94
Table 4.12	FT-IR peak listing reported for baclofen in 2-propanol	96
Table 4.13	Presentation of the concentrations obtained for the different solvents	97
Table 4.14	FT-IR peak listing reported for melt recrystallised baclofen	99
Table 4.15	XRPD peak listing reported for melt recrystallised baclofen	101

CHAPTER 5

SOLUBILITY, DISSOLUTION AND PERMEABILITY STUDIES OF BACLOFEN

5.1	Introduction	104
5.2	Equilibrium solubility in bio-relevant media	104
5.2.1	Distilled water	104
5.2.2	0.1 M Hydrochloric acid buffer (HCl)	107
5.2.3	Citrate buffer solution (pH 4.5)	110
5.2.4	Phosphate buffer solution (pH 6.8)	113
5.2.5	Conclusion	116
5.3	Powder dissolution	117
5.3.1	Distilled water	117
5.3.2	0.1 M Hydrochloric acid (HCl) – pH 1.2	118
5.3.3	Citrate buffer solution (pH 4.6)	119
5.3.4	Phosphate buffer solution (pH 6.8)	119
5.3.5	Conclusion	120
5.4	<i>In vitro</i> membrane permeation	120
5.4.1	Permeability in the apical to basolateral direction	120
5.4.2	Permeability in the basolateral to apical direction	121
5.4.3	Conclusion	122
	References	125

Figures & tables

Figure 5.1	The solubility profile obtained for baclofen anhydrate in distilled water over a period of 24 h at 37°C ± 0.5°C	105
Figure 5.2	The DSC thermogram obtained for baclofen in distilled water at 1 h (blue) and 24 h (red) with a heating rate 10°C/min	106
Figure 5.3	XRPD diffractograms obtained for baclofen in distilled water at 1 h (red), 24 h (blue) and baclofen anhydrate (green)	107

Figure 5.4	Solubility profile of baclofen raw material in different pH level HCl buffer solution concentrations at $37^{\circ}\text{C} \pm 0.5^{\circ}\text{C}$	108
Figure 5.5	The DSC thermogram obtained for baclofen in HCl buffer solution 1 h (blue) and 24 h (red) with heating rate $10^{\circ}\text{C}/\text{min}$	109
Figure 5.6	XRPD diffractograms obtained for baclofen in HCL buffer solution at 1 h (red), 2 h (blue), 24 h (green) and baclofen anhydrate (grey)	110
Figure 5.7	The solubility profile obtained for baclofen anhydrate in citrate buffer solution over a period of 24 h at $37^{\circ}\text{C} \pm 0.5^{\circ}\text{C}$	111
Figure 5.8	The DSC thermogram obtained for excess baclofen in citrate buffer solution (a) 1 h, (b) 4 h and (c) 24 h with heating rate $10^{\circ}\text{C}/\text{min}$	111
Figure 5.9	XRPD diffractograms obtained for baclofen in citrate buffer solution at 1 h (red), 2 h (blue), 4 h (green), 24 h (grey) and baclofen anhydrate (brown)	113
Figure 5.10	The solubility profile obtained for baclofen anhydrate in phosphate buffer solution over a period of 24 h at $37^{\circ}\text{C} \pm 0.5^{\circ}\text{C}$	114
Figure 5.11	The DSC thermogram obtained for baclofen in phosphate buffer solution at 1 h (blue) and 24 h (red) with heating rate $10^{\circ}\text{C}/\text{min}$	114
Figure 5.12	XRPD diffractograms obtained for baclofen in phosphate buffer solution at 1 h (red), 4 h (blue) and baclofen anhydrate (green)	115
Figure 5.13	Summary of solubilities of baclofen in the different bio-relevant media obtained at $37^{\circ}\text{C} \pm 0.5^{\circ}\text{C}$	116
Figure 5.14	The dissolution profile obtained for 2 g and 25 mg baclofen in distilled water at $37 \pm 0.5^{\circ}\text{C}$ and 100 rpm paddle stirring speed	117
Figure 5.15	The dissolution profile obtained for 4 g and 25 mg baclofen in HCl buffer solution at $37 \pm 0.5^{\circ}\text{C}$ and 100 rpm paddle stirring speed	118
Figure 5.16	The dissolution profile obtained for 2.5 g and 25 mg baclofen in citrate buffer solution at $37 \pm 0.5^{\circ}\text{C}$ and 100 rpm paddle stirring speed	119
Figure 1.17	The dissolution profile obtained for 2.3 g and 25 mg baclofen in phosphate at $37 \pm 0.5^{\circ}\text{C}$ and 100 rpm paddle stirring speed	120
Figure 5.18	Permeability (% transport) in baclofen in the apical to basolateral direction across Caco-2 cell monolayers	121
Figure 5.19	Permeability (% transport) in baclofen in the basolateral too apical direction across Caco-2 cell monolayers	122
Table 5.1	FT-IR peak listing reported for baclofen in distilled water	106
Table 5.2	FT-IR peak listing reported for baclofen in HCl buffer solution	109
Table 5.3	Solubility concentrations of baclofen in different HCl buffer solutions with differing pH values	110
Table 5.4	FT-IR peak listing reported for excess baclofen in citrate buffer solution	112

Table 5.5	FTIR peak listing reported for excess baclofen in phosphate buffer solution	114
Table 5.6	Presentation of the concentrations obtained for the different bio-relevant media	116

CHAPTER 6

CONCLUSION

Conclusion	126
References	130

ACKNOWLEDGEMENTS

I hereby wish to express my thanks and gratitude to the following people and organisations without whose help I would not have been able to complete this dissertation successfully:

Prof Anita Wessels a special thank you not only for helping me with my masters but also just for being there when I needed you. You gave me your time and advice the most thoughtful gift of all and for that I can't be more grateful.

Dr Marique Aucamp it takes a special person to light that fire, to raise the expectations that I had for myself and not giving up on me, no matter how challenging it might have been. Without you, I would have been lost. Thank you for teaching, guiding and inspiring me.

Prof Sias Hamman for helping me to understand and complete the chapters on *in vitro* cell cultures.

My mother Jenny, father Christo, brother Clinton and sister Bianca who supported and believed in me throughout my masters. Without you I could not have done this.

Dr Clarissa Willers for all the help and taking so much trouble and time to assist me with the cell cultures in the lab.

Dr Angelique Lewies for all the help and advice you gave me and always answering all my questions.

Chané Erasmus, my best friend, for being there through it all not only in terms of support in the lab but also in every other aspect. Without you this would have been a lot more difficult.

Elisca Boneschans and Juandré Saayman for your friendship, lending an ear always making me laugh and helping me to realise things are not as bad as it seems.

Daniel Forde for all the support, a shoulder to cry on and someone to talk to in the last few months. I don't think you fully understand how you've touched my life.

Francois du Rand for your patience and willingness to drop everything and help me when I needed it and being there when I just needed someone to talk to.

Tannie Marianne thank you for the coffees, taking the time to listen to all my stories and all your advice.

NRF and the North-West University, for the financial support during my master's study.

ABSTRACT

Baclofen is a centrally acting muscle relaxant that acts as an agonist of the inhibitory neurotransmitter gamma-aminobutyric acid (GABA). It is primarily used to treat muscle spasticity in patients with multiple sclerosis and spinal cord injuries. On the South African market, baclofen is available in a solid pharmaceutical dosage form (tablets) for oral administration. Despite it being already commercially available for a relatively long period, very little in terms of the physico-chemical properties of baclofen, is known. Some scientific publications reported that baclofen exhibited a relatively low bioavailability (40%) due to a narrow absorption window in the upper gastro-intestinal tract, while other literature articles reported a 70 to 80% bioavailability of baclofen. To complicate matters even further, baclofen can exist in at least two solid-state forms namely an anhydrate and a monohydrate, however, there exists almost no information on the physico-chemical properties of these two solid-states of baclofen and no mention is made towards how the different hydration levels of baclofen might influence its solubility, stability, and bioavailability.

In this study, solid state investigations were employed with certain physico-chemical investigations to determine if different solid-state forms of baclofen exist. Physico-chemical investigations using different instruments (including differential scanning calorimetry, thermogravimetric analysis, thermal microscopy, scanning electron microscopy, Fourier-Transform infrared spectroscopy, X-ray powder diffraction and vapour sorption analysis) were done on baclofen raw material and the product obtained from recrystallisation with water and quench cooling. The physico-chemical investigations indicated that baclofen may exist in the anhydrate and the monohydrate form. However, on further investigation it was found that the monohydrate only exists in solution or environments where sufficient water is available. Recrystallisation studies using different organic solvents proved to be unsuccessful and therefore it was concluded that no other solid-state form of baclofen exists.

Furthermore, the solubility, dissolution and membrane permeability of baclofen in different solvents and bio-relevant media were investigated to determine the biopharmaceutics classification system (BCS) of baclofen. Equilibrium solubility concentrations of baclofen anhydrate in different solvents (acetone, 1-butanol, 2-butanol, ethanol, methanol, 1-propanol and 2-propanol) and different bio-relevant media (water, HCl-, citrate- and phosphate buffer solutions) were determined. Apparent phase transformations were observed with the solvents: acetone, 2-butanol and ethanol, however, after further examination by means of Differential scanning calorimetry (DSC), Fourier-transform infrared spectroscopy (FT-IR) and X-ray powder diffraction (XRPD) the same physico-chemical properties as for baclofen raw material (anhydrate) was observed. There was also apparent phase transformation observed within the bio-relevant media. These transformations could possibly be the formation of salts or salt complexes, however, further

investigation would be necessary to clarify the observed phenomena. Additionally, it was observed that baclofen was highly sensitive to small changes in low pH-levels.

Powder dissolutions were performed on baclofen anhydrate in the different bio-relevant media (water, HCl-, citrate- and phosphate buffer solutions) using 25 mg baclofen anhydrate and using sufficient baclofen quantities that would result in saturated solutions. These 'saturated solution' dissolutions were performed in an effort to identify possible solution-mediated phase transformation of baclofen anhydrate.

During this study, the *in vitro* Caco-2 cell model was used for permeation studies. Caco-2 cells were originally derived from human colon adenocarcinoma. Despite their origin, Caco-2 cells grow in culture to form a polarised monolayer with tight junctions and an apical brush border that differentiate on a semi-permeable membrane that displays similar morphological and functional characteristics as small intestinal enterocytes. The results obtained for the *in vitro* permeability studies (Caco-2 monolayer studies) showed low permeability for baclofen raw material in the apical to basolateral direction and in the basolateral to apical direction.

This study provided information regarding the physico-chemical properties, solubility and membrane permeability characteristics of baclofen. The information obtained is adequate to classify baclofen in class 3 of the biopharmaceutical classification system as well as sufficient evidence towards possible bio-waiver applications for this drug.

Keywords: baclofen, recrystallisation, solubility, dissolution, permeability

RESEARCH PROBLEM

Baclofen can exist in at least two crystalline states, namely anhydrate and monohydrate. Little information is available on the physico-chemical and stability properties of these two solid-state forms; in addition, there are contradictory reports on the bioavailability class to which baclofen belong and whether different solid-states will significantly affect the intestinal epithelial permeability.

AIM AND OBJECTIVES

The aim of this study is to determine if baclofen can exist in more than one solid-state form and to characterise these forms in terms of physico-chemical properties and physical stability. This study also aims to provide a clear and distinctive classification of baclofen in terms of the biopharmaceutics classification system (BCS) based on its solubility and membrane permeability.

The objectives of this study are:

- Preparation of different solid-state forms of baclofen by means of recrystallisation and quench cooling, subsequently aiding in the screening of possible unknown solid-state forms;
- Investigation of the physico-chemical properties of identified solid-state forms of baclofen, in terms of melting point, loss of moisture upon heating, water content, crystallinity and vapour sorption isotherms;
- Determination of the equilibrium solubility of each of the solid-sates of baclofen within bio-relevant media (pH 1.2, pH 4.6, pH 6.8 and distilled water) as well as in typical organic solvents (e.g. ethanol, methanol, octanol, acetone);
- Investigation of the physical stability of the solid-state forms, i.e. susceptibility to solid-state phase transformations either through solid-, solvent- or solution-mediated processes;
- To conduct dissolution studies of each of the solid-sates of baclofen within bio-relevant media (pH 1.2, pH 4.6, pH 6.8 and distilled water) and to investigate phase transformations if it was identified during investigation of the previous objective;
- To investigate the *in vitro* permeability of each of the solid-sates of baclofen across Caco-2 cell monolayers;
- To indicate the BCS classification of baclofen based on the combined data obtained during this study.

CHAPTER 1

SOLID-STATE PROPERTIES OF DRUGS

1.1 Introduction

It is a well-known fact that organic compounds can either exist in the solid-, liquid- or gas-state. Most drugs exist in the solid-state. The solid-state in which drugs can exist can be broadly classified as either crystalline or amorphous. These crystalline or amorphous solid-states can further be sub-classified into different solid-state forms being governed by different molecular arrangements. Furthermore, it is well-known that different solid-state forms have a significant impact on the physico-chemical properties of a particular drug. These physico-chemical properties include melting point, physical and chemical stability, solubility, particle morphology and ultimately processability and bioavailability. This chapter focuses on the differences between crystalline and amorphous states as well as the different types of solid-state forms in which a drug may exist. In addition, this chapter will elaborate on the physico-chemical attributes of a drug that are affected by different solid-state forms. Furthermore, the physical stability of different solid-state forms will be discussed, and the aspect of phase transformations will be elaborated on. Lastly, this chapter will bring into context the importance of proper solid-state form characterisation of drugs and the influence that different forms may ultimately have on the bioavailability of a drug.

1.2 Classification of different solid-state forms

1.2.1 Crystalline

As mentioned in the preceding paragraph, drugs can exist in different solid-state forms. Crystalline solids show regular, repetitive arrangement of molecules that repeat in three dimensions (Datta & Grant, 2004). The molecules aggregate together with the short-range order (neighbouring molecules) and long-range order (regularity of molecules, aggregating first through short-range, spreading to a significant distance, to form a phase), where molecules in the amorphous form aggregate only within the short-range order (Cui, 2007; Yu, 2001). These differences between crystal and amorphous molecules will affect their physical and chemical properties. The regular arrangement of structural units, called unit cells that contain all structural features and symmetry elements of the molecule, repeat in three dimensions (Datta & Grant, 2004). The arrangement of molecules in the crystalline state is in a definite order (Aulton & Taylor, 2013). Molecules arranged in an orderly fashion within the unit cell leads to more efficiently packed molecules that are closer together and this reduces the specific volume of the molecules and thus present with lower potential energy levels and crystalline solids are therefore thermodynamically more stable than amorphous solids (Cui, 2007).

The molecules in the unit cell have directional specific intermolecular interactions that include hydrogen or covalent bonding, which leads to an orderly arrangement of neighbouring molecules. After the molecules aggregate in a certain short-range arrangement, the arrangements can continuously spread in three-dimensions without any voids between them, reducing the interfacial area between the molecular aggregate (solid) and the neighbouring phases (Cui, 2007).

A basic unit cell, illustrated in figure 1.1, shows a certain orientation and shape that can be characterised by translational vectors a , b and c (axial lengths), with individual angles α , β and γ , and show a definite volume, V (Datta & Grant, 2004; Vippagunta *et al.*, 2001; Ymén, 2011). In a unit cell, α defines the angle between the axis of b and c , β defines the angle between the axis of a and c and γ defines the angle between the axis of a and b (Brittain, 1999).

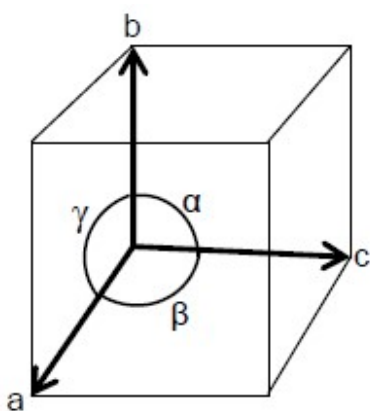


Figure 1.1: Representation of a basic unit cell (Datta & Grant, 2004)

Crystals can be classified in at least one of seven possible three-dimensional systems that are defined by the relationship between the translation vectors and individual angles of the unit cells. The seven crystal systems include cubic, tetragonal, orthorhombic, monoclinic, triclinic, hexagonal and trigonal unit cells. The crystals can then be further assigned to one of the 14 Bravais lattices that consist of cubic-P, cubic-I, cubic-F, orthorhombic-P, orthorhombic-I, orthorhombic-F, orthorhombic-C, tetragonal-P, tetragonal-I, monoclinic-P, monoclinic-B, triclinic-P, hexagonal-P and trigonal-R lattices (Brittain, 1999). The crystals can further be classified to one of the 230 possible space groups (Brittain, 1999; Datta & Grant, 2004; Vippagunta *et al.*, 2001).

Crystalline solids can exist as either singular molecular entities that show polymorphism or molecular adducts that includes hydrates, solvates, salts and co-crystals (Datta & Grant, 2004). These sub-phases show different arrangements of molecular packing. Although polymorphs have different crystal structures, they have the same chemical composition. Hydrates, solvates, salts, and co-crystals are similar in the sense that they all consist of more than one type of molecule (Cui, 2007) as illustrated in Figure 1.2.

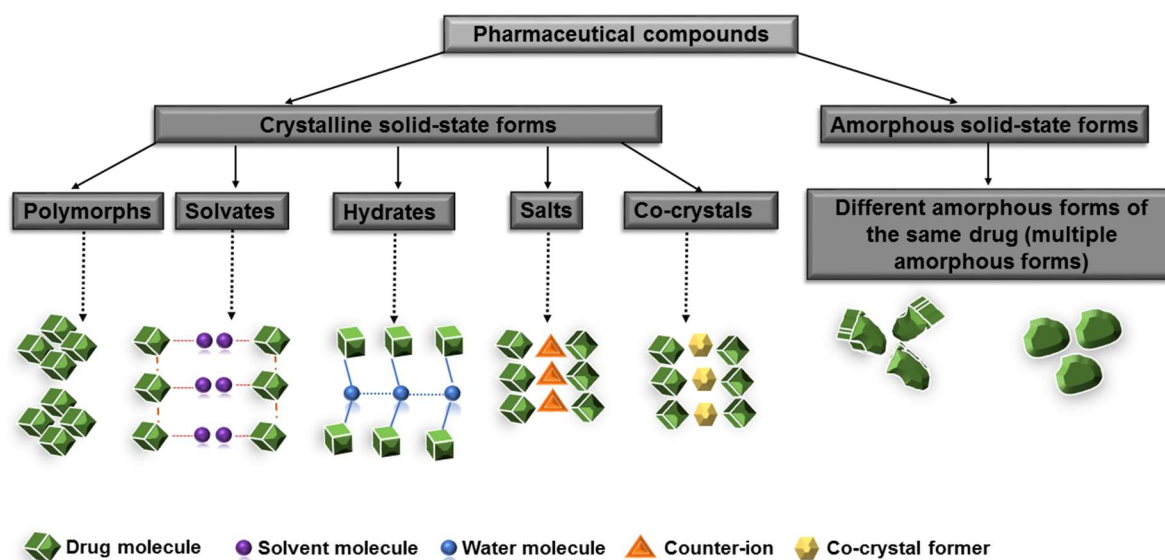


Figure 1.2: Classification of the different solid-state forms in which pharmaceutical compounds can exist (Aucamp, 2015a)

a. Polymorphism

Polymorphism can be defined as the ability of a compound to exist in two or more crystalline phases with different arrangements and/or conformations of the molecules in the crystal lattice (Datta & Grant, 2004; Grant & Lohani, 2006; Gu *et al.*, 2001; Patel *et al.*, 2015). It should be stressed that the possibility of new polymorphs appearing even after a century after the initial discovery of the drug, could never be excluded. Polymorphic compounds present the following challenges:

- Gradual generation of different polymorphic forms that cause diversity in the solid mass. Once a polymorphic form is identified, the concern is raised that other forms may be discovered.
- The selection of the preferred polymorphic form for further development, requires investigation regarding the thermodynamic as well as kinetic properties of the non-preferred polymorphic form.
- There is also an analytical challenge to monitor the specific polymorph content within the dosage form, since there exists a possibility for other polymorphs to form.
- Lastly, there is a concern regarding the impact of different polymorphs on the manufacturing as well as the bioavailability that may lead to therapeutic problems (Morissette, 2004).

Polymorphs can be classified as either monotropic or enantiotropic (Figure 1.3). In monotropic polymorphism, one of the polymorphic forms is stable and the metastable form will convert to the stable form (Aulton & Taylor, 2013; Datta & Grant, 2004; Vippagunta *et al.*, 2001; Zhang *et al.*, 2004). The metastable form can exist for a period of time, thus appearing stable, but when given the chance, it will convert to the more stable form (Aulton & Taylor, 2013). In monotropic polymorphism, there is no reversible transition below the melting point (Brittain, 1999). In the case of enantiotropic polymorphism, reverse transformation can occur between polymorphic forms, under different conditions such as temperature and pressure (Aulton & Taylor, 2013; Datta & Grant, 2004; Vippagunta *et al.*, 2001). The reversible transition can be observed at a transition temperature below the melting point (Brittain, 1999; Patel *et al.*, 2015).

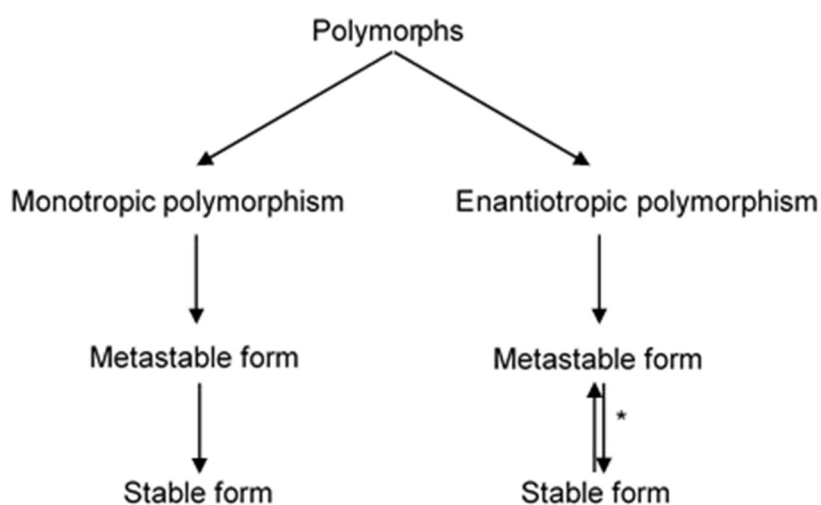


Figure 1.3: Diagram illustrating the transitions in monotropic and enantiotropic polymorphism.

*Transition takes place under different conditions such as temperature and pressure (Adapted from Aulton & Taylor, 2013; Datta & Grant, 2004; Vippagunta *et al.*, 2001)

Molecules are capable of forming different crystal lattices through two mechanisms namely, packing polymorphism and conformational polymorphism. Packing polymorphism is conformational relatively rigid molecules assembled in different three-dimensional structures through different intermolecular mechanisms. Conformational polymorphism is non-conformational rigid molecules folded in different arrangements, packed in different alternative crystal structures (Datta & Grant, 2004; Grant & Lohani, 2006; Vippagunta *et al.*, 2001).

Polymorphs can be prepared through a variety of methods. One of the methods include recrystallisation. The solids are introduced to the solvents under different experimental conditions that include: temperature, initial supersaturation, the rate of desupersaturation and rate of agitation. Other methods available to crystallise different polymorphs include cooling of melts, sublimation, recrystallisation from single or mixed solvents, changing the pH of the solution and the presence or addition of tailor-made additives (Grant & Lohani, 2006).

b. Hydrates

Hydrates can be described as compounds in which water molecules are trapped within the crystal lattice (Ahlqvist & Taylor, 2002; Aulton & Taylor, 2013; Datta & Grant, 2004; Vippagunta *et al.*, 2001). The water molecule is small enough to fill the structural spaces occupying definite positions within the crystal lattice, linking the molecules through hydrogen bonds into stable crystal structures (Brittain, 1999; Khankari & Grant, 1994; Vippagunta *et al.*, 2001).

Hydration leads to a change in volume of the unit cell that will lead to a change in the molar volume and in the density of the compound. Incorporation of water molecules in the crystal lattice of the anhydrate or lower hydrates changes the behaviour of the crystals in the following ways: interaction of the electron vibrations with light quanta changing the refractive index, interactions of the molecular motions with heat quanta changing the thermal conductivity and movement of the electrons in an electric field changing the electrical conductivity. Additional bonds form between the host molecule and the water molecules that change the bonding between the host molecules themselves altering the co-operativity in the crystal lattice and thus altering the melting point (Khankari & Grant, 1994).

Drug molecules can come in contact with water during several manufacturing processes that include: crystallisation, lyophilisation, wet granulation, aqueous film coating or spray drying. Other than the manufacturing processes that can expose the drug to water during storage is when the drug is in an atmosphere with a high humidity or if the drug is formulated in a dosage form that contains excipients that contain water and is capable of transferring the water to the drug or other excipients (Khankari & Grant, 1994).

Compounds can consist of different levels of hydration such as monohydrate, dihydrate, and trihydrate. Monohydrates contain one molecule of water for each molecule of compound in the crystal, where dihydrate and trihydrate contain two and three molecules of water for each compound molecule, respectively (Aulton & Taylor, 2013). Furthermore, hydrates can be classified into three categories namely: isolated site hydrates, channel hydrates (that can further be subdivided in expanded or non-stoichiometric hydrates and planar hydrates), and ion associated hydrates (Ahlqvist & Taylor, 2002; Brittain, 1999; Datta & Grant, 2004; Vippagunta *et al.*, 2001).

- Isolated site hydrates: water molecules are isolated from direct contact with other water molecules by intervening drug molecules.
- Channel hydrates: water molecules lie next to other water molecules of adjoining unit cells, along with the axis of the crystal lattice. Channel hydrates can subdivide into two groups: expanded hydrated or non-stoichiometric hydrates where the molecule can take up additional moisture in the channels when the molecules are exposed to high humidity and

the crystal lattice may expand when hydration occurs or contract when dehydration occurs changing the dimensions of the unit cell. Planar hydrates form when water is in a two-dimensional order.

- Ion associated hydrates: metal ions are associated with the water molecules, the interaction between the metal and the water can be strong, and dehydration can only take place at very high temperatures (Brittain, 1999; Datta & Grant, 2004; Vippagunta *et al.*, 2001).

Hydrates are very common within the pharmaceutical industry and mostly the impact that different hydration levels can have on the physico-chemical properties of a particular drug is a critical aspect that is overlooked.

c. Solvates

Solvates are crystalline molecular compounds that form when a pure organic solvent or a mixture of solvents, other than water, is used to crystallise a compound. Molecules of the solvent are incorporated into the host lattice (Aulton & Taylor, 2013; Grant & Lohani, 2006; Vippagunta *et al.*, 2001; Zhang *et al.*, 2004).

Solvent molecules form a part of the unit cell of the crystal lattice and are in a stoichiometric ratio to the principal substrate. The solvents are bound into the crystal lattice through hydrogen bonding. Removal of the solvent, in this case, cannot occur without structural disruption and the conversion of the compound can either be to an amorphous or re-ordered, non-solvated crystal. The temperature where the solvent removal takes place is usually significantly higher than the melting point of the solvent and this temperature is determined by the energy input required to bring disruption to the lattice structure (Brittain, 1999).

Solvates can also include solvent molecules that are not incorporated into the crystal lattice. These solvent molecules are lodged at the surface, in voids or channels of the crystal structure. In the case where the solvent is lodged at the surface of the crystal structure, it can be driven off by temperatures slightly above the solvents' boiling point. Thermal stability is the primary factor that determines if the structure will be disrupted or not. Removal of the solvent within the voids or channels of the crystal structure (desolvation) from the lattice structure may or may not lead to structural disruption depending on both thermal stability and the mechanical effects. In this case, desolvation occurs at temperatures significantly higher than the solvents' boiling point (Brittain, 1999).

Solids can be exposed to solvent or solvent vapors throughout the manufacturing process. The most common methods in the chemical and pharmaceutical industry include precipitation,

crystallisation or recrystallisation from a suitable solvent or a mixture of solvents. Other methods include wet granulation, spray-drying, lyophilisation, to name but a few (Griesser, 2006).

Solvates must be analysed for toxicity, interactions with the drug and mobile solvent molecules with excipients in storage before they can be used (Singhal & Curatolo, 2003). This analysis is necessary since organic solvents have a potential risk for human health due to their toxicity, undesirable side effects and it has an effect on the physico-chemical properties and the excipients of pharmaceutical products (Witschi & Doelker, 1997). Some solvents are known to cause unacceptable toxic effects and are classified as class 1 solvents. These solvents should be avoided in pharmaceutical products unless the use of them can be strongly justified in a risk-benefit assessment. Class 2 solvents are associated with less severe toxicity and their use should also be limited to protect patients from potential adverse effects. Ideally, class 3 solvents that are less toxic should be used in pharmaceutical products.

Table 1.1: Class 3 solvents

Class 3 Solvents	
Acetic acid	Isobutyl acetate
Acetone	Isopropyl acetate
Anisole	Methyl acetate
1-Butanol	3-Methyl-1-butanol
2-Butanol	Methylethyl ketone
Butyl acetate	Methyl isobutyl ketone
<i>tert</i> -Butylmethyl ether	2-Methyl-1-propanol
Dimethyl sulfoxide	Pentane
Ethanol	1-Pentanol
Ethyl acetate	1-Propanol
Ethyl ether	2-Propanol
Ethyl formate	Propyl acetate
Formic acid	Triethylamine
Heptane	

d. Co-crystal

Co-crystals can be defined as mixed crystals that contain two different molecules, made from reactants that are solids at ambient temperature thus as a stoichiometric multi-component system connected by non-covalent interactions that exclude salts that contain ions rather than molecules (Brittain, 2009; Qiao *et al.*, 2011; Savjani, 2015, Thakuria *et al.*, 2013; Ymén, 2011).

It can be classified in zero-, one-, two- or three-dimension assemblies. The assembly depends on the type of intermolecular interactions within and between the collections of certain molecules. Interactions include van der Waals forces, π - π stacking interaction and hydrogen bonds. Further classifications of co-crystals can be based on the chains, dimers, rings and intermolecular hydrogen bonding forming these crystal forms (Qiao *et al.*, 2011; Savjani, 2015).

Co-crystals can be divided into two groups of material development namely: non-linear optical properties and host-guest complexes. Non-linear optical materials were designed by combining ionic and hydrogen bonds. Host-guest complexes involve the construction of a host with channels. Potential advantages of co-crystals include the improvement of solubility, dissolution rate, stability and other physical properties (Brittain, 2009).

Co-crystals can be formed through a solid and an appropriate co-former that include: carboxylic acid, amides, carbohydrates, alcohols, amino acids, flavonoids and nutraceuticals such as quercetin, pterostilbene and p-coumaric acid (Qiao *et al.*, 2011; Thakuria *et al.*, 2013). Co-crystallization of drugs can be achieved by using different methods that include solvent evaporation (solution co-crystallisation), drop grinding method, anti-solvent addition, melt crystallisation and ultrasound-assisted co-crystallisation (Savjani, 2015; Thakuria *et al.*, 2013).

Solution co-crystallisation is the most common method where the appropriate stoichiometric amount is taken and dissolved in a solvent. The solvent is allowed to evaporate, or the solution is allowed to be cooled. A disadvantage of this method is that individual components may crystallise separately, and it may result in the formation of undesirable solvates and hydrates with a risk of homomeric molecules forming (Qiao *et al.*, 2011; Savjani, 2015; Thakuria *et al.*, 2013). The solvent drop grinding method is the most environmentally friendly method and involves only a few drops of solvent. The method does not involve evaporation of large quantities of the solvent, purification or filtering procedures. On the other hand, excessive heating with the solvent drop grinding method can cause accidental phase transition, leading to crystallisation or polymorphism (Qiao *et al.*, 2011; Savjani, 2015).

e. Salts

Salt formation is preferred for weak bases and acids (Brough & Williams, 2013). More than 50% of the drugs on the market are in the form of a salt (Sarmah *et al.*, 2015) and 20-30% of new

molecules can form a salt easily (Brough & Williams, 2013). The salt formation is used to improve the physico-chemical properties of drugs through an acid-base reaction between the drug and an acidic or basic compound (Savjani, 2015). For this reaction to take place, the drug must be ionisable (anionic, cationic or zwitterionic) (Elder *et al.*, 2012; Savjani, 2015).

The most common acidic (anionic) counter-ions are hydrochloride, sulphate, tartrate, hydrobromide, maleate, mesylate, phosphate to name but a few. In addition, basic (cationic) counter-ions are sodium, potassium, calcium, magnesium, meglumine, ammonium, aluminium, etc. (Brittain, 2009). Salt formation requires a difference of 2.7 pKa units between the conjugated acid and the conjugated base ($\text{pKa}[\text{base}] - \text{pKa}[\text{acid}] \geq 2.7$) (Sarmah *et al.*, 2015; Savjani, 2015).

1.2.2 Amorphous

Amorphous solids demonstrate only a certain level of order found in short-range order; regularity does not extend beyond this (Cui, 2009). The feature that distinguishes amorphous solids from crystalline solids is the lack of three-dimensional long-range order (Brittain, 2009). Accompanying the more random arrangement of molecules in amorphous materials are a higher free volume, compared to crystalline solids. The higher free volume and molecular mobility lead to liquid-like behaviour in temperatures below the crystal-to-liquid transition temperature (Brittain, 2009). This being said, amorphous solids have a characteristic temperature where there is a major change in its properties, called the glass transition temperature (T_g). T_g is the point where the molecule in the glass shows a major change in mobility. Due to the lack of mobility when the solid is in a glassy state, it will allow the amorphous form to exist for a longer period of time, whereas an increase in molecular mobility allows fast conversion to the crystalline form. If the solid is stored below its T_g the amorphous form would be brittle (in the glassy state). If the solid is stored above its T_g it will become rubbery (Aulton & Taylor, 2013).

Amorphous solids can occur due to one of three sets of circumstances: firstly, the drug may be deliberately manufactured to be an amorphous solid through quenching of melts, rapid precipitation by addition of an anti-solvent, freeze-drying, spray-drying and introduction of impurities to enhance product performance characteristics, for example, the preparation of glassy drugs to enhance dissolution or freeze-drying behaviour. Secondly, the drug may inherit amorphous or partially amorphous qualities (examples include: D/L polylactic acid, polyvinylpyrrolidone or polyethylene glycol) at ambient temperatures that can be observed during processing or delivering conditions. Dosage forms that use these materials can be partially amorphous. Thirdly, an amorphous solid can be produced accidentally through manufacturing processes that can introduce mechanical or chemical stress through milling, grinding, wet granulation, compression, or introduction of impurities. The production of accidental amorphous

forms can be problematic leading to significant changes in product performance (Burnett *et al.*, 1999; Craig *et al.*, 1998; Yu, 2001).

1.3 Physico-chemical properties of different solid-state forms

Each of the solid-state forms displays unique physico-chemical properties that can influence the manufacturability, purification, physico-chemical stability, melting point, solubility, dissolution rate, hygroscopicity and ultimately the bioavailability of a drug (Babu & Nangia, 2011; Morissette, 2004; Rodríguez-Spong *et al.*, 2004). It is important to understand the relationship between the specific solid-state form of the drug and its functional properties (Morissette, 2004).

The preferred solid-state form is usually the thermodynamically stable form of the specific drug; however, this may show inadequate solubility or dissolution rates that will ultimately result in poor bioavailability of orally administered drugs, especially for drugs that are water-insoluble. In these cases, an alternative solid-state form can be investigated (Morissette, 2004). Stability is a closely studied parameter especially during the development of a new chemical entity. Stability considerations are different depending on the structure and characteristics of the molecule. Physico-chemical stability data are commonly gained from accelerated stability conditions that will determine the developability and the shelf life of the compound (Schultheiss & Newman, 2009).

Melting point is an important factor to consider during drug development. A high melting point is desirable; however, it can contribute to poor solubility. On the other hand, a low melting point can be problematic during the manufacturing process especially during drying, and it can cause stability problems (Schultheiss & Newman, 2009).

Poor aqueous solubility is a significant problem in the development of new compounds. Poor aqueous solubility is related to poor dissolution rates and bioavailability. There are, however, numerous approaches to enhance the solubility and/or dissolution rates and thus the oral bioavailability of drugs. Solubility and dissolution rates can be enhanced through salt or co-crystal formulation, reducing drug particle size, modification in the solid-state from one polymorph to another, solvation, hydration or amorphization (Censi & Di Martino, 2015).

Bioavailability measures the rate and extent of an active drug that reaches the systemic circulation. During early development, *in vitro* membrane permeation and animal bioavailability are important aspects to consider during the development of new forms of compounds to determine pharmacokinetic data quickly (Schultheiss & Newman, 2009).

During the next section, each solid-state form that has been mentioned throughout sections 1.2.1 and 1.2.2 will be discussed further with emphasis on the physico-chemical properties of these forms.

1.3.1 Polymorphism

Polymorphism is a quite common phenomenon among a variety of organic crystals (Morissette, 2004). Due to the differences in the potential energy levels, it can have a significant impact on stability, solubility, and bioavailability. A metastable polymorph presents higher molecular mobility leading to lower chemical stability relative to the stable polymorph (Cui, 2007; Singhal & Curatolo, 2004). Metastable polymorphs exhibit a higher solubility and dissolution rate, therefore, the bioavailability is higher than that of the stable polymorph (Cui, 2007). The higher lattice free energy leads to faster drug dissolution rates, releasing a higher amount of lattice free energy that will result in increased solubility (Brittain, 1999). Thus, the difference in solubility and dissolution rates between the polymorphic forms are determined by the differences in the lattice energy of the involved polymorphs (Brittain, 1999; Cui, 2007). Different polymorphs show a correlation between the melting point and the dissolution rate. Solids with high melting points have strong crystal lattices and removal of molecules is therefore more difficult due to the lower available free energy, thus resulting in lower dissolution rates. Solids with low melting points have weak crystal lattices and will easily remove molecules, thus resulting in faster dissolution rates (Aulton & Taylor, 2013).

An example of a drug where polymorphism has an impact on the solubility and dissolution rate is the protease inhibitor, ritonavir. After the release of the commercial product containing ritonavir, a new thermodynamically stable form of the drug (i.e. Form II) with a lower solubility was discovered. The dosage form on the market was a semi-solid formulation that consisted of a nearly saturated solution of Form I. However, in respect to Form II, the formulation was supersaturated since Form II is much less soluble in the solvents that were used (Huang & Tong, 2003).

1.3.2 Hydrates

Water molecules incorporated into the crystal lattice produces a new unit cell that is different from the anhydrate (Aulton & Taylor, 2013; Khankari & Grant, 1994) or lower hydrates with changes in the dimensions, shapes, symmetry and capacity of the unit cell. These changes can cause the hydrate to have different physico-chemical properties than the anhydrate. Changes in thermodynamic activity of the drug can occur due to hydration changes properties of the drug such as solubility and the physico-chemical stability. The change in solubility usually changes the dissolution rate that will ultimately change the bioavailability and performance of the drug (Khankari & Grant, 1994).

Hydrated forms can have a faster or slower dissolution rate than the anhydrous form. Usually, the hydrated forms have slower dissolution rates than the anhydrous counterpart, for example, theophylline monohydrate. The water molecules form a greater number of intermolecular

hydrogen bonds between the molecules and this will tie the lattice together providing a stronger, more stable lattice (higher mechanical strength than anhydrous theophylline) resulting in a slower dissolution rate. The anhydrous form will initially form supersaturated conditions whereas the hydrated form comes to true equilibrium solubility (Aulton & Taylor, 2013; Datta & Grant, 2004).

Although the anhydrous form is usually more soluble with faster dissolution rates, the opposite can also be true. An example of this is erythromycin monohydrate and dihydrate, where the water can act as a wedge between the molecules, pushing them apart thus preventing optimum interaction. The water molecules present in the crystal weakens the structure of the lattice and this will result in a more rapid dissolution rate (Aulton & Taylor, 2013).

1.3.3 Solvates

Solvates demonstrate different solubilities and consequently different dissolution rates per unit surface area than their unsolvated counterparts, thus resulting in different bioavailability of solvates. Solvates formed from different solvents will differ in terms of solubility (Grant & Lohani, 2006; Haung & Tong, 2003).

Solvates can enhance aqueous solubility, while hydrates often decrease it (Cui, 2007). Phase changes due to solvation or desolvation and hydration or dehydration of a drug can therefore affect the bioavailability of the drug from solid dosage forms (Vippagunta *et al.*, 2001).

1.3.4 Co-crystals

Co-crystals can improve properties such as melting point, stability, solubility and dissolution rates of drugs (Brittain, 1999; Cui, 2007; Qiao *et al.*, 2011). One of the main reasons to study co-crystals is to increase the solubility of a poorly soluble compound (Schultheiss & Newman, 2009). Co-crystals can influence the crystal lattice, lowering the lattice energy and the solvation of co-crystals increasing solvent affinity thus increasing the solubility. The higher solubility is dependent on the activities or concentrations of co-crystal components in solution (Thakuria *et al.*, 2013).

The melting point of the co-crystal depends on the co-former that was used. If a higher melting point is desired for the co-crystal than a co-former with a higher melting point should be considered and *vice versa*. There are few reports on the chemical stability of co-crystals, however, it is possible that co-crystals may exhibit superior chemical stability. In the case where the stability is an issue with the specific compound that is used, crystal engineering techniques can provide different approaches to prevent degradation pathways if there are known (Schultheiss & Newman, 2009).

An example of a co-crystal that improves the solubility and bioavailability is the anti-inflammatory, antipyretic and analgesic drug, indomethacin. Indomethacin is a biopharmaceutical classification

system (BCS) class II drug that exists in polymorphic forms α and γ . The polymorphic form γ is thermodynamically stable at room temperature, very slightly soluble (2.4 – 4 $\mu\text{g/ml}$) that can explain the low bioavailability. The co-crystals were prepared using saccharin through both slow evaporation and co-grinding. Indomethacin-saccharin co-crystals showed a higher solubility and faster dissolution rates than the stable indomethacin (form γ). The improved solubility led to an improved bioavailability (Qiao *et al.*, 2011; Thakuria *et al.*, 2013).

An example of a co-crystal that does not improve the solubility or dissolution rates but is nevertheless equivalent to the existing compound, despite it being a different form, is the carbamazepine:saccharin co-crystal. The stability of this co-crystal was compared to carbamazepine (form III) at 5°C, 40°C and 60°C at an ambient humidity as well as elevated relative humidity (RH) conditions of 25°C/60% RH and 40°C/75 RH over a period of two months. Degradation was not observed for either the co-crystal or carbamazepine (from III) at the elevated temperatures, however, both compounds showed a similar degradation pattern at elevated RH conditions. In this case chemical stability does not need to be improved. The co-crystal proved to be as stable as the existing compound under similar conditions (Schultheiss & Newman, 2009).

1.3.5 Salt

As previously mentioned, the preparation of salts is usually formed from ionizable compounds using acceptable acids and bases (Morissette, 2004). However, salt formation offers a convenient method to improve physico-chemical properties of drugs (Tilborg *et al.*, 2014). The physico-chemical properties of the molecules that can be changed by salt formation include the melting point, hygroscopicity, solubility, dissolution rate, physico-chemical stability, refractive index, thermal conductivity, surface activity, density, habit, electrostatic, mechanical, and optical properties (Datta & Grant, 2004; Guerrieri *et al.*, 2010; Haung & Tong, 2003). These properties are significant because of their effect on the manufacturing, therapeutic efficacy, toxicity and bioavailability of drugs (Guerrieri *et al.*, 2010).

The most important property that is improved by salt formation is the solubility and dissolution rate in water (Guerrieri *et al.*, 2010; Morissette, 2004; Tilborg *et al.*, 2014; Ymén, 2011). Ionizable species such as a salt will therefore be more soluble in water and the drug will have a better chance of reaching its biological target regardless of the required administration pathway (e.g. intravenous, oral, to name but a few) due to a higher concentration gradient (Tilborg *et al.*, 2014). In some cases, salts may also be used to reduce the solubility of drugs for certain usages such as controlled release dosage forms (Morissette, 2004).

1.3.6 Amorphous solids

Amorphous solids show higher solubility and therefore often higher dissolution rates than crystalline solids, nonetheless they are physically and chemically less stable than the corresponding crystal forms. It possesses entropy, enthalpy and free energy that accounts for the improved solubility (Datta & Grant, 2004; Graeser *et al.*, 2008; Yu, 2001) due to the lack of a three-dimensional crystalline lattice, more intermolecular mobility, higher intermolecular distance and higher free energy (Cui, 2009; Graeser *et al.*, 2008; Singhal & Curatolo, 2004). Amorphous solids express excess thermodynamic properties making it unstable and therefore recrystallisation may occur (Graeser *et al.*, 2008).

During the processing and handling of drugs, there are numerous situations where mechanical properties are important for manufacturing, stability, and the performance of a drug. In the case of external stress crystalline materials tend to show high levels of elasticity and brittleness. While, in contrast, the amorphous state tends to show different degrees of viscoelasticity. These differences are a result of dependence of their temperature relative to the glass transition temperature (Hancock & Zografi, 1996).

Powder cohesion is expressed as interchangeable closely related phenomena known as caking and stickiness in powders. The transformation of powder in lumps followed by agglomeration can be described as caking in amorphous solids (Paterson *et al.*, 2005). Caking is an unfavorable phenomenon where a free-flowing powder with low moisture transforms into lumps, then into an agglomerated solid and finally into a sticky material that will result in the loss of function (e.g. a change in solubility, dissolution rates or stability) (Aguilera *et al.*, 1995). Different stages in the caking process are defined as free flowing, bridging, agglomeration, compaction, and liquefaction as illustrated in Figure 1.4 (Aguilera *et al.*, 1995; Paterson *et al.*, 2005). The process depends on temperature, moisture and the position of the particles within the powder (Aguilera *et al.*, 1995). During caking the particles involved must bridge together for the powder to cake also known as sticking or lumping. The caking of the powder is determined by the extent of the stickiness before the solidification of the bridges (Paterson *et al.*, 2005).

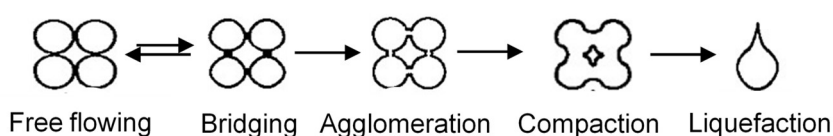


Figure 1.4: Stages during a typical caking process (Aguilera *et al.*, 1995)

As mentioned above, amorphous solids are more soluble than crystalline solids and this is often more significant than the solubility advantage of a metastable polymorph. Amorphous

atorvastatin calcium can be prepared through spray drying or through a supercritical anti-solvent process. The initial dissolution rate of both amorphous forms of atorvastatin was 3.3 times that of the crystalline solid. Solution-mediated phase transformation during powder dissolution studies in water showed a rapid increase in the concentrations that is followed by a decline at 10 min for both of the amorphous forms. The amorphous form that was prepared through the supercritical anti-solvent process was administered to rats and resulted in an area-under-the-curve (AUC) that was 2.8 times that of the crystalline material. The bioavailability of the spray-dried amorphous atorvastatin calcium was only two times that of the crystalline material. Compared with the crystalline form, the AUC is somewhat less than expected, suggesting a possible solution-mediated phase transformation *in vivo* from the amorphous to crystalline forms (Greco and Bogner, 2012). Phase transformations will be discussed in detail in the next section.

1.4 Solid-state transformations

A solid-state transformation may be defined as any transition from one solid-state form of a compound to another solid-state form resulting in the same chemical composition, but different packing arrangement. These transformations can be classified as thermodynamic, kinetic and molecular that can be affected by mechanical, thermal and chemical stresses (Aucamp *et al.*, 2015b; Govindarajan & Suryanarayanan, 2006). Phase transitions that may affect the performance of drugs in solid dosage forms include inter-conversion among polymorphs, formations of solvates or hydrates and conversion to the amorphous form. These transformations can affect the physico-chemical and mechanical properties of the drug (Zhang *et al.*, 2004).

Exposing a solid dosage form to the manufacturing process induces stress to the system that can result in phase transformation (Govindarajan & Suryanarayanan, 2006; Morris *et al.*, 2001). Stress, in this instance, implies a physical change that moves the system from or towards equilibrium. Stress can be thermal, mechanical or as a result of a second factor such as solubilisation or moisture that can induce a phase transition. A transition can be thermodynamically favoured, resulting in a phase that is stable under stress. While the system is under stress it may be trapped in another equilibrium, however, if the stress is removed from the system it can relax back into the original equilibrium state. There are two subdivisions of trapping newly generated phases: first, stress can move the system to a point where the new phase is the stable phase and it will become metastable only when the stress is removed, for example tableting. Secondly, the stress can be used kinetically to stabilise a metastable phase (partial or complete amorphisation due to mechanical processing, vitrification of solutes) and in this circumstance it is not the thermodynamically stable form. An example would be the formulation of a metastable polymorph in a monotropic system *via* a melting process or a hydrate that forms during wet granulation (Govindarajan & Suryanarayanan, 2006; Morris *et al.*, 2001).

Manufacturing processes such as milling, granulation, spray-drying, blending and compression may affect the stability and induce a transformation of the solid also depending on further factors such as temperature, pressure and the relative humidity of the environment (Aucamp *et al.*, 2015b; Vippagunta *et al.*, 2001; Zhang *et al.*, 2004). Multiple phase transformations can occur during the different manufacturing processes. The effect of the transformed phase of each of the processes on the solid and on its behaviour can be understood by monitoring the phases during the manufacturing process (Govindarajan & Suryanarayanan, 2006). If the transformation is not intended, it can lead to an array of problems that can affect any further processing during manufacturing (Aucamp *et al.*, 2015b). The phase changes can either be within the arrangement of molecules in the crystal lattice or in the lattice order that can lead to amorphisation, crystallization or polymorphic transition (Govindarajan & Suryanarayanan, 2006).

Granulation is usually executed when the drug is combined with some of the excipients. There are two types of granulation: wet and dry granulation. Wet granulation creates favourable conditions for solvent-mediated or solution-mediated transformations and it is the most likely to result in a solid-state transformation. The liquid used can lead to hydration/solvation, polymorphic conversions, vitrification or crystallisation (Aucamp *et al.*, 2015b). During dry granulation, mechanical stress is induced when powder blends are subjected to compression (Govindarajan & Suryanarayanan, 2006), this can lead to solid-solid transformations that might ultimately lead to solvent-mediated or solution-mediated transformations further along the manufacturing process. For both wet- and dry granulation, mixing with excipients can lead to solid-state transformations (Aucamp *et al.*, 2015b).

Spray-drying produces homogenous particles that have a uniform shape and size. The process requires partial or complete dissolution in the solvent leading to likely solvent or solution-mediated transformations. Solvent removal is a rapid process that can lead to crystallization of the metastable form (Aucamp *et al.*, 2015b; Govindarajan & Suryanarayanan, 2006).

After compression, a coating process can be either required or desired. The tablet is subjected to the solution for a minimal period leading to unlikely solid-state transitions, however, in the case of modified release, the drug layer is applied by spraying the drug-excipient solution or suspension on the tablet surface. The drug can dissolve or suspend in liquid thus increasing the probability of solvent or solution-mediated transformations. The rapid removal of the solvent after applying the coat could lead to precipitation of an altered solid-state form in the coated layer (Aucamp *et al.*, 2015b).

There are three underlying mechanisms for phase transformations (solid-solid, solvent-mediated and solution-mediated transformations) that are discussed in the section below.

1.4.1 Solid-solid transformations

This transformation occurs as a result of a direct conversion from one solid-state form to another solid-state form without an intermediate solution, melt- or vapour phase (Aucamp *et al.*, 2015b; Vippagunta *et al.*, 2001; Zhang *et al.*, 2004). Solid-solid transformations without the addition of a solvent as a catalyst is a relatively slow process and need to be thermodynamically favoured. Therefore, they can only result in products that are more stable than the starting material. These transformations are accelerated through solvents or solvent vapour that acts as a catalyst that reduces the energy barrier and increases the rate at which the transformation occurs (Aucamp *et al.*, 2015b).

Melt-induced transformation occurs when the solid-state form is heated above the melting point, then cooled back to room temperature resulting in another solid-phase. Parameters determining the solid-state form that will be produced include cooling rate, nucleation rate and the presence of impurities or seed crystals. This can result in both the initial product and final product being either crystalline or amorphous (Aucamp *et al.*, 2015b; Zhang *et al.*, 2004). Milling, usually the first step in the manufacturing process, is used to reduce the size of drug particles. It imparts mechanical stress and often generates heat and vibrational energy that can lead to dehydration or complete/partial vitrification of the drug (Aucamp *et al.*, 2015b; Govindarajan & Suryanarayanan, 2006). This is characterised as a solid-solid transformation process. Compression is another process that can lead to solid-solid transformations of the metastable form (Aucamp *et al.*, 2015b).

1.4.2 Solvent-mediated transformations

These transformations are mediated by an interaction between the undissolved material and a solvent that is in liquid or vapour form that was introduced. Examples of this transformation include an anhydrous form of a drug converting to a hydrated form or to a solvate, solvent exchange that can lead to change in the structure and crystallisation of an amorphous form to a solvate or a hydrate (Aucamp *et al.*, 2015b).

1.4.3 Solution-mediated transformations

Solution-mediated transformations always occur from the metastable to the stable phase if a saturated solution of the metastable form exists (Aucamp *et al.*, 2015b; Zhang *et al.*, 2004). The transition is driven by the difference in solubility between the two phases that occur when the metastable phase is in contact with the supersaturated solution (Zhang *et al.*, 2004).

Solution-mediated transformation from the metastable to the stable phase occurs in three steps as listed below and illustrated in Figure 1.5 (Cardew and Davey, 1985; Greco & Bogner, 2012; Gu *et al.*, 2001; Murphy *et al.*, 2002; Zhang *et al.*, 2004):

1. Dissolution of the metastable phase into the solution to reach and exceed the solubility of the stable phase.
2. Nucleation of the stable phase.
3. Growth of the stable phase coupled with the continuous dissolution of the metastable phase.



Figure 1.5: Steps of solution-mediated transition (Gu *et al.*, 2001)

Step 2 and 3 are usually the slowest steps. In the case where step 2 is the rate-determining step, any factors that affect the nucleation will influence the overall transformation. The factors that will affect this include solubility, solubility difference between phases, processing temperature, contact surface, agitation and soluble excipients/impurities. In the case where step 3 is the rate-determining step, the kinetics of the conversion is determined by solubility difference, solid/solvent ratio, agitation, processing temperature, the particle size of the original form and soluble excipients/impurities (Zhang *et al.*, 2004).

Supersaturation can be created by numerous methods that can be regulated by the activity of the solid or the solute that include: solvent removal through evaporation leading to the concentration of the solute to rise in the remaining solvent, freezing or cooling of the solution that will result in most material becoming less soluble as the temperature decreases, addition of different salts with ions that participate in precipitation and dissolution of the metastable phase (Aulton & Taylor, 2013; Rodríguez-Hornedo & Murphy, 1999; Ymén, 2011). Other than these methods, supersaturations can be created by regulating the solute solubility through pH change and the addition of a solvent that will lower the solubility of the solute (anti-solvent) (Aulton & Taylor, 2013; Rodríguez-Hornedo & Murphy, 1999).

Nucleation is the formation of the nuclei in a supersaturated solution that acts as the centre of crystallisation (Grant & Lohani, 2006). Nucleation can be divided in primary and secondary nucleation. Primary nucleation is when there are no crystals present in the initial solution. Primary nucleation can further be divided in homogeneous and heterogeneous nucleation (Grant & Lohani, 2006; Rodríguez-Hornedo & Murphy, 1999; Ymén, 2011). Homogeneous nucleation occurs spontaneously in bulk solution. Heterogeneous nucleation is an interaction on surfaces and it may be induced by foreign particles through the use of different types of equipment, impurities, to name but a few. Secondary nucleation is when the crystals of the solute are already present, or it is deliberately added as seeds to the solutions (Grant & Lohani, 2006). Nucleation is a more demanding process than crystal growth and it requires more energy. There are,

however, regions in the supersaturated solution where the nucleation is suppressed but crystal growth proceeds. The nucleation rate will increase by increasing the supersaturation, while other variables are constant, however, at a constant supersaturation, the nucleation rate will increase with an increase in solubility (Rodríguez-Hornedo & Murphy, 1999).

Nucleation rate can experimentally be controlled by the following parameters: molecular or ionic transport, viscosity, supersaturation, solubility, solid-liquid interfacial tension, and temperature. Nucleation kinetics can experimentally be determined from the measurements of nucleation rates, introduction times and the metastability zone widths that include the supersaturation or undercooling that is necessary for the formation of spontaneous nuclei as a function of initial supersaturation (Rodríguez-Hornedo & Murphy, 1999).

Crystal growth is known as the stage where the nucleation step has been overcome and the nucleus has grown into macroscopic crystals. Crystal size distribution will be determined by the nucleation and growth processes that compete for the solute in terms of their dependence of supersaturation and their relative rates (Rodríguez-Hornedo & Murphy, 1999; Ymén, 2011). The size and number of crystals obtained, depend on the supersaturation so that high supersaturation leads to many small crystals whereas low supersaturation leads to fewer larger crystals (Ymén, 2011). Internal and external factors can govern crystal growth. Internal factors include the three-dimensional crystal structure and crystal defects will determine the nature and strength of the intermolecular interactions between the crystal surface and the solution. External factors include temperature, supersaturation, solvent and the presence of impurities that will affect the type of interactions at the solid-liquid interface. Growth rate can be expressed as overall linear growth that is the rate of change of the volume equivalent diameter with time, linear growth rate of a face that is the rate of displacement of a crystal face in a direction perpendicular to the face and velocity, height and spacing of growth steps spreading across a crystal surface (Rodríguez-hornedo & Murphy, 1999).

1.5 Biopharmaceutics Classification System/Drug like properties

The biopharmaceutical classification system (BCS) is a scientific framework that classifies a drug based on its aqueous solubility and intestinal membrane permeability properties (Blume & Schug, 1999; Chavda *et al.*, 2010; Kawabata *et al.*, 2011; Lennernäs *et al.*, 2007; Reddy & Karunakar, 2011; Sinai Kunde *et al.*, 2015; Varma *et al.*, 2004). The BCS concept can be elaborated to include the dose number, dissolution number and absorption number of an orally administered drug, which can predict the systemic availability of a drug. The dose number can be defined by the volume that is required to solubilise the maximum dose strength of the drug and the solubility of the drug. The dissolution number can be defined by the time that is required for dissolution in the gastro-intestinal tract that is the ratio of the intestinal residence time and the dissolution time.

The absorption number can be defined by the ratio of the mean residence time to the mean absorption of a dose administered orally (Reddy & Karunakar, 2011; Varma *et al.*, 2004).

These three numbers are associated with different factors that include the physico-chemical properties of the drug (solubility/dissolution), stability of the drug in the gastro-intestinal (GI) environment (acid degradation), enzymatic stability in the GI lumen, epithelium and liver, membrane permeability (molecular weight, log P, H-bonding efficiency) and substrate specificity to various biological transporters and efflux systems of intestinal epithelium including P-glycoprotein (P-gp) (Varma *et al.*, 2004).

This BCS system gives an indication of the *in vivo* pharmacokinetics of immediate-release (IR) orally administered drugs (Reddy & Karunakar, 2011; Sinai Kunde *et al.*, 2015). Drugs can be classified into four different classes (Table 2) based on their solubility related to the dose and membrane permeability properties in combination with the dissolution properties of the dosage form (Blume & Schug, 1999; Lennernäs *et al.*, 2007; Reddy & Karunakar, 2011; Sinai Kunde *et al.*, 2015). BCS is also based on the framework describing three rate limiting steps in the oral absorption process, which are necessary for a drug to be absorbed after oral administration:

- Release of the drug from the dosage form.
- Maintenance of the dissolved state through the gastro-intestinal (GI) tract.
- Permeation across the GI membrane into the hepatic circulation (Sinai Kunde *et al.*, 2015).

This classification system therefore depends on the understanding that the dissolution of the dosage form depends on the solubility of the drug and thereafter the absorption of the drug across the gastro-intestinal tract epithelial membrane is dependent on the permeability properties of the drug substance. Dissolution may be affected by the characteristics of the dosage form and the absorption rate from the intestine (Blume & Schug, 1999).

Table 1.2: BCS classification of drug substances (Blume & Schug, 1999; Ku & Dulin, 2010; Reddy & Karunakar, 2011)

Class	Solubility	Permeability
I	High	High
II	Low	High
III	High	Low
IV	Low	Low

BCS Class I - Drugs in this class has a high solubility and a high membrane permeability (Kawabata *et al.*, 2011; Sinai Kunde *et al.*, 2015; Varma *et al.*, 2004). These drugs are ideal for effective oral delivery (Varma *et al.*, 2004). These drugs are well absorbed with an absorption rate usually higher than the excretion rate (Reddy & Karunakar, 2011; Sinai Kunde *et al.*, 2015). The drugs show a high absorption as well as a high dissolution number, thus indicating the drug is in solution throughout the GI tract and it is available for permeation across the GI epithelial membrane (Chavda *et al.*, 2010; Reddy & Karunakar, 2011; Sinai Kunde *et al.*, 2015; Varma *et al.*, 2004). If the drug is formulated in an immediate release dosage form, it will dissolve rapidly and will be transported across the GI wall in a rapid manner (Sinai Kunde *et al.*, 2015). In this class, the rate-determining step is dissolution, however, if the dissolution is relatively rapid, the gastric-emptying rate will become the rate-determining step (Chavda *et al.*, 2010; Reddy & Karunakar, 2011; Sinai Kunde *et al.*, 2015).

BCS Class II - Drugs in this class has a low solubility, but a high membrane permeability (Chavda *et al.*, 2010; Kawabata *et al.*, 2011; Sinai Kunde *et al.*, 2015). These drugs have a high absorption number and a low dissolution number (Chavda *et al.*, 2010; Reddy & Karunakar, 2011; Sinai Kunde *et al.*, 2015). These drugs have a variable bioavailability, therefore these compounds are suitable for slow release (SR) and controlled release (CR) formulations that will control the dissolution and in effect give a more predictable bioavailability (Sinai Kunde *et al.*, 2015). The rate-determining step is *in vivo* drug dissolution, except in cases of a very high dose number (Chavda *et al.*, 2010; Reddy & Karunakar, 2011; Sinai Kunde *et al.*, 2015; Varma *et al.*, 2004).

BCS Class III - Drugs in this class has a high solubility and low membrane permeability (Chavda *et al.*, 2010; Kawabata *et al.*, 2011; Sinai Kunde *et al.*, 2015). The rate-determining step is the membrane permeation of the drug molecules (Chavda *et al.*, 2010; Reddy & Karunakar, 2011; Sinai Kunde *et al.*, 2015). Absorption is limited by a slow permeation rate. These drugs have a variable absorption rate and extent. Because the dissolution is rapid, the variation is attributable to changes in the physiology of the different regions of the GIT and membrane permeability rather than the dosage form factors (Chavda *et al.*, 2010; Reddy & Karunakar, 2011; Sinai Kunde *et al.*, 2015).

BCS Class IV - Drugs in this class has a low solubility as well as low membrane permeability (Kawabata *et al.*, 2011; Sinai Kunde *et al.*, 2015; Varma *et al.*, 2004). These compounds have a low bioavailability and they are usually not well absorbed through the intestinal mucosa and a high variability can therefore be expected (Reddy & Karunakar, 2011; Sinai Kunde *et al.*, 2015). These drugs can be highly problematic for effective oral administration (Chavda *et al.*, 2010; Reddy & Karunakar, 2011; Sinai Kunde *et al.*, 2015).

1.5.1 Solubility

Solubility is the ability of a solute to dissolve in a solvent (i.e. quantity of solute per volume solvent) to form a homogeneous solution that will be influenced by temperature, pressure and the nature of the drug (Censi & Di Martino, 2015; Khankari & Grant, 1994).

When the solute is placed in the solvent and mixing of the solute- and solvent molecules takes place due to randomization then in effect entropy and enthalpy takes place. Entropy is the driving factor of the mixing process, while enthalpy is the molecular interactions and hydrogen bonds between the solute and solvent molecules. It was found that the hydrogen bonds between molecules of the solute and molecules of the solvent are stronger compared to solute-solute and solvent-solvent interactions (Babu & Nangia, 2011).

Molecules will start to mix at the surface and continue until the solution reached saturation. The solute molecules will leave the solid phase from the surface and will go into solution. The molecules will re-attach and become an equal state of dynamic equilibrium. The amount of solute that dissolves in the solvent at equilibrium state can be defined as the solubility of the substance (Babu & Nangia, 2011). The typical aqueous solubility describing terms are indicated in Table 1.3.

Table 1.3: Solubility terms (Aulton & Taylor, 2013; BP 2017; USP 2017)

Descriptive term	Parts per solvent required for 1 part of solute	Solubility range (mg/ml)
Very soluble	<1	≥1000
Freely soluble	1-10	100-1000
Soluble	10-30	33-100
Sparingly soluble	30-100	10-33
Slightly soluble	100-1000	1-10
Very slightly soluble	1000-10 000	0.1-1
Practically insoluble	≥10 000	≤0.1

1.5.2 Permeability

The overall characteristics of drug permeability across the epithelium of the small intestine have been investigated extensively (Hidalgo *et al*, 1989). The small intestine is approximately 2 – 6 m and divided in three sections namely the duodenum, jejunum and the ileum. The division of these sections are 5%, 50% and 45% in length respectively. Approximately 90% of drug absorption of the GI tract takes place in the small intestine (Balimane *et al.*, 2000).

In order to exhibit ideal membrane permeability, drugs need to have certain desirable physico-chemical properties such as pKa, lipophilicity and solubility values within specific ranges. These physico-chemical properties have to be supported by aspects such as being non-toxic, non-degradable and not metabolised before, during or after permeation of the intestine to ensure good bioavailability (Bjarnason *et al.*, 1995; Hidalgo *et al.*, 1989). Intestinal membrane permeability is a critical feature that will determine the rate and extent of drug absorption and therefore ultimately the bioavailability of the drug (Nožinić *et al.*, 2010).

For a drug to be absorbed from the GI tract, it requires certain drug-like properties (i.e. physico-chemical and molecular properties). Lipinski proposed the rule of five based on physico-chemical properties of compounds in order to be absorbed at an acceptable rate and extent, which include the following (Lipinski *et al.*, 1996; Varma *et al.*, 2004):

- Molecular weight of the compound should be smaller than 500 g/mol;
- Number of hydrogen bond acceptors of the compound should be less than 10 (expressed in terms of the number of O's and N's);
- Number of hydrogen bond donors of the compound should be less than 5 (expressed in terms of the number of OH's and NH's);
- Log P of the compound should be less than 5 (or in the case if the MLog P over 4.1);
- Other physico-chemical and molecular properties of compounds that can influence the solubility can be seen in Table 1.4.

Lipinski's rule of 5 is implemented on a registration system especially for large numbers of newly synthesised compounds. If two or more of the parameters are not in range, an alert appears indicating the possibility for poor absorption and permeability. The alert does not completely prevent a chemist from registering the compound. This is due to the fact that drug compounds that are substrates for biological transporters are exceptions to the rule of 5, examples of these substrates include certain antibiotics, antifungals, vitamins as well as cardiac glycosides (Lipinski *et al.*, 1996).

Table 1.4: Physico-chemical and molecular property requirements for permeability and solubility (Müller, 2009)

Parameter	Requirement
Molecular weight	< 500 g/mol
Lipophilicity	Log P < 5 ^a
Solubility	> 0.1 mg/ml ^b
Charge	≤140 Å (for peripheral active drugs)
Polar surface area (PSA)	≤ 60 - 80 Å (for brain penetration)
H-bond donors (OH and NH)	≤5
H-bond acceptors (O and N)	≤10
Number of rotatable bonds	≤10

^a High enough to allow for passive diffusion.

^b Depending on the potency of the drug (very potent drugs, a lower solubility will be efficient to require sufficient blood levels).

Intestinal absorption or membrane permeability of a drug can be determined by *in vitro*, *ex vivo*, *in situ* and *in vivo* models (Alqahtani *et al.*, 2013). *In vitro* models include Caco-2 cells that form monolayers and are by far the most used cell model to simulate the intestinal epithelium. Madin-Darby canine kidney cells (MDCK) is an alternative to Caco-2 cells. Monolayers of MDCK cells are highly correlated with the Caco-2 cell model particularly for drugs that are passively absorbed (Sarmiento *et al.*, 2012). One of the most common *ex vivo* models is the Ussing chamber, which is a technique where excised animal intestinal segments are mounted between diffusion cells. Another model is the everted intestinal sac that is prepared from freshly isolated animal intestinal pieces that are turned inside out and closed at the ends to form a sac. An *in situ* perfusion model is used to perfuse a drug solution through an isolated intestinal segment, which is still part of a living animal (e.g. a rat). Drug absorption is determined by calculating the difference in concentration of the inlet and outlet flow. *In vivo* animal models involve oral administration of the drugs to the animals with subsequent blood sample withdrawal at predetermined time intervals. The samples are then analysed to determine the drug concentration at each time point in the blood plasma (Alqahtani *et al.*, 2013).

1.6 *In vitro* models for screening of membrane permeability properties

In vitro models used for screening of membrane permeability should ideally mimic the conditions in the human mucosa (Sarmiento *et al.*, 2012). There are a variety of *in vitro* methods that can be used in intestinal absorption for potential drug candidates (Balimane *et al.*, 2000). These methods require less labour with a high through put rate, it is more cost-effective and require less ethical

considerations compared to that of *in vivo* animal models and there is adequate predictability of absorption in humans. Some of the overall issues of these methods include gastric emptying rate, gastro-intestinal transit rate, gastro-intestinal pH, to name but a few that cannot be included in the data interpretation. Apart from those mentioned above, every *in vitro* method has its own advantages and limitations based on the specific goal of the method used (Balimane *et al.*, 2000; Sarmiento *et al.*, 2012).

1.6.1 Cell culture models

Cell culture models can be very useful for drug permeability screening assessments. In order to determine a specific mechanism of membrane permeation or absorption, different cell lines can be used (summarised in Table 1.5). *In vitro* cell models have been optimised to become more complex and to incorporate more than one type of cell in order to resemble *in vivo* tissues (Sarmiento *et al.*, 2012). During this study, the Caco-2 cell model was used and therefore this model is discussed in more detail.

Table 1.5: The cell culture models that are most commonly used to estimate intestinal transcellular transport (Balimane *et al.*, 2000)

Cell line	Species/tissue origin	Cell type
Caco-2	Human/colon	Epithelial
HT-29	Human/colon	Epithelial
T-84	Human/colon	Epithelial
MDCK	Canine/kidney	Epithelial
LLC-PK-1	Porcine/kidney	Epithelial

1.6.1.1 Caco-2 cell line

Caco-2 cells were originally derived from human colon adenocarcinoma (Alqahtani *et al.*, 2013; Gan & Thakker, 1997; Le Ferrec *et al.*, 2001). Despite their origin, Caco-2 cells grow in culture to form a polarised monolayer with tight junctions that differentiate to form a semi-permeable membrane and displays similar morphological and functional characteristics as small intestinal enterocytes (Alqahtani *et al.*, 2013; Le Ferrec *et al.*, 2001; Sarmiento *et al.*, 2012). When culturing these cells on membranes in Transwell® plates, they will separate the wells in an apical compartment and in a basolateral compartment (Figure 1.6) that corresponds to the lumen and the serosal of the intestine, respectively (Le Ferrec *et al.*, 2001). It therefore resembles the small intestinal epithelium through differentiating spontaneously into enterocytes under conventional cell culture conditions (Gan & Thakker, 1997).

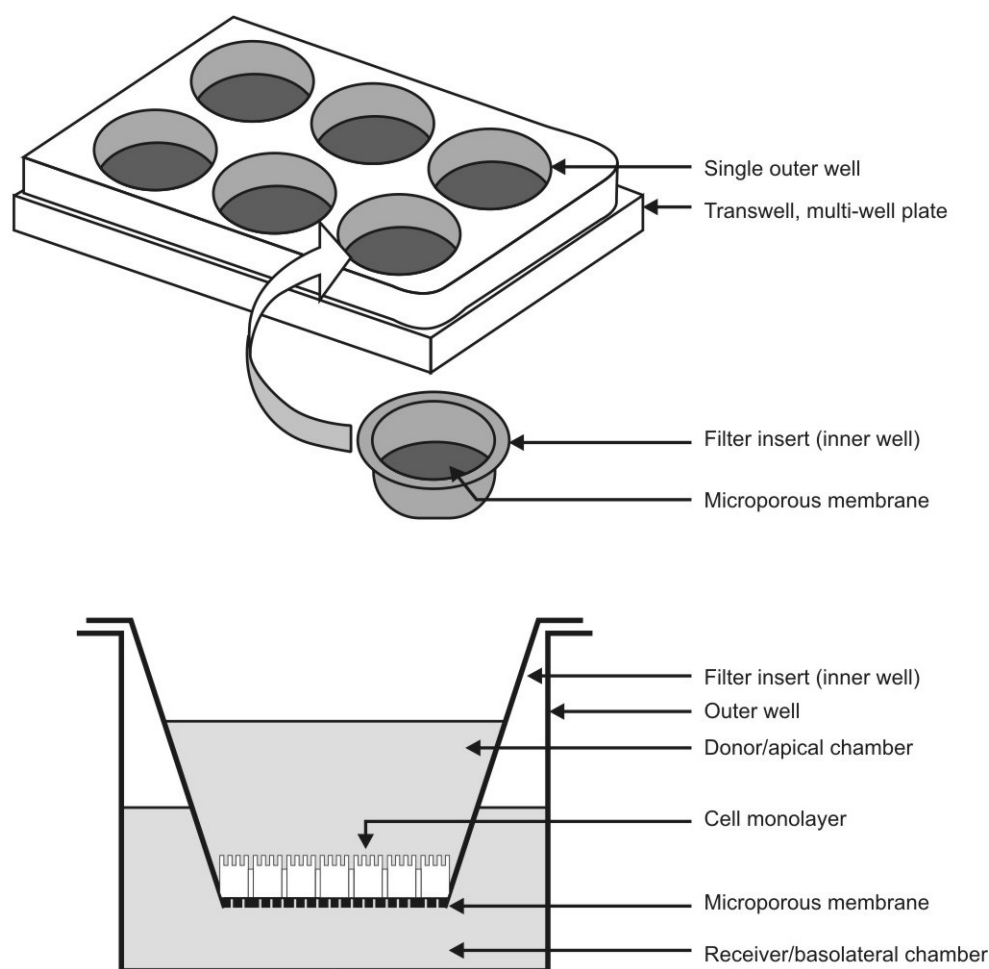


Figure 1.6: A schematic representation of a cultured monolayer of Caco-2 cells on a microporous membrane in a Transwell® plate (Hamman, 2007).

Most of the *in vitro* studies that include drug transport across cell monolayers are performed using Caco-2 cells. The aim is to examine whether the drug will be actively or passively transported across the GI epithelium. In the case of active transport, the identification of the relevant carriers is necessary. The majority of studies that focus on active drug transporters in Caco-2 cells examined two transport systems: the dipeptide carrier and the P-glycoprotein (P-gp) (Artursson *et al.*, 2001).

There are several studies that show that the active transport systems that are located in the intestinal epithelium can also be expressed in Caco-2 cells. These transport systems include glucose, amino acids, dipeptide, bile acids, vitamins and cobalamin intrinsic factor (Alqahtani *et al.*, 2013; Gan & Thakker, 1997). Enzymes that is found in the brush border of the GI tract that is also present in Caco-2 cells are aminopeptidase, alkaline phosphatase, sucrase, dipeptidyl aminopeptidase and γ -glutamyl transpeptidase (Gan & Thakker, 1997). There are also existence of phase I and phase II metabolizing enzymes in Caco-2 cells (Gan & Thakker, 1997). An example of an enzyme that is expressed as part of phase I metabolism is cytochrome-P450 iso-enzyme 1A1 (CYP1A1) (Gan & Thakker, 1997) and enzymes expressed in phase II metabolism

are glutathione S-transferase, glucuronidase, N-acetyl transferase, hydrolases and sulfotransferase (Alqahtani *et al.*, 2013; Gan & Thakker, 1997; Le Ferrec *et al.*, 2001). Caco-2 cells express CYP3A very weakly, however, treatment with 1 α ,25-dihydroxyvitamine D3 can induce CYP3A4 at the mRNA level in Caco-2 cells and transfection of CYP3A4 cDNA. However, despite the treatment levels, CYP3A iso-enzymes do not reach the levels that are observed *in vivo* (Le Ferrec *et al.*, 2001).

Advantages of Caco-2 cells include the following (Gan & Thakker, 1997; Le Ferrec *et al.*, 2001):

- It is a flexible *in vitro* permeation method;
- Caco-2 cell monolayers can serve as a relatively fast and simple screening tool for drug permeation studies;
- It can provide information at cellular level on the absorption, metabolism and transport of drug molecules across the GI mucosa, which is an advantage over the intestinal loop and everted sacs that are more suitable for the study of drug uptake into the mucosal cells;
- It can provide information on possible mucosal toxicity caused by therapeutic agents;
- There are no interspecies differences in the morphological and physiological characteristics of GI cells, since it is of human origin;
- There is no use of animals, unlike many other *in vitro* GI absorption models;
- It can be used for high through put drug screening testing.

Despite the advantages Caco-2 cells also have some limitations that include (Gan & Thakker, 1997; Le Ferrec *et al.*, 2001):

- The tight junctions in the appropriately differentiated Caco-2 cell monolayers are more characteristic of those in the colon than in the small intestine, thus resulting in higher trans-epithelial resistance (TEER) than what normally is found across the small intestinal epithelium;
- Caco-2 cell monolayers are devoid of the mucin producing goblet cells, therefore they are devoid of the mucus layer that are found on the intestinal epithelium;
- The role of the physiological parameter such as intestinal mobility or transit time, in the absorption of drug molecule are not present with the use of Caco-2 cell monolayers;
- It is not always possible to relate the rates of transport across the Caco-2 cell to the extent of intestinal absorption;
- It is a static permeation screening model;
- The cells have a tumoral origin;
- It is a model providing only one cell type;
- The influence of P-gp may be difficult to estimate.

Despite the limitations of the Caco-2 cells, they are still established as an excellent model to study the transport of drugs across the GI barrier, provided these limitations are taken into account when the results are interpreted (Gan & Thakker, 1997).

1.7 Conclusion

It is well known that pharmaceutical solids can exist in different forms such as polymorphs, hydrates, solvates, co-crystals, salts and amorphous forms. Polymorphs have different crystal structures with the same chemical composition of the crystals (Cui, 2007). Hydrates and solvates are formed when water or organic solvents are trapped within the crystalline structure, respectively (Aulton & Taylor, 2013). Co-crystals contains two different molecules that is made from reactants. Amorphous forms are non-crystalline with only short range molecular order (Cui, 2007).

The arrangement of molecules in a crystal determines its physico-chemical properties and affects the drugs' performance (Datta & Grant, 2004). These effects include, physical and chemical stability, solubility, dissolution rates and in some cases bioavailability (Rodríguez-Spong *et al.*, 2004). Interactions with water can induce phase transitions that can lead to changes in the pharmaceutical and biopharmaceutical performance of the drug. The bioavailability of the drug can change as a result of polymorphic inter-conversions, alteration of crystallinity or formation of hydrates (Sandler *et al.*, 2005).

The biopharmaceutics classification system is a framework that classifies a drug based on its aqueous solubility and membrane permeability (Blume & Schug, 1999). Caco-2 cells are derived from human colon adenocarcinoma. Caco-2 cells, in culture, grow to form a polarised monolayer with tight junctions with an apical brush border that differentiate on a semi-permeable membrane and displays similar morphological and functional characteristics as intestinal enterocytes (Alqahtani *et al.*, 2013; Le Ferrec *et al.*, 2001; Sarmento *et al.*, 2012). For any given drug to be pharmacologically effective, it is important that it will reach the preferred target site at a specified concentration. This requires the critical step of sufficient intestinal epithelial permeability. The relationship between the physico-chemical properties of molecules and their ability to cross the gastro-intestinal (GI) epithelium is rather complex (Gan & Thakker, 1996). Each transport mechanism depends on certain physico-chemical properties of absorbed molecules, such as partition coefficient, molecular weight, molecular volume, pKa, solubility, chemical stability, and charge distribution (Le Ferrec *et al.*, 2001). In the following chapter an in depth literature discussion will be provided on baclofen as this is the drug that will be used during this study.

References

- Aguilera, J., del Valle, J. & Karel, M. 1995. Caking phenomena in amorphous food powders. *Trends in food science & technology*, 6(5):149-155.
- Ahlqvist, M.U.A. & Taylor, L.S. 2002. Water dynamics in channel hydrates investigated using H/D exchange. *International journal of pharmaceuticals*, 241:253-261.
- Alqahtani, S., Mohamed, L.A. & Kaddoumi, A. 2013. Experimental models for predicting drug absorption and metabolism. *Expert opinion on drug metabolism and toxicology*, 9(10):1-14.
- Artursson, P., Palm, K. & Luthman, K. 2001. Caco-2 monolayers in experimental and theoretical predictions of drug transport. *Advanced drug delivery reviews*, 46:27-43.
- Aucamp, M.E. 2015a. Solid-state chemistry of drugs, *Lecture notes*.
- Aucamp, M.E., Liebenberg, W. & Stieger, N. 2015b. Solvent-interactive transformations of pharmaceutical compounds. (In Mastai, Y. ed. Crystallization. InTech:Rijeka. p. 2-26.).
- Aulton, M.E. & Taylor, K.M.G. 2013. Aulton's pharmaceuticals: the design and manufacture of medicines, 4th Edition. Spain: Harcourt Publishers Limited.
- Babu, N.J. & Nangia, A. 2011. Solubility advantage of amorphous drugs and pharmaceutical cocrystals. *Crystal growth & design*, 11:2662–2679.
- Balimane, P.V., Chong, S. & Morrison, R.A. 2000. Current methodologies used for evaluation of intestinal permeability and absorption. *Journal of pharmacological and toxicological methods*, 44:301-312.
- Bjarnason, I., Macpherson, A. & Hollander, D. 1995. Intestinal Permeability: An Overview. *Gastroenterology*, 108(5)1566-1581.
- Blume, H.H. & Schug, B.S. 1999. The biopharmaceutics classification system (BCS): Class III drugs-better candidates for BA/BE waiver BP see British Pharmacopoeia. *European journal of pharmaceuticals*, 9:117-121.
- Brittain, H. 1999. Polymorphism in pharmaceutical solids. New York: M. Dekker.
- Brough, C. & Williams, R.O. 2013. Amorphous solids dispersions and nano-crystal technology for poorly water-soluble drug delivery. *International journal of pharmaceuticals*, 453:157-166.
- Burnett, D.J., Thielmann, F. & Booth, J. 1999. Determining the critical relative humidity for moisture-induced phase transitions. *International journal of pharmaceuticals*, 287:123-133.

- Cardew, P.T. & Davey, R.J. 1985. The kinetics of solvent-mediated phase transformations. *Proceedings of the royal society*, 398:415-428.
- Censi, R. & Di Martino, P. 2015. Polymorph impact on the bioavailability and stability of poorly soluble drugs. *Molecules*, 20(10):18759-18776.
- Chavda, H.V., Patel, C.N. & Anand, I.S. 2010. Biopharmaceutics classification system. *Systematic reviews in pharmacy*, 1(1):62-69.
- Craig, D.Q.M., Royall, P.G., Kett, V.L. & Hopton, M.L. 1998. The relevance of the amorphous state to pharmaceutical dosage forms: glassy drugs and freeze dried systems. *International journal of pharmaceutics*, 179:179-207.
- Cui, Y. 2007. A material science perspective of pharmaceutical solids. *International journal of pharmaceutics*, 339(1-2):3-18.
- Datta, S. & Grant, D. 2004. Crystal structures of drugs: advances in determination, prediction and engineering. *Nature reviews drug discovery*, 3(1):42-57.
- Elder, D.P., Holm, R. & de Diego, H.L. 2012. Use of pharmaceutical salts and cocrystals to address the issue of poor solubility. *International journal of pharmaceutics*, 453:88-100.
- Gan, L.L. & Thakker, D.R. 1997. Applications of the Caco-2 model in the design and development of orally active drugs: elucidation of biochemical and physical barriers posed by the intestinal epithelium. *Advanced drug delivery reviews*, 23:77-98.
- Govindarajan, R. & Suryanarayanan, R. 2006. Processing-induced phase transformation and their implication on pharmaceutical product quality. (In Hilfiker, R. *ed.* Polymorphism in the pharmaceutical industry. Weinheim, Germany: Wiley. p.333-364).
- Graeser, K., Strachan, C., Patterson, J., Gordon, K. & Rades, T. 2008. Physicochemical Properties and Stability of Two Differently Prepared Amorphous Forms of Simvastatin. *Crystal growth & design*, 8(1):128-135.
- Grant, D.J.W. & Lohani, S. 2006. Thermodynamics of polymorphs. (In Hilfiker, R. *ed.* Polymorphism in the pharmaceutical industry. Weinheim, Germany: Wiley. p. 21-42).
- Greco, K. & Bogner, R. 2012. Solution-mediated phase transformation: significance during dissolution and implications for bioavailability. *Journal of pharmaceutical sciences*, 101(9):2996-3018.

- Griesser, U.J. 2006. The importance of solvates. (In Hilfiker, R. *ed.* Polymorphism in the pharmaceutical industry. Weinheim, Germany: Wiley. p. 211-234).
- Gu, C., Young, V. & Grant, D.J.W. 2001. Polymorph screening: influence of solvents on the rate of solvent-mediated polymorphic transformation. *Journal of pharmaceutical sciences*, 90(11): 1878-1890.
- Guerrieri, P., Rumondor, A., Li, T. & Taylor, L. 2010. Analysis of Relationships Between Solid-State Properties, Counterion, and Developability of Pharmaceutical Salts. *AAPS PharmSciTech*, 11(3):1212-1222.
- Hamman, J.H. 2007. Drug development (Oral drug delivery. Tshwane University of Technology. p. 3-50).
- Hancock, B.C. & Zografi, G. 1996. Characteristics and significance of the amorphous state in pharmaceutical systems. *Journal of pharmaceutical sciences*, 86(1):1-12.
- Hidalgo, I.J., Raub, T.J. & Borchardt R.T. 1989. Characterization of the human colon carcinoma cell line (Caco-2) as a model system for intestinal epithelial permeability. *Gastroenterology*, 96(3):736-749.
- Huang, L. & Tong, W. 2003. Impact of solid state properties on developability assessment of drug candidates. *Advanced drug delivery review*, 56:321-334.
- Kawabata, Y., Wada, K., Nakatani, M., Yamada, S. & Onoue, S. 2011. Formulation design for poorly water-soluble drugs based on biopharmaceutics classification system: Basic approaches and practical applications. *International journal of pharmaceuticals*, 420:1-10.
- Khankari, R.K. & Grant, D.J.W. 1994. Pharmaceutical hydrates. *Thermochimica acta*, 248:61-79.
- Le Ferrec, E., Chesne, C., Artusson, P., Brayden, D., Fabre, G., Gires, P., Guillou, F., Rousset, M., Rubas W. & Scarino, M. 2001. In vitro models of the intestinal barrier. *Alternatives to laboratory animals*, 29:649-668.
- Lennernäs, H., Abrahamsson, B., Persson, E.M. & Knutson, L. 2007. Oral drug absorption and the biopharmaceutics classification system. *Journal of drug delivery science and technology*, 17(4):237-244.
- Lipinski, C.A., Lombardo, F., Dominy, B.W. & Feeney, P.J. 1996. Experimental and computational approaches to estimate solubility and permeability in drug discovery and development settings. *Advanced drug delivery reviews*, 46:3-26.

- Morissette, S. 2004. High-throughput crystallization: polymorphs, salts, co-crystals and solvates of pharmaceutical solids. *Advanced drug delivery reviews*, 56(3):275-300.
- Morris, K.R., Griesser, U.J., Eckhardt, C.J. & Stowell, J.G. 2001. Theoretical approaches to a physical transformation of active pharmaceutical ingredients during manufacturing processes. *Advanced drug delivery reviews*, 48:91-114.
- Müller, C.E. 2009. Prodrug approaches for enhancing the bioavailability of drugs with low solubility. *Chemistry & biodiversity* 6:2071-2083.
- Murphy, D., Rodríguez-Cintrón, F., Langevin, B., Kelly, R.C. & Rodríguez-Hornedo, N. 2002. Solution-mediated phase transformation of anhydrous to dihydrate carbamazepine and the effect of lattice disorder. *International journal of pharmaceutics*, 24:121-134.
- Nožinić, D., Milić, A., Mikac, L., Ralić, J., Padovan, J. & Antolović, R. 2010. Assessment of macrolide transport using PAMPA, Caco-2 and MDCKII-hMDR1 assays. *Croatica chemica acta*, 83(3):323-331.
- Patel, J., Jagia, M., Bansal, A. & Patel, S. 2015. Characterization and thermodynamic relationship of three polymorphs of a xanthine oxidase inhibitor, Febuxostat. *Journal of pharmaceutical sciences*, 104(11):3722-3730.
- Paterson, A., Brooks, G., Bronlund, J. & Foster, K. 2005. Development of stickiness in amorphous lactose at constant T–T_g levels. *International dairy journal*, 15(5):513-519.
- Qiao, N., Li, M., Schlindwein, W., Malek, N., Davies, A. & Trappitt, G. 2011. Pharmaceutical cocrystals: An overview. *International journal of pharmaceutics*, 419:1-11.
- Reddy, B.B.K. & Karunakar, A. 2011. Biopharmaceutics classification system: A regulatory approach. *Dissolution technologies*, 18(1):31-37.
- Rodríguez-Hornedo, N. & Murphy, D. 1999. Significance of controlling crystallization mechanisms and kinetics in pharmaceutical systems. *Journal of pharmaceutical sciences*, 88(7):651-660.
- Rodríguez-Spong, B., Price, C.P., Jayasankar, A., Matzger, A.J. & Rodríguez-Hornedo, N. 2004. Principals of pharmaceutical solid polymorphism: a supramolecular perspective. *Advanced drug delivery reviews*, 56(3):241-247.
- Sarmah, K.K., Sarma, A., Roy, K., Rao, D.R. & Thakuria, R. 2016. Olanzapine salt and diversity in molecular packing. *Crystal growth & design*, 16(2):1047-1055.

- Sarmiento, B., Andrade, F., da Silva, S.B., Rodrigues, F., das Neves, J. & Ferreira, D. 2012. Cell-based in vitro models for predicting drug permeability. *Expert opinion on drug metabolism and toxicology*, 8(5):607-621.
- Savjani, J.K. 2015. Co-crystallization: An approach to improve the performance characteristics of active pharmaceutical ingredients. *Asian journal of pharmaceuticals*, 9(3):147-151.
- Schultheiss, N. & Newman, A. 2009. Pharmaceutical Cocrystals and Their Physicochemical Properties. *Crystal growth & design*, 9(6):2950-2967.
- Sinai Kunde, S.D., Bhilegaonkar, S., Godbole, A.M. & Gajre, P. 2015. Biopharmaceutical Classification System: A Brief Account. *International journal of research methodology*, 1(1):21-46.
- Singhal, D. & Curatolo, W. 2004. Drug polymorphism and dosage form design: a practical perspective. *Advanced drug delivery reviews*, 56(3):335-347.
- Thakuria, R., Delori, A., Jones, W., Lipert, M.P., Roy, L. & Rodríguez-Hornedo, N. 2013. Pharmaceutical cocrystals and poorly soluble drugs. *International journal of pharmaceuticals*, 453:101-125.
- Tilborg, A., Norberg, B. & Wouters, J. 2014. Pharmaceutical salts and cocrystals involving amino acids: A brief structural overview of the state-of-art. *European journal of medicinal chemistry*, 74:411-426.
- Varma, M.V.V., Khandavilli, S., Ashokraj, Y., Jain, A., Dhanikula, A., Sood, A., Thomas, N.S., Pillai, O., Sharma, P., Gandhi, R., Agrawal, S., Nair, V. & Panchagnula, R. 2004. Biopharmaceutic classification system: A scientific framework for pharmacokinetic optimization in drug research. *Current drug metabolism*, 5:375-388.
- Vippagunta, S.R., Brittan, H.G. & Grant, D.J.W. 2001. Crystalline solids. *Advanced drug delivery reviews*, 48(1):3-26.
- Witschi, C. & Doelker, E. 1997. Residual solvents in pharmaceutical products: acceptable limits, influences on physicochemical properties, analytical methods and documented values. *European journal of pharmaceuticals and biopharmaceutics*, 43(3):215-242.
- Ymén, I. 2011. Introduction to the solid state-physical properties and processes. (In Storey, R.A. & Ymén, I. ed. Solid state characterization of pharmaceuticals. West Sussex, United Kingdom: Wiley. p. 1-34).

Yu, L. 2001. Amorphous pharmaceutical solids: preparation, characterization, and stabilization. *Advanced drug delivery reviews*, 48(1):27-42.

Zhang, G., Law, D., Schmitt, E.A. & Qiu, Y. 2004. Phase transformation considerations during process development and manufacture of solid oral dosage forms. *Advanced drug delivery reviews*, 56(3):371-390.

CHAPTER 2

BACLOFEN

2.1 Introduction

Baclofen is a central acting muscle relaxant that acts as an agonist of the inhibitory neurotransmitter gamma-aminobutyric acid (GABA), specifically on the metabotropic GABA_B receptors. Currently, baclofen is the drug of choice for the alleviation of long-term spasticity in patients with multiple sclerosis and is especially prescribed for the relief of flexor spasms and subsequent pain, clonus, and muscular rigidity. There is also some evidence that baclofen can be of value in patients suffering from diseases which affect the spinal cord or patients presenting with spinal cord injuries (Abdelkader *et al.*, 2007; Bahri *et al.*, 2007; Dario *et al.*, 2006; Gande & Rao, 2011; Kochak *et al.*, 1985). Recently, the pharmaceutical industry became more interested in supplying generic baclofen formulations. The lack of reliable solubility and bioavailability data on this drug significantly complicates bio-waiver applications by industry. As mentioned in the aims and objectives section, this study is aimed at investigating the physico-chemical properties of this GABA-agonist, to provide sound solubility data and to establish an accurate BCS (biopharmaceutics classification system) characterisation. The main goal of this study is, therefore, to assist the pharmaceutical knowledge base and industry in terms of reporting the information that is necessary for successful bio-waiver applications on baclofen. This chapter will mainly focus on the physico-chemical properties reported in the literature for this centrally acting drug.

2.2 Synthesis of baclofen

Baclofen was first synthesised in 1962 (Felluga *et al.*, 2005) and since then there are several reports in literature regarding the total synthesis of baclofen (Coelho *et al.*, 1997; Tehrani *et al.*, 2003). Although the literature reports different synthesis strategies for baclofen, none of them mention whether the product is the anhydrate or the monohydrate form.

A synthesis process reported by Coelho *et al.* (1997) shows a cyclo-addition between the dichloroketene as illustrated in Figure 2.1. The addition of the cyclo-adduct (2) is the only detectable regiosomer between the *in situ* generated dichloroketene and the commercial 4-chlorostyrene (1) with a yield of 82%. Reductive dichlorination (2) in acid/Zn dust provides the cyclobutanone derivate (3) with a yield of 92%. Preparation of the baclofen lactam (4) was accomplished by extending the cyclobutanone ring *via* a Beckmann re-arrangement, using a nitrogen source N-hydroxylamine-O-sulponic acid, with a yield of 43%. The acid hydrolysis of the lactam (4) furnished baclofen (5) as a white solid with a yield of 70%.

In conclusion, this reaction sequence provides a cost-effective, commercial starting material with an overall yield of 22%. As several substituted styrenes are commercially available or could be easily prepared, this approach should provide a convenient method of synthesis of baclofen.

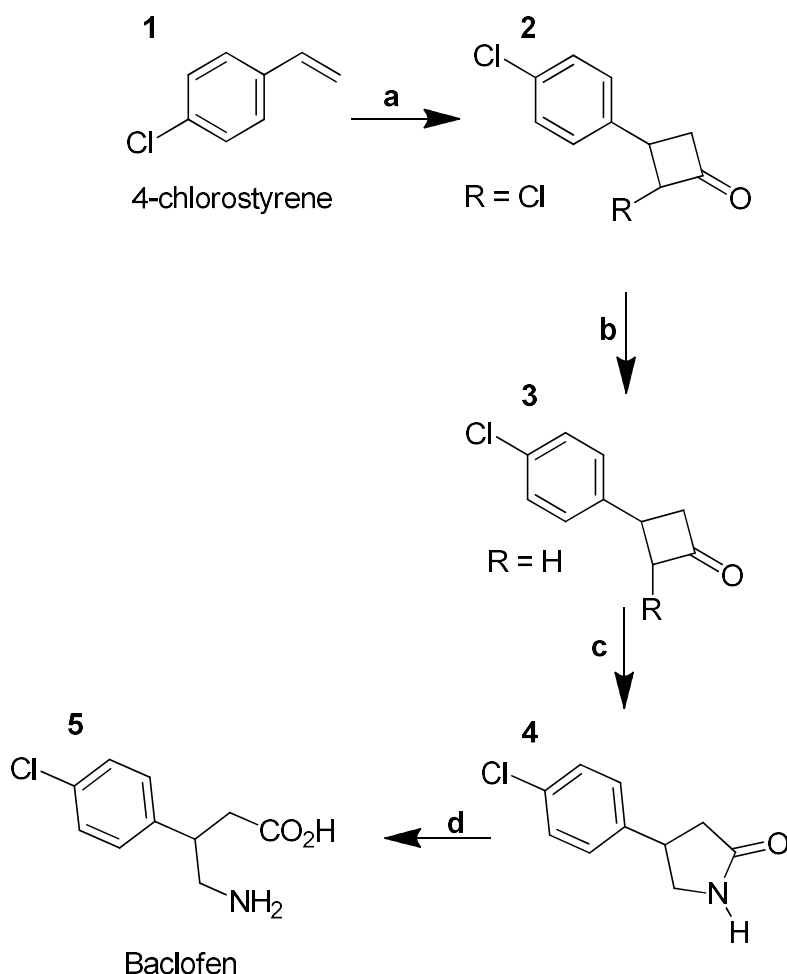


Figure 2.1: Synthesis of baclofen. Reagents and conditions: a) Cl_3CCOCl , Zn-Cu, PoCl_3 , ether, reflux, 20 h, 82%; b) Zn/ $\text{CH}_3\text{CO}_2\text{H}$, 70°C , 14 h, 93%; c) $\text{H}_2\text{NOS}_3\text{H}$, HCO_2H 98%, reflux, 10 h, 43%; d) HCl, reflux, 12 h, 70% (Coelho *et al.*, 1997).

An alternative approach for the synthesis of baclofen is a strategy that consists of the following three general steps: 1) aldol condensation, 2) Michael addition and 3) reduction and decarboxylation (Figure 2.2). The preparation of the β -nitrostyrenes required mainly two different conditions: firstly, a medium with a weak base and a high temperature such as ammonium acetate in boiling acetic acid (this condition however did not provide a good enough purity of the styrene) and secondly, a medium with a strong base and a low temperature such as sodium hydroxide in cold methanol (this condition resulted in a good enough purity and yield) (Tehrani *et al.*, 2003).

The reaction of the malonate diethyl ester with the β -nitrostyrene will need a strong base such as sodium alkoxide to make the malonate an active nucleophile that undergoes a Michael addition reaction. There are several methods that can be considered for the reduction of the nitro group

to take place, which includes H₂ (gas) with Raney nickel, HCl with Zn, Fe or Sn powder. In the case where Raney nickel is used, it is necessary to ensure the medium is acidic to prevent lactam from forming. The acidic medium will also help with the hydrolysis and decarboxylation steps (in a reflux condition). Hydrolysis of the amine compound may also be performed in a basic medium. To obtain the final baclofen raw material, there has to be a pH adjustment of the amino acid (Tehrani *et al.*, 2003).

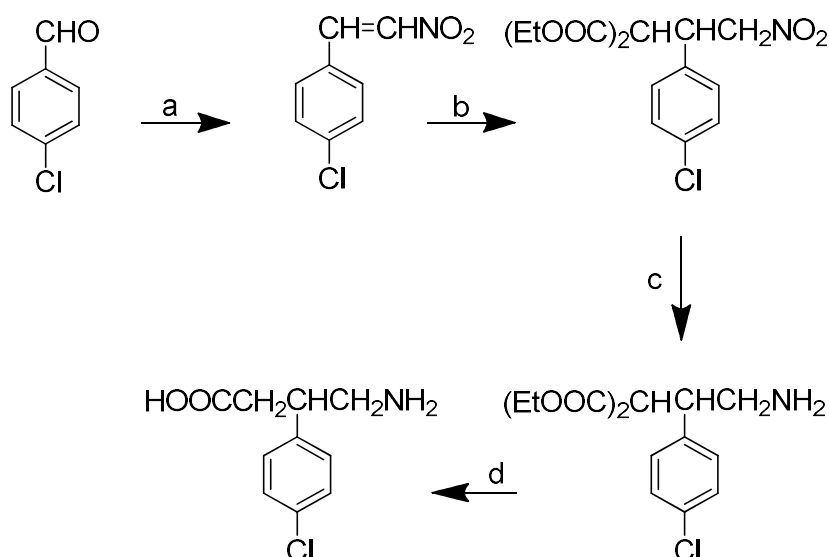


Figure 2.2: Synthesis of baclofen. Reaction conditions: a) CH₃NO₂, NaOH, CH₃OH, 0°C; b) diethyl malonate, ethanol, NaOEt, 8-10°C; c) H₂, Raney nickel, CH₃OH, room temperature; d) OH⁻, reflux then H₃O⁺ or H₃O⁺, reflux then OH⁻ (Tehrani *et al.*, 2003).

2.3 Enantiomers of baclofen

Metabolic processes are mediated through biological systems that are sensitive to stereochemistry of substrates and precise molecular recognition of enzymes, receptors and other natural binding sites occur within the biological systems. Enantiomers can interact in different ways causing different pharmacological and/or toxicological profiles in the biological system (Hefnawy & Aboul-Enein, 2003; Rat'ko & Stefan-van Staden, 2004).

In the case of drugs with a single stereogenic centre, both enantiomers can be pharmacologically active. In some cases, only one of the enantiomers is capable of causing the main pharmacological effect. Several possibilities exist for the other enantiomer such as inactivity, a qualitatively different effect, an antagonistic effect or even severe toxicity (Hefnawy & Aboul-Enein, 2003; Rat'ko & Stefan-van Staden, 2004).

The baclofen molecule contains a chiral centre and is marketed as a racemic mixture that consists of equal amounts of R- and S-enantiomers (Desiderio *et al.*, 2008; Hefnawy & Aboul-Enein, 2003; Rat'ko & Stefan-van Staden, 2004; Sanchez-Ponce *et al.*, 2012). The enantiomers of baclofen

(Figure 2.3) possess of different properties (Hefnawy & Aboul-Enein, 2003; Zhu & Neirinck, 2003). The configuration of the (R)-(-)- enantiomer is stereospecifically active at the GABA_B-receptors, while the (S)-(+)-enantiomer is virtually inactive (Desiderio *et al.*, 2008; Hefnawy & Aboul-Enein, 2003; Kerr *et al.*, 1995). The R(-)-enantiomer can be up to 100-times more active than the S-(+)-enantiomer and the S-(+)-enantiomer interferes with the binding of the R(-)-enantiomer to the receptor (Bhushan & Kumar, 2008 Desiderio *et al.*, 2008; Hefnawy & Aboul-Enein, 2003; Rat'ko & Stefan-van Staden, 2004; Zhu & Neirinck, 2003).

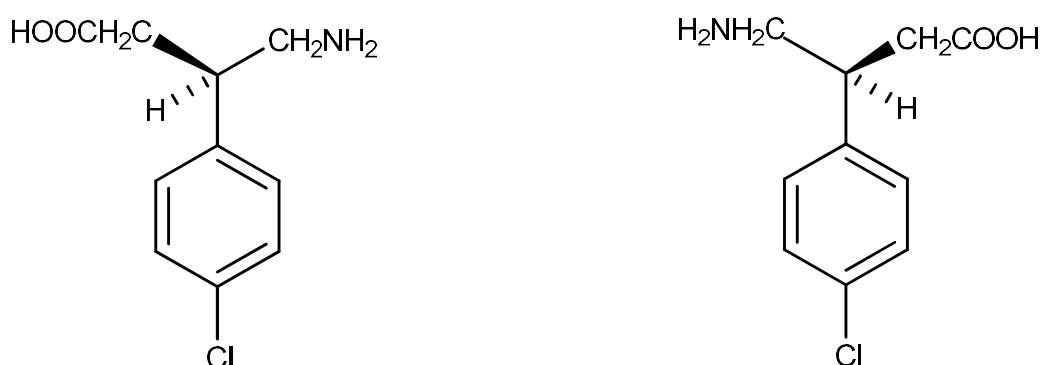


Figure 2.3: Enantiomers of baclofen (Right: R-isomer; Left: S-isomer) (Smith, 1984).

Considering the abovementioned and from a pharmaceutical quality control perspective, it will be critical for the industry to know which baclofen enantiomer is included into a manufactured baclofen containing product since this can greatly affect the treatment success of patients.

2.4 Indications and pharmacological properties of baclofen

GABA is an inhibitory neurotransmitter that is related to the control of the neuronal activity in the central nervous system and the regulation of several physiological mechanisms. It has been shown to act through at least two different receptor sites, GABA_A and GABA_B receptors, with different binding properties (Chênevert & Desjardins, 1994).

Baclofen is a chemical analog of GABA, but unlike GABA, baclofen can cross the blood-brain barrier selectively stimulating the GABA_B receptor that is located on the presynaptic nerve terminals (Bahri *et al.*, 2007; Chênevert & Desjardins, 1994; Hosseinimehr *et al.*, 2010). This effect is due to the balance between the inhibition of neurotransmitter release (mediated by presynaptic GABA_B receptors) and the inhibition of neuronal excitability (mediated by postsynaptic GABA_A receptors) (Bahri *et al.*, 2007; Dario *et al.*, 2006).

Activation of the GABA_B receptors reacts with G_i to inhibit adenylyl cyclase that results in increased K⁺ conductance, reducing the calcium influx and the release of excitatory transmitters in the brain as well as the spinal cord (Figure 2.4) (Brunton *et al.*, 2011; Katzung *et al.*, 2012; Misgeld *et al.*, 1995).

Baclofen administered orally, has been studied in several other medical conditions that include intractable back pain, reducing cravings in recovering alcoholics and prophylaxis of migraine headaches in some patients (Katzung *et al.*, 2012). Baclofen may also be successful in treating the symptoms that are associated with gastro-esophageal reflux disease (GERD) of non-acidic stomach content through a transient lower esophageal sphincter relaxation (TLESR) inhibiting mechanism (Thakar *et al.*, 2012).

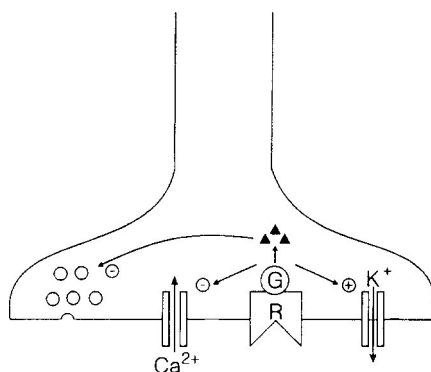


Figure 2.4: Site of action for the pre-synaptic GABA_B receptors. Pre-synaptic GABA_B receptors (R) can activate (+) a K⁺ current and/or reduce (-) a Ca²⁺ current in a membrane-delimited pathway with G-protein requirement and/or through second messengers (▲). In addition, GABA receptor activation may reduce release independently from an activation of K⁺ conductance or reduction of Ca²⁺ conductance (Misgeld *et al.*, 1995).

2.5 The physico-chemical properties of baclofen

Baclofen is a white to off-white, odourless or practically odourless crystalline powder with a melting point between 190°C and 207°C. It has a molecular weight of 213.66 g/mol, calculated on the anhydrous base and a pK_{a1} of 3.8 ± 0.1 and pK_{a2} of 9.62 ± 0.1 at 20°C (Jakaria *et al.*, 2014; Moffat *et al.*, 2011; Rustum, 1989; Sznitowska *et al.*, 1996; Tarannum & Singh, 2012; Trissel & Zhang, 2013; USP, 2017). However, Godwin *et al.* (2001) reported the pK_{a1} as 5.4 and pK_{a2} as 9.5.

Some literature sources mention the solubility characteristics of baclofen, however; it does not provide sufficient solubility information of baclofen in organic solvents typically used within the pharmaceutical industry (BP, 2016; Moffat *et al.*, 2011; USP, 2016). The reports on the water solubility of baclofen are contradictory. Baclofen is reported to be soluble in water (Abdelkader *et al.*, 2008; Faisal *et al.*, 2013; Jakaria *et al.*, 2014), whilst other sources report it as slightly soluble in water (USP, 2017; Trissel & Zhang, 2013; Moffat *et al.*, 2011; Godwin *et al.*, 2001) and others report it to be difficult to obtain stable solutions in water of concentrations greater than approximately 2 mg/ml. Furthermore, it has been reported that concentrations that are higher than 2 mg/ml can lead to powder that may not dissolve completely or it can lead to an

unacceptable tendency to precipitate during storage (Trissel & Zhang, 2013). In addition, baclofen is very slightly soluble in methanol, insoluble in chloroform and poorly soluble in other organic solvents (Faisal *et al.*, 2013; USP 2017; Trissel & Zhang, 2013; Moffat, *et al.*, 2011). Other reports state that baclofen solubility shows pH dependence and dissolves freely in very high pH (0.1 N NaOH) and very low pH (0.1 N HCl) solutions, however, the solubility will drop rapidly as the pH increase or decreases to a more neutral pH (Abdelkader *et al.*, 2008; Faisal *et al.*, 2013; Trissel & Zhang, 2013; Ranpise *et al.*, 2013).

Chemically, baclofen is a zwitterionic molecule (Figure 2.5) that has ionisable groups namely amino and a carboxylic acid group. These groups can ionise and attain charge from +1 to 0 to - 1, depending on the pH of the baclofen solution (Hanafi *et al.*, 2011; Tarannum & Singh, 2012).

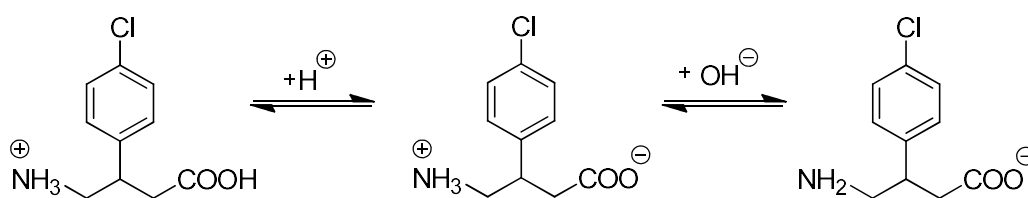


Figure 2.5: Zwitterionic properties of baclofen (adapted with permission from Sznitowska *et al.*, 1996).

Baclofen can exist in at least two solid-state forms namely an anhydrate and a monohydrate; however, almost no information on the physico-chemical properties of these two solid-states is available and no mention is made on how the different hydration levels of baclofen might influence its solubility, stability, and bioavailability (Mirza *et al.*, 2007). In addition to this, some literature report that baclofen shows a low bioavailability of 40% due to a narrow absorption window in the upper gastro-intestinal tract (Gande & Roa, 2011; Jivani *et al.*, 2010; Ranpise *et al.*, 2013), while other literature reports a 70 to 80% bioavailability of baclofen (Bahri *et al.*, 2007; Thakar *et al.*, 2012). However, it is reported that baclofen has a low permeability (Hakkarainen *et al.*, 2012b) using Caco-2 cell monolayers (Hakkarainen *et al.*, 2010a). As a result of all the contradicting literature regarding the solubility and bioavailability of baclofen, a reliable classification of this drug in the BCS can't be made.

2.6 Dose and baclofen products

On the South African market, baclofen is available in a solid pharmaceutical dosage form (tablets) for oral administration (Rossiter, 2012), however, baclofen is available for oral administration as well as intrathecal administration on the global market (Ghasemian *et al.*, 2017). The initial dose starts at 5 – 10 mg daily, increased to 15 mg twice daily and can be increased to a maximum dosage of 100 – 200 mg daily if necessary (Brunton *et al.*, 2011; Katzung *et al.*, 2012). Oral

administration is the most popular route due to the ease of ingestion, pain avoidance and patient compliance (Faisal *et al.*, 2013).

Alternatively, baclofen can be delivered directly into the spinal cord using a surgically implanted pump and an intrathecal catheter (Brunton *et al.*, 2011). Intrathecal administration can be used to control severe spasticity and muscle pain that does not respond to other medication (Katzung *et al.*, 2012) or it can be used for severe spasticity of spinal or cerebral origin (Lagarce *et al.*, 2005b). Long-term intrathecal baclofen therapy can improve the quality of life for patients with severe spastic disorders (Katzung *et al.*, 2012). Despite the advantages of this route, there are risks of surgery itself, spinal infection, catheter malfunctioning (often leading to discontinuation of therapy), several side effects and high expenses of implantation and follow-ups (Ghasemian *et al.*, 2017; Lagarce *et al.*, 2005a; Lagarce *et al.*, 2005b).

2.7 Conclusion

Baclofen is an agonist of GABA_B and the drug of choice for long-term treatment of spasticity. Despite the benefits as well as its potential uses, one of the biggest disadvantages is an unreliable BCS classification. If the BCS classification of baclofen could be precisely determined, it will determine if it is eligible for a biowaiver (e.g. BCS class I drug). The physico-chemical properties of baclofen reported in literature are contradictory, especially regarding the solubility and bioavailability. Furthermore, to date, there are limited studies available regarding the different physico-chemical properties of the anhydrate and monohydrate solid-state forms in which it is claimed baclofen can exist. This study will aim to look into the physico-chemical characterisation of baclofen and in the process, clarify the current discrepancies that exist in terms of reported solubility and bioavailability thereof.

References

- Abdelkader, H., Abdalla, O.Y. & Salem, H. 2007. Formulation of Controlled-Release Baclofen Matrix Tablets: Influence of Some Hydrophilic Polymers on the Release Rate and In Vitro Evaluation. *AAPS PharmSciTech*, 8(4):1-11.
- Bahri, L.E., Ghorbel, A. & Hassine T.B. 2007. Baclofen. *Compendium-Pharm profile*, 629-631.
- Bhushan, R. & Kumar, V. 2008. Indirect resolution of baclofen enantiomers from pharmaceutical dosage form by reversed-phase liquid chromatography after derivatization with Marfey's reagent and its structural variants. *Biomedical chromatography*, 22(8):906-911.
- British Pharmacopoeia. 2017. <https://www-pharmacopoeia-com.nwulib.nwu.ac.za/bp-2017/general-notice/part-ii-1.html?published-date=2016-08-23&text=Solubility+range> 16 Date of access 17 May 2017.
- Brunton, L., Chabner, B. & Knollmann, B. 2011. *Goodman & Gilman's the pharmacological basis of therapeutics*. New York, NY: McGraw-Hill Medical.
- Chênevert, R. & Desjardins, M. 1994. Chemoenzymatic enantioselective synthesis of baclofen. *Canadian journal of chemistry*, 72:2312-2317.
- Coelho, F., de Azevedo, M.B.M., Boschiero, R. & Resende, P. 1997. A Simple and Efficient New Approach to the Total Synthesis of (±)-4-Amino-3-(4-Chlorophenyl)-Butyric Acid (BACLOFEN). *Synthetic communications*, 27(14):2455-2465.
- Dario, A., Pisani, R., Sangiorgi, S., Soragna, A., Reguzzoni, M., Protasoni, M., Pessina, F., Fesce, R., Peres, A. & Tomei, G. 2006. Baclofen and potential therapeutic use: Studies of neuronal survival. *European journal of pharmacology*, 550(1-3):33-38.
- Desiderio, C., Rossetti, D., Perri, F., Giardina, B., Messana, I. & Castagnola, M. 2008. Enantiomeric separation of baclofen by capillary electrophoresis tandem mass spectrometry with sulfobutylether-β-cyclodextrin as chiral selector in partial filling mode. *Journal of chromatography B*, 875(1):280-287.
- Faisal, M., Vishal, G., Dinesh, S. & Dinesh, B. 2013. Formulation and optimization of mouth dissolving tablet of baclofen by direct compression method using two different superdisintegrants. *Journal of medical pharmaceutical and allied sciences*, 5:1-13.
- Felluga, F., Gombac, V., Pitacco, G. & Valentin, E. 2005. A short and convenient chemoenzymatic synthesis of both enantiomers of 3-phenylGABA and 3-(4-chlorophenyl)GABA (Baclofen). *Tetrahedron: Asymmetry*, 16(7):1341-1345.

Gande, S. & Rao, Y.M. 2011. Sustained-release effervescent floating matrix tablets of baclofen: development, optimization and in vitro-in vivo evaluation in healthy human volunteers. *DARU*, 202-209.

Ghasemian, E., Vatanara, A., Navidi, N. & Rouini, M. 2017. Brain delivery of baclofen as a hydrophilic drug by nanolipid carriers: Characteristics and pharmacokinetics evaluation. *Journal of drug delivery science and technology*, 37:67-73.

Godwin, D.A. Kim, N. & Zungia, R. 2001. Stability of a baclofen and clonidine hydrochloride admixture for intrathecal administration. *Hospital pharmacy*, 36(9):950-954.

Hakkarainen, J., Jalkanen, A., Kääriäinen, T., Keski-Rahkonen, P., Venäläinen, T., Hokkanen, J., Mönkkönen, J., Suhonen, M. & Forsberg, M. 2010a. Comparison of *in vitro* cell models in predicting *in vivo* brain entry of drugs. *International journal of pharmaceutics*, 402(1-2):27-36.

Hakkarainen, J., Pajander, J., Laitinen, R., Suhonen, M. & Forsberg, M. 2012b. Similar molecular descriptors determine the in vitro drug permeability in endothelial and epithelial cells. *International journal of pharmaceutics*, 436(1-2):426-443.

Hanafi, H., Mosad, S., Abouzid, K., Nieß, R. & Spahn-Langguth, H. 2011. Baclofen ester and carbamate prodrug candidates: A simultaneous chromatographic assay, resolution optimized with DryLab. *Journal of pharmaceutical and biomedical analysis*, 56:569-576.

Hefnawy, M.M.H. & Aboul-Enein, H.Y. 2003. Enantioselective high-performance liquid chromatographic method for the determination of baclofen in human plasma. *Talanta*, 61:667-673.

Hosseinimehr, S.J., Pourmorad, F., Moshtaghi, E. & Amini, M. 2010. Colorimetric determination of baclofen with ninhydrin reagent and compare with HPLC method in tablet. *Asian journal of chemistry*, 22(1):522-526.

Jakaria, M., Data, S.C., Hossain, S., Masum, A. & Fahad, A.B. 2014. Effect of acid, base and heat on different brands of baclofen available in Bangladesh. *International journal of pharmacology and pharmaceutical sciences*, 2(2):9-12.

Jivani, R.R., Patel, C.N., Patel, D.M. & Jivani, N.P. 2010. Development of a novel floating in-situ gelling system for stomach specific drug delivery of the narrow absorption window drug baclofen. *Iranian journal of pharmaceutical research*, 9(4):359-368.

Katzung, B.G., Masters, S.B. & Trevor, A.J. 2012. *Basic & clinical pharmacology*. New York: McGraw-Hill Medical.

- Kerr, D.I.B, Ong, J., Doolette, D.J. Schafer, K. & Prager, R.H. 1995. The (S)-enantiomer of 2-hydroxysaclofen is the active GABA_B receptor antagonist in central and peripheral preparations. *European journal of pharmacology*, 287:185-189.
- Kochak, G., Rakhit, A., Wagner, W., Honc, F., Waldes, L. & Kershaw, R. 1985. The pharmacokinetics of baclofen derived from intestinal infusion. *Clinical pharmacology and therapeutics*, 38(3):251-257.
- Lagarce, F., Faisant, N., Desfontis, J., Marescaux, L., Gautier, F., Richard, J., Menei, P. & Benoit, J. 2005a. Baclofen-loaded microspheres in gel suspensions for intrathecal drug delivery: In vitro and in vivo evaluation. *European journal of pharmaceutics and biopharmaceutics*, 61(3):171-180.
- Lagarce, F., Renaud, P., Faisant, N., Nicolas, G., Cailleux, A., Richard, J., Menei, P. & Benoit, J. 2005b. Baclofen-loaded microspheres: preparation and efficacy testing in a new rabbit model. *European journal of pharmaceutics and biopharmaceutics*, 59(3):449-459.
- Mirza, S., Miroshnyk, I., Rantanen, J., Aalonen, J., Harjula, P., Kiljunen, E., Heinämäki, J. & Yliruusi, J. 2007. Solid-state properties and relationship between anhydrate and monohydrate of baclofen. *Journal of pharmaceutical sciences*, 96(9):2399-2408.
- Misgeld, U., Bijak, M. & Jarolimek, W. 1995. A physiological role for GABA_B receptors and the effect of baclofen in the mammalian central nervous system. *Pergamon*, 46:423-462.
- Moffat, A., Osselton, M., Widdop, B. & Watts, J. 2011. *Clarke's analysis of drugs and poisons*. 14th ed. London: Pharmaceutical Press.
- Ranpise, N.S., Kolhe, S.R. & Ranade, A.N. 2013. Development and evaluation of bilayer gastroretentive floating drug delivery system for baclofen. *Indian journal of pharmaceutical education and research*, 47(1):41-46.
- Rat'ko, A. & Stefan-van Staden, R. 2004. Determination of baclofen enantiomers in pharmaceutical formulations using maltodextrin-based enantioselective, potentiometric membrane electrodes. *Il Farmaco*, 59(12):993-997.
- Rossiter, D. 2012. South African medicines formulary. 10th edition. Rondebosch, South Africa: Health and medical publication group.
- Rustum, A.M. 1989. Simple and rapid reversed-phase high performance liquid chromatography determination of baclofen in human plasma with ultra violet detection. *Journal of chromatography*, 487:107-115.

Sanchez-Ponce, R., Wang, L., Lu, W., von Hehn, J., Cherubini, M. & Rush, R. 2012. Metabolic and pharmacokinetic differentiation of STX209 and racemic baclofen in humans. *Metabolites*, 2:596-613.

Smith, D.F. 1984. Stereoselectivity of spinal neurotransmission: Effects of baclofen enantiomers on tail-flick reflex in rats. *Journal of neuronal transmission*, 60:63-67.

Sznitowska, M., Janicki, S. & Gos, T. 1996. The effect of sorption on percutaneous of a model zwitterion-baclofen. *International journal of pharmaceutics*, 137:125-132.

Tarannum, N. & Singh, M. 2012. Water-compatible surface imprinting of baclofen on silica surface for selective recognition and detection in aqueous solution. *Analytical methods*, 4(9):3019-3026.

Tehrani, M.H.H., Farnia, M. & Nazer, M.S. 2003. Synthesis of baclofen; an alternative approach. *Iranian journal of pharmaceutical research*, 1-3.

Thakar, K., Joshi, G. & Sawant, K.K. 2012. Bioavailability enhancement of baclofen by gastroretentive floating formulation: statistical optimization, in vitro and in vivo pharmacokinetic studies. *Drug development and industrial pharmacy*, 39(6):880-888.

Trissel, L.A. & Zhang, Y. 2013. High concentrations baclofen preparations. (Patent: US 8357379).

USP see United States Pharmacopoeia.

United States Pharmacopeia. 2017.
<http://www.uspnf.com/uspnf/pub/index?usp=39&nf=34&s=2&officialOn=December%201,%202016> Date of access: 10 May 2017.

Zhu, Z. & Neirinck, L. 2003. Chiral separation and determination of R-(2)- and S-(1)-baclofen in human plasma by high-performance liquid chromatography. *Journal of chromatography B*, 785:277–283.

CHAPTER 3

RESEARCH METHODOLOGY

3.1 Introduction

As already mentioned in Chapter 2, baclofen can exist in at least two solid-state forms namely an anhydrate and a monohydrate; however, almost no information is available on the physico-chemical properties of these two forms. During typical physico-chemical characterisation studies, it is important to make use of different and complimentary techniques. The different techniques used during this study focused on the preparation and characterisation of the anhydrate and monohydrate forms of baclofen as well as testing the permeability characteristics of baclofen.

3.2 Materials

Anhydrous baclofen (Batch number: 20160615) was purchased from DB Fine Chemicals (Johannesburg, South Africa). All organic solvents used during recrystallisation, equilibrium solubility studies and high-performance liquid chromatography (HPLC) analyses were obtained from either Associated Chemical Enterprise (ACE) (Johannesburg, South Africa) or Merck (Johannesburg, South Africa). All solvents were of either analytical or chromatography grade. Potassium dihydrogen orthophosphate, sodium citrate and hydrochloric acid, that was used to prepare bio-relevant solubility and/or dissolution media was obtained from ACE (Johannesburg, South Africa) and was of analytical grade.

For the *in vitro* membrane permeability studies, the materials purchased are listed in Table 3.1.

Table 3.1: Materials used during permeability studies

Material/reagent	Supplier
Caco-2 cell line	European Collection of Cell Cultures (ECACC) from Sigma Aldrich (Johannesburg, South Africa)
High-glucose Dulbecco's Modified Eagles Medium (DMEM)	Separations (Randburg, South Africa)
non-essential amino acids (NEAA)	Whitehead Scientific (Cape Town, South Africa)
foetal bovine serum	Merck (Modderfontein, South Africa)
penicillin/streptomycin	Separations (Randburg, South Africa)

Table 3.1 continued: Materials used during permeability studies

Material/reagent	Supplier
Amphotericin B (250 µg/ml)	The Scientific Group (Johannesburg, South Africa)
L-glutamine (2 mM)	Whitehead Scientific (Cape Town, South Africa)
Phosphate buffered saline solution (PBSS)	Sigma Aldrich (Johannesburg, South Africa)
Trypsin-versene (EDTA)	Whitehead Scientific (Cape Town, South Africa)
Transwell® 6-well membrane filters	Corning Costar® Corporation (Tewksbury, USA)
Trypan blue	Sigma Aldrich (Johannesburg, South Africa)
(2-[4-(2-hydroxyethyl)piperazin-1-yl]ethanesulfonic acid)	Scientific group, Biochrom (Randburg, South Africa)

3.3 Methods

3.3.1 Solid-state form screening of baclofen

This screening was done to identify if other solid-state forms of baclofen, not currently reported in the literature, can be prepared. During this objective of the study, possible metastable forms that could accidentally arise through exposure of a certain baclofen solid-state form to heat, moisture or solvent were also investigated. The techniques that were used included slow evaporation of organic solvents from baclofen solutions and quench cooling of the melt.

The slow evaporation entailed the preparation of a saturated solution of baclofen in various selected organic solvents including acetonitrile, butanol-1, butanol-2, ethanol, methanol, propanol-1, propanol-2, n-octanol and acetone. A sufficient quantity of baclofen was added to each organic solvent whilst stirring the solvent and heating it to the relevant solvent boiling point. Once a saturated solution was obtained, the solution was removed from the magnetic stirrer hot plate and subsequently covered with Parafilm® (Neenah, USA). The solution was left at ambient temperature for slow evaporation of the solvent to occur.

The quench cooling of the melt method involved spreading a thin layer of the purchased baclofen bulk material onto a sheet of tin foil. Subsequently, the sample was placed in a pre-heated conventional laboratory oven (Binder, Germany). The sample was heated until melting occurred, followed by removal of the sample from the oven and quenching it on a cold surface.

Subsequently, all the prepared solid-state forms were characterised in terms of physico-chemical and stability characteristics as outlined in the section below.

3.3.2 Physico-chemical characterisation

3.3.2.1 Differential scanning calorimetry (DSC)

Differential scanning calorimetry (DSC) measures the energy changes of a sample. It measures the amount of energy absorbed (endothermal event) or released (exothermal event) by a sample as the sample is heated or cooled continuously or when the sample is held at a constant temperature (isothermal). It also measures the temperatures where these changes take place (Lu & Rohani, 2009; Rodríguez-Spong *et al.*, 2004; Saunders & Gabbott, 2011). Thus, DSC detects any phenomenon where a change in energy is involved (Giron, 2002). The energy changes are related to the difference in heat flow between the reference and the compound under investigation (Rodríguez-Spong *et al.*, 2004).

Using the technique of DSC, samples can be submitted to a variety of temperature. This variety will allow characterisation of the substance at the temperature during manufacturing or it can be used to distinguish the peaks that overlap, that is observed by desolvation (Giron, 2002). DSC will provide data about the melting point, heat capacity, heat of fusion as well as polymorphic transitions of the sample (Lu & Rohani, 2009).

A Shimadzu (Kyoto, Japan) DSC-60 instrument was used to record the DSC thermograms of the different baclofen samples obtained from the solvent evaporation and quench cooling techniques. Samples weighing approximately 3 - 5 mg was accurately weighed and sealed in aluminium crimp cells. The samples were subsequently heated from 25°C to 250°C with a heating rate of 10°C/min and a nitrogen gas purge of 35 ml/min. In all instances, the onset temperatures of the thermal events were reported.

3.3.2.2 Thermogravimetric analysis (TGA)

Thermogravimetric analysis (TGA) is used to determine the loss of drying and information about simultaneous weight-change and heat-flow (Giron, 2002; Yu *et al.*, 1998). It provides quantitative evidence on the stoichiometry of solvates and hydrates (Zhang *et al.*, 2003). TGA is used since the mass change evaluation allows specific determinations (Giron, 2002). Method validation is done in terms of precision, accuracy, robustness, and limit of quantitation. TGA is efficient for validation of drying, milling and stability analyses (Giron, 2002).

A Perkin Elmer TGA 4000 (Waltham, USA) instrument was used for thermogravimetric analysis. This was used to determine the percentage weight loss (%) of the sample during heating.

Samples weighing 3 - 5 mg were accurately weighed into open ceramic crucibles and heated from 25°C to 250°C with a heating rate of 10°C/min and a nitrogen gas purge of 40 ml/min.

3.3.2.3 Thermal microscopy (TM)

Thermal microscopy (TM) is also known as thermo-microscopy or hot-stage microscopy (HSM). It is one of the most used methods to identify different polymorphs of a specific drug through visualising their crystal habits and determining their melting points as well as observing the physical appearance of the sample (Stieger *et al.*, 2012). Thermal microscopy is an analytical technique that combines the properties of microscopy and thermal analysis. This will enable characterization of the samples' physico-chemical properties as a function of temperature and time (Lu & Rohani, 2009; Stieger *et al.*, 2012).

Thermal microscopy will provide information on melting and recrystallisation behaviour of the sample through varying temperatures, while simultaneously viewing it through the microscope. During the process of heating and cooling, thermal microscopy can be used to study solid-state form transformations. It also offers detection of solvates or hydrates through the observation of the evolution of gas or liquid from a crystal. Thermal microscopy can further be used to obtain valuable data about solid-state characterisation, evaluation of crystal forms, hydrates and other physico-chemical properties (Lu & Rohani, 2009; Stieger *et al.*, 2012).

TM analyses were performed with a Nikon Eclipse E4000 microscope, fitted with a Nikon DS-Fi1 camera (Nikon, Japan Linkam THMS600 equipped with a T95 LinkPad temperature controller (Surrey, England). A heating rate of 10°C/min was used starting from 20°C up to 250°C and in some instances, a polarised filter was used to investigate amorphicity and identify crystalline nuclei in samples.

3.3.2.4 Scanning electron microscopy (SEM)

Scanning electron microscopy (SEM) can simulate a visual image with a magnification range that is big enough to study micro- and macro-structures of a surface of the sample. The interaction of the primary electron beam with the surface of the sample is associated with a flux of secondary and back-scattered electrons that form and are collected by the detectors. Secondary electrons will form near the area of impact of the primary electron beam. This will be used to produce images with a spatial resolution that is closely related to the cross-sectional area of the scanning beams of the electrons (Castle & Zhdan, 1997).

The samples were adhered to a small piece of carbon tape mounted onto a metal stub and coated with a gold-palladium film. Subsequently, the samples were placed into the FEI Quanta 200 ESEM & Oxford INCA 400 EDS system and photomicrographs were obtained for each sample.

3.3.2.5 Fourier-Transform infrared spectroscopy (FT-IR)

Fourier-Transform infrared spectroscopy (FT-IR) is a well-known method for the qualitative analysis of drugs. FT-IR is used to study molecular vibrations that provide a fingerprint of the specific solid (Rojek *et al.*, 2013; Yu *et al.*, 1998). The vibrations of the atoms can provide information of the structure and the molecular conformation. Spectroscopic differences will result in the identification of transmission bands that is useful for the quantitative analysis of polymorph mixtures (Lu & Rohani, 2009).

IR-spectra were recorded on a Shimadzu IR Prestige-21 spectrophotometer (Kyoto, Japan) over a range of 400 - 4000 cm^{-1} . Potassium bromide (KBr) was used as a background. The diffuse reflectance method was implemented and involves grinding the sample with KBr and measuring its IR spectrum in a reflectance cell.

3.3.2.6 X-ray powder diffraction (XRPD)

X-ray powder diffraction (XRPD) is one of the most reliable techniques for solid-state form differentiation and can be used for definite proof of existence and identification of different solid-state forms. XRPD can be used to determine the three-dimensional structure, captured in a two-dimensional plot, of micro- and macromolecules. It can produce an impression of a phase having numerous peaks that corresponds with a periodic spacing of atoms in the solid state, resulting in different lattice constants that will peak on different positions (Lu & Rohani, 2009, Rodríguez-Spong *et al.*, 2004; Yu *et al.*, 1998). XRPD provides structural information about crystals which includes unit cell parameters, density, crystal disorder, molecular conformation, molecular packing as well as hydrogen-bonding pattern (Yu *et al.*, 1998).

Samples were evenly distributed on a zero-background sample holder and then placed into the PANalytical Empyrean diffractometer (PANalytical, Almelo, Netherlands) for analysis. The measurement conditions were as follows: target, Cu; voltage, 40 kV; current, 40 mA; divergence slit, 2 mm; antiscatter slit, 0.6 mm; detector slit, 0.2 mm; monochromator; scanning speed, 2°/min (step size, 0.025°; step time, 1.0 sec).

3.3.2.7 Vapour sorption analysis

Vapour sorption is used to study the affinity of powders towards the water, this will reflect the interaction between the powder material and water by relating the humidity of air in equilibrium with the water content of the solid material at a constant temperature and pressure (Punčochová *et al.*, 2014). The degree of water absorption is determined by certain environmental factors that include temperature, vapour pressure, solid-state properties of the sample and the number of polar functional groups on the structure that are capable of forming hydrogen bonds with water (Crowley & Zografi, 2002).

Vapour sorption analysis studies were performed on baclofen using a VTI-SA from TA Instruments (Delaware, USA) with a nitrogen gas flow rate of 20 ml/min. The microbalance was calibrated and set to zero prior to weighing the sample in a platinum sample container. Approximately 25 - 100 mg of the powdered sample was carefully weighed into the sample container and care was taken to evenly distribute the sample. The percentage relative humidity (% RH) / temperature program was set using TA Instruments Isotherm software. The % RH ramp was set from 5 to 95% RH, followed by a decrease in % RH from 95 to 5%. The last absorption phase was also set to ramp from 5 to 95% RH. A drying phase with a weight loss criterion of not more than 0.01% weight loss in 2 minutes was set to run, prior to the % RH ramp program. The temperature was held at a constant 25°C throughout the % RH ramp. The program criteria was set to 0.0001% weight change or 2 minute stability of weight gained or lost before the program would continue to the next set parameter.

3.3.2.8 High-performance liquid chromatography (HPLC)

The mobile phase consisted of HPLC water and methanol mixed in a ratio of 55:45 % v/v. The mobile phase was filtered and degassed prior to use. A Phenomenex® Kinetex® C₁₈ (250 mm x 4.6 mm) column with particle size 2.6 µm and a detection wavelength of 220 nm were used. The flow rate was 1.0 ml/min. A Hitachi Chromaster chromatographic system was used for all HPLC analyses in this study. The system consisted of a 5410 UV detector, an auto-sampler (5260) with a sample temperature controller and a solvent delivery module (5160). Method verification was done in terms of repeatability, linearity, system suitability, limit of detection (LOD), limit of quantification (LOQ) and specificity (Moffat *et al.*, 2011), which are further elaborated on in Chapter 4.

3.3.2.9 Equilibrium solubility

Solubility is a crucial property of drugs that influence the bioavailability thereof (i.e. availability of the drug at the site of action). Drugs need to dissolve before they can be absorbed and pass through the gastro-intestinal (GI) epithelium to reach the site of action (Aulton & Taylor, 2013; Censi and Di Martino, 2015). For drugs to be absorbed from the GI epithelium, it requires certain physico-chemical and molecular properties.

The solubility studies were performed in a water bath consisting of a submerged axis rotating at approximately 50 rpm at 37°C ± 2°C. An excess of baclofen was added to test tubes and approximately 10 ml of the solvent was added into every tube to produce saturated or more ideally over-saturated solutions. The test tubes were sealed with Parafilm® (Neenah, USA) and a screw cap was tightly fitted onto every test tube to prevent leakage. Each test tube was placed on the rotating axis in the water bath and rotated for 24 h. In the 24 h period withdrawals of 3 test tubes at a time were made on 1, 2, 4, 8 and 24 h intervals. From each test tube, a sample was collected,

filtered through 0.45 μm PVDF filters and assayed using HPLC. Solubility studies of baclofen were performed within bio-relevant media (pH 1.2, pH 4.6, pH 6.8 and distilled water) as well as in typical organic solvents (acetone, 1-butanol, 2-butanol, chloroform, ethanol, methanol, octanol, 1-propanol and 2-propanol). Solubility studies were also performed on pH 1, pH 1.2, pH 1.4 and pH 1.6 to determine if the concentration is affected in small differences in a low pH. For each solubility study, a total of 15 samples were prepared. The remaining undissolved baclofen powder was sampled from at least one test tube at each mentioned time interval. The powder was placed on filter paper in order to absorb the excess solvent. These samples were analysed by means of DSC, XRPD, and FT-IR. This was done in order to investigate possible solid-state transformations during the solubility studies.

3.3.2.10 Powder dissolution studies

Dissolution describes the process where drug particles dissolve in a solvent. The dissolved drug molecules move through the dissolving fluid to the mucosa where the drug will be absorbed. Physico-chemical factors of the drugs can affect the drug dissolution in the gastro-intestinal tract (Aulton & Taylor, 2013).

A VanKel700 (Varian, USA) dissolution bath was used for dissolution testing. USP apparatus 2 (paddle) was set up at $37^{\circ}\text{C} \pm 2^{\circ}\text{C}$ with a rotational speed of 100 rpm, 900 ml dissolution medium was added to each dissolution vessel. All dissolution media used were prepared according to USP specifications (USP, 2016). A sufficient quantity of powder (determined from solubility results) was weighed into 10 ml test tubes, to which 50% of the powder weight, glass beads, $\leq 106 \mu\text{m}$ (Sigma-Aldrich, Johannesburg, South Africa) were added. To each test tube, 5 ml of dissolution medium pre-heated to $37^{\circ}\text{C} \pm 2^{\circ}\text{C}$ was added. The mixtures were agitated for a period of 120 s using a vortex mixer. The resulting mixtures were transferred to each dissolution vessel. An aliquot of the solution was withdrawn from each dissolution vessel at predetermined time intervals (5 min, 10 min, 15 min, 20 min, 40 min, 60 min, 120 min and 180 min). The volume (5 ml) of solution withdrawn was replaced by the same volume pre-heated dissolution medium. In the instances where solution-mediated phase transformation was investigated, the dissolution medium was not replaced after each withdrawal of 5 ml since a supersaturated solution is required to observe such transformations. After withdrawal, the samples were filtered through 0.45 μm PVDF filters into HPLC vials. The filtered solutions were analysed by the HPLC method described in paragraph 3.3.2.8.

3.3.2.11 Permeability

The use of Caco-2 cell monolayers for classifying the permeability of drug compounds are recommended by both the US FDA and European agency EMEA. The Caco-2 cell monolayers can be used as a correlation between drug permeability and the fraction of the drug that is

absorbed (Bock *et al.*, 2003). The Caco-2 cell monolayers have the ability to mimic the complexity of the drug absorption process (Sarmiento *et al.*, 2012).

The Caco-2 cells were cultured in high-glucose DMEM and were supplemented with 1% non-essential amino acids (NEAA), 10% foetal bovine serum, 1% penicillin/streptomycin, 1% amphotericin B (250 µg/ml) and 2 mM L-glutamine.

The Caco-2 cells were cultured at 37°C in 95% humidified air and 5% carbon dioxide in a Forma Steri-cycle CO₂ incubator. The cells were inspected by use of a light microscope (Nikon Eclipse TS100/TS100F, Nikon Instruments, Tokyo, Japan) to determine the percentage confluence. The growth medium was replaced every second day upon which it was decanted and was removed from the cell culture flask and then replaced with 10 ml of growth medium that was pre-warmed at 37°C through a pipettor and a serological pipette. This was done in a laminar flow hood equipped with HEPA filters, under sterile conditions.

The Caco-2 cells were sub-cultured, upon reaching 50% confluency (Natoli *et al.*, 2012) by means of trypsinisation. Phosphate buffered solution (PBS) and growth medium was pre-warmed in a circulating water bath to 37°C. The growth medium was decanted and removed from the cell culture flask and the cells were rinsed twice with 10 ml PBSS using serological pipettes and a pipettor. This was done in a laminar flow hood under sterile conditions. Trypsin-versene (EDTA) mixture (3 ml) was added to the cell culture flask and the mixture was evenly distributed on the cell layer. The cell culture flask was then placed in the CO₂ incubator at 37°C for 5 min. Cell detachment was determined by using a light microscope. Upon complete cell detachment, 6 ml of growth medium (pre-warmed at 37°C) was added to the content of the flask in order to inactivate the action of the trypsin mixture. The cell suspension was gently agitated with a pipette to ensure that all cells were rinsed from the bottom of the flask and divided evenly for transfer to new cell culture flasks. Cells were maintained in normal cell culture conditions prior to seeding.

The Caco-2 cells were seeded onto Transwell® 6-well membrane filters with a surface area of 4.67 cm² and a pore diameter of 0.4 µm. A cell suspension was obtained from the growth flasks by trypsinisation with Trypsin-versene as previously described. After cell detachment, 6 ml of growth medium (pre-warmed at 37°C) were added to the flask and the suspension agitated extensively through a pipette to ensure de-agglomeration and complete detachment, resulting in a suspension consisting of single cells. The cell suspension was transferred to a 50 ml tube. To ensure homogenous distribution of the cells throughout the suspension, a Pasteur pipette was used to agitate the suspension. Cells were counted employing a haemocytometer using Trypan blue as staining agent to monitor the percentage cell death. In a 2.5 ml Eppendorf tube, a volume of 15 µl PBSS, 10 µl cell suspension and 25 µl Trypan blue was mixed and incubated for 3 min, after which a volume of 10 µl of the mixture was placed on either side of the cover slip of the

haemocytometer. Cells were counted on five of the nine squares on the haemocytometer's grid on each side by means of a light microscope. The average number of cells was calculated (per square), which was then multiplied with the dilution factor (5×10^4). This would establish the total number of cells per ml in the cell suspension. The suspension was diluted to a concentration of approximately 20 000 cells per ml using equation 1

$$C1 \times V1 = C2 \times V2 \quad (3.1)$$

Where V1 represents the initial volume and V2 final volume and C1 represents the initial concentration and C2 final concentration. Cell seeding onto Transwell® filter membranes occurred in a laminar flow hood under sterile conditions by pipetting 2.5 ml of the final cell suspension into each apical chamber of the membrane filter plate wells. The Caco-2 cells were grown for 21 to 24 days on the membrane filters to produce intact epithelial cell monolayers. The growth medium was replaced every second day under sterile conditions.

Prior to the transport studies, the TEER of each cell monolayer was measured using a Millicell ERS II meter (Millipore, Billerica, Massachusetts, USA) to ensure that confluent monolayers would be formed. A resistance of at least 150 Ω per well was required to commence the experiment (Alqahtani *et al.*, 2013). For the apical-to-basolateral (AP-BL) transport studies, the growth medium was removed from the basolateral chamber (acceptor chamber) and replaced with 2.5 ml of pre-warmed (37°C) DMEM buffered with HEPES (2-[4-(2-hydroxyethyl)piperazin-1-yl]ethanesulfonic acid) and was incubated at 37°C for 30 min, after which TEER measurements were performed. The growth medium was removed from the apical chamber (donor chamber) and was replaced with 2.5 ml of test solution (drug solution was tested in triplicate), after which TEER measurements were performed. For the basolateral-to-apical (BL-AP) transport studies, the same method was used, but the basolateral chamber served as the donor chamber and the apical chamber served as the acceptor chamber.

For all test solutions, supersaturated solutions were prepared where approximately 2.6 mg of baclofen compound was weighed into test tubes and 20 ml of DMEM was added as a solvent and pre-heated to 37°C. A 200 μ l sample was withdrawn from the basolateral chamber every 20 min over a period of 120 min. The chamber from which the sample was withdrawn was immediately replenished by the same volume of fresh pre-heated DMEM. The samples were placed into HPLC vials containing inserts. To ensure that the monolayer integrity was maintained, final TEER measurements were performed at the end of the study. All samples were then analysed by means of HPLC to determine baclofen concentration.

The concentration of baclofen in the transport samples were corrected for dilution and its transport was expressed as a percentage of the initial concentration of baclofen applied to the donor

chamber. The percentage transport was plotted as a function of time to produce percentage transport curves.

The apparent permeability coefficient (P_{app}) value for baclofen was calculated from the percentage transport curves (Equation 3.2) (Zhao *et al.*, 2016).

$$P_{app} = \frac{dQ}{dt} \left(\frac{1}{A \cdot 60 \cdot C_0} \right) \quad (3.2)$$

Where P_{app} is the apparent permeability coefficient ($\text{cm} \cdot \text{s}^{-1}$), dQ/dt is the permeability rate (amount permeated per minute), A is the diffusion area of the membrane (cm^2) and C_0 is the initial concentration of baclofen.

3.3.3 Conclusion

This chapter discussed a variety of solid-state characterisation methods used during this study. All techniques were used in a complimentary fashion to one another. The methods described included the screening for different solid-state forms of baclofen; investigation of the physico-chemical properties of the identified solid-state forms of baclofen as well as the determination of the equilibrium solubility of each of the solid-state forms of baclofen within bio-relevant media (pH 1.2, pH 4.6, pH 6.8 and distilled water) as well as in typical organic solvents (ethanol, methanol, octanol, acetone, to name but just a few). Furthermore, the physical stability of the solid-state forms, i.e. susceptibility to solid-state phase transformations either through solid-, solvent- or solution-mediated processes were described. Investigation of the bi-directional *in vitro* permeability of each of the solid-states of baclofen across Caco-2 cell monolayers was described. The following chapters will focus on the results obtained and the conclusions made throughout this study.

References

- Alqahtani, S., Mohamed, L.A. & Kaddoumi, A. 2013. Experimental models for predicting drug absorption and metabolism. *Expert opinion on drug metabolism and toxicology*, 9(10):1-14.
- Aulton, M.E. & Taylor, K.M.G. 2013. Aulton's pharmaceuticals: the design and manufacture of medicines, 4th Edition. Spain: Harcourt Publishers Limited.
- Bock, U., Kottke, T., Gindorf, C. & Haltner, E. 2003. Validation of the Caco-2 cell monolayer system for determining the permeability of drug substances according to the biopharmaceutic classification system (BCS). *Across barriers*, 1-7.
- Castle, J.E. & Zhdan, P.A. 1997. Characterization of surface topography by SEM and SFM: problems and solutions. *Journal of physics D - Applied physics*, 30:722-740.
- Censi, R. & Di Martino, P. 2015. Polymorph impact on the bioavailability and stability of poorly soluble drugs. *Molecules*, 20(10):18759-18776.
- Crowley, K.J. & Zografi, G. 2002. Water vapor absorption into amorphous hydrophobic drug/poly(vinylpyrrolidone) dispersions. *Journal of pharmaceutical sciences*, 91(10):2150-2165.
- Giron, D. 2002. Applications of thermal analysis and coupled techniques in pharmaceutical industry. *Journal of thermal analysis and calorimetry*, 68:335-357.
- Lu, J. & Rohani, A. 2009. Polymorphism and the crystallization of active pharmaceutical ingredients (APIs). *Current medicinal chemistry*, 16:884-905.
- Moffat, A., Osselton, M., Widdop, B. & Watts, J. 2011. *Clarke's analysis of drugs and poisons*. London: Pharmaceutical Press.
- Natoli, M., Leoni, B.D., D'Agnano, I., Zucco, F. & Felsani, A. 2012. Good caco-2 cell culture practices. *Toxicology in vitro*, 26:1243-1246.
- Punčochová, K., Heng, J., Beránek, J. & Štěpánek, F. 2014. Investigation of drug–polymer interaction in solid dispersions by vapour sorption methods. *International journal of pharmaceuticals*, 469(1):159-167.
- Rojek, B., Wesolowski, M. & Suchacz, B. 2013. Detection of compatibility between baclofen and excipients with aid and infrared spectroscopy and chemometry. *Molecular and biomolecular spectroscopy*, 116:532-538.

Rodríguez-Spong, B. Price, C.P. Jayasankar, A. Matzger, A.J. & Rodríguez-Hornedo, N. 2004. Principals of pharmaceutical solid polymorphism: a supramolecular perspective. *Advance drug delivery reviews*, 56(3):241-247.

Sarmiento, B., Andrade, F., da Silva, S.B., Rodrigues, F., das Neves, J. & Ferreira, D. 2012. Cell-based in vitro models for predicting drug permeability. *Expert opinion on drug metabolism and toxicology*, 8(5):607-621.

Saunders, M. & Gabbott, P. 2011. Thermal analysis: conventional techniques. (In Storey, R.A. & Ymén, I. ed. Solid state characterization of pharmaceuticals. West Sussex, United Kingdom: Wiley. p. 135-186).

Stieger, N., Aucamp, M., Zhang, S.W. & de Villiers, M.M. 2012. Hot-stage optical microscopy as an analytical tool to understand solid-state changes in pharmaceutical materials. *American pharmaceutical review*, 1-9.

USP see United States Pharmacopoeia.

United states pharmacopoeia - national formulary. 2017.
<http://www.uspnf.com/uspnf/pub/index?usp=40&nf=35&s=0&officialOn=May%201,%202017>
Date of access: 17 May 2017.

Yu, L., Reutzel, S.M. & Stephenson, G.A. 1998. Physical characterization of polymorphic drugs: an integrated characterization strategy. *Pharmaceutical science and technology today*, 1 (3):118-127.

Zhao, W., Uehera, S., Tanaka. K., Tadokoro. S., Kusamori, K., Katsumi, H., Sakane, T. & Yamamoto, A. 2016. Effects of polyoxyethylene alkyl ethers on the intestinal transport and absorption of rhodamine 123: a P-glycoprotein substrate by in vitro and in vivo studies. *Journal of pharmaceutical sciences*, 105:1526-1534.

Zhang, G., Law, D., Schmitt, E.A. & Qiu, Y. 2004. Phase transformation considerations during process development and manufacture of solid oral dosage forms. *Advanced drug delivery reviews*, 56(3):371-390.

CHAPTER 4

PHYSICO-CHEMICAL PROPERTIES OF BACLOFEN AND SOLID-STATE FORM SCREENING

4.1 Introduction

Currently, there is a relatively small number of literature and research reports found on the physico-chemical properties of baclofen anhydrate and more specifically the monohydrate. Different pharmaceutical processing techniques may result in different forms of baclofen each with different physico-chemical and thermodynamic properties. The first part of this study focussed on characterising the anhydrate and there after different methods were used to prepare different forms of baclofen. The primary goal of this section was to investigate the physico-chemical properties, solubility and dissolution profile of the different forms. An in depth discussion of the different methods that were used can be seen in Chapter 3.

4.2 High performance liquid chromatography (HPLC) method verification

Analytical method verification is confirming that specified requirements of the method has been met through the provision of objective evidence. A validated method can be published to provide a standard for future use by other scientists or it can be bought from a manufacturer. Even though an analytical method is used that was previously validated, method verification is still necessary to confirm the ability of the method to provide acceptable, accurate and trustworthy results. Different parameters are used to verify a method and include linearity to determine that the method will deliver acceptable detection data that correlate with the concentration of the analyte, limit of detection (LOD) to know the lowest concentration of baclofen that can be detected and limit of quantification (LOQ) to establish the lowest level where analytical measurement (Magnusson & Örnemark, 2014) of baclofen is acceptable. LOD and LOQ are determined since solubility, dissolution and permeability may require the analyses of very low concentrations (see Figures 4.1 - 4.6). Since solubility, dissolution and permeability were studied in different media, specificity of the method was done within the different media.

During linearity testing, a concentration range of 0.25 µg/ml - 500.0 µg/ml of baclofen was analysed on the HPLC. Seven solutions were prepared with concentrations of 0.25 µg/ml, 2.5 µg/ml, 25.0 µg/ml, 50.0 µg/ml, 100.0 µg/ml, 200 µg/ml, and 500 µg/ml. These solutions were all analysed in duplicate. A duplicate solution of 200 µg/ml was analysed six times to determine repeatability and to calculate the percentage recovery. The response of linearity was plotted on a graph as a function of concentration (Figure 4.1). An acceptable linearity was obtained ($R^2 = 0.9961$), and the method was deemed suitable for further analyses.

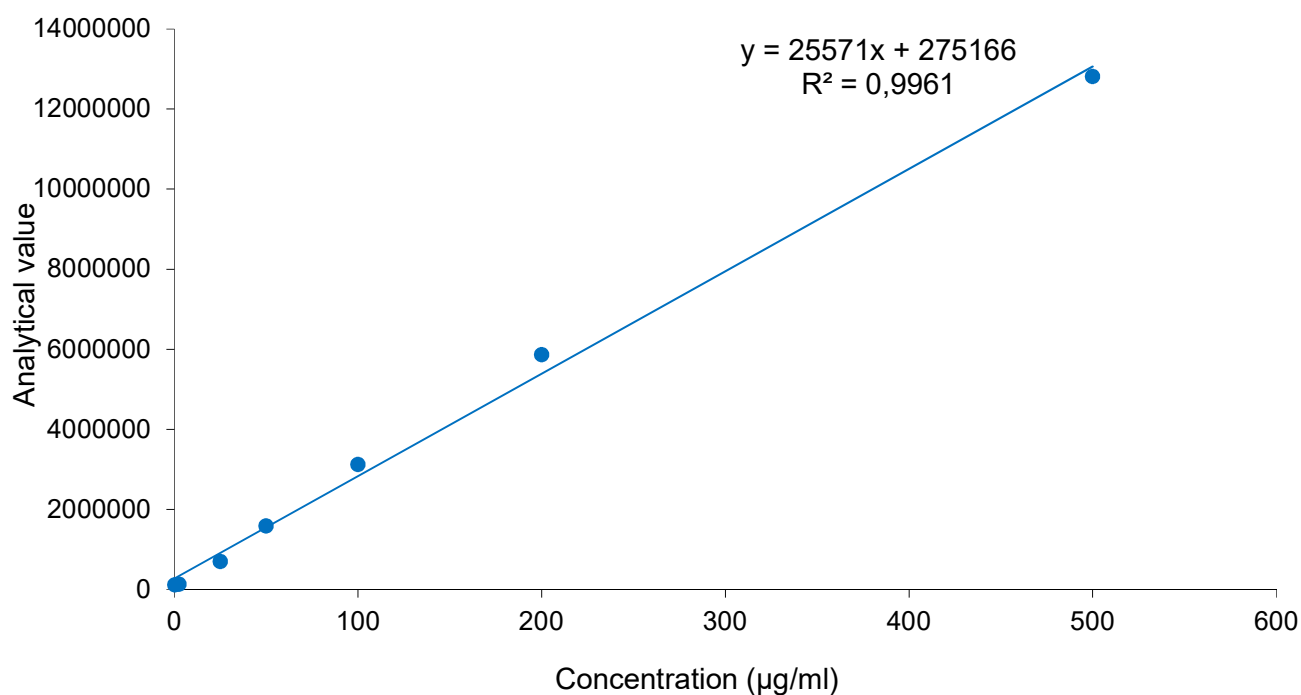


Figure 4.1: HPLC linearity of baclofen obtained using a concentration range of 0.25 µg/ml – 500 µg/ml

Due to the fact that various solvents were used throughout this study to investigate the solubility and behaviour of baclofen in organic or inorganic solutions, it was deemed necessary to investigate the specificity of the analytical method. It was considered important to investigate if any peak overlapping, poor peak shape or faster or slower elution of baclofen will occur when dissolved in various solvents. In order to investigate this, baclofen was dissolved in the various solvents that were used in the project (listed in Table 4.1). These solutions were injected and correlated with injections of the blank solutions (only the solvent, without any baclofen added) to investigate whether any chromatography issues will occur during the full analyses of solubility, dissolution or permeability samples. The method proved to be specific enough with no peak overlapping or changed baclofen retention.

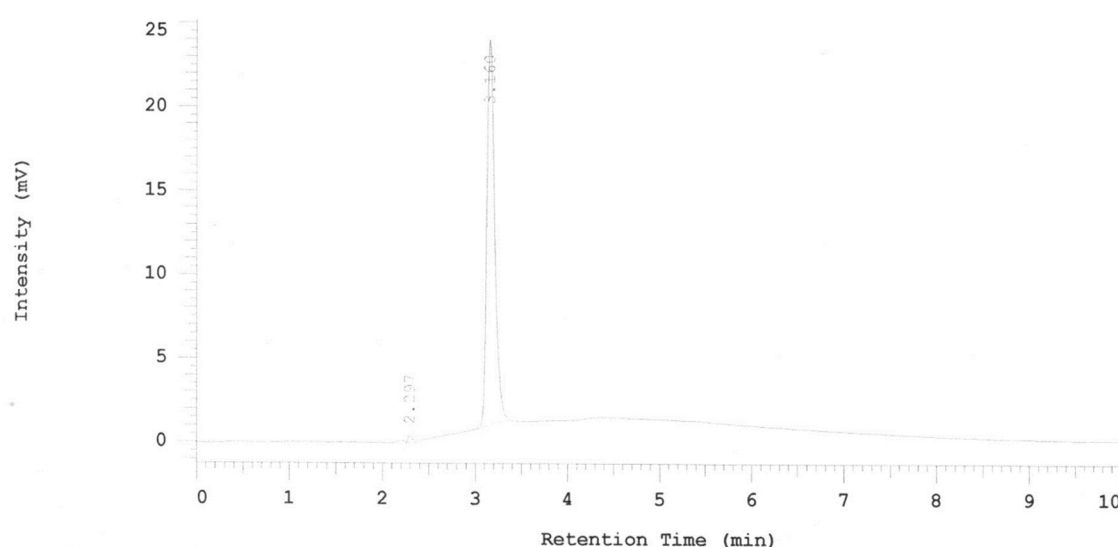
Table 4.1: Retention time of baclofen in different solvents

Solvent	Baclofen retention time (minutes)	Retention time of solvent peak (minutes)
Distilled water	3.13	No solvent peak
0.1 M HCl	2.92	No solvent peak
2-butanol	2.84	2.27, 2.60, 4.32

Table 4.1 continued: Retention time of baclofen in different solvents

Solvent	Baclofen retention time (minutes)	Peak due to solvent used (minutes)
Ethanol	3.07	2.17, 2.28, 2.51
Methanol	3.14	No solvent peak
n-octanol	3.11	2.23
1-propanol	2.58	2.27, 3.23
2-propanol	2.24	2.27, 3.21
Citrate	3.08	2.11
Phosphate	3.07	2.14
Acetone	3.16	2.29, 2.57, 4.03
1-butanol	3.05	2.26, 2.64, 3.31, 4.39

Due to the fact that solubility, dissolution or permeability testing can lead to the analysis of very small concentrations of the active ingredient, it was important to test the limit of detection (LOD) and limit of quantification (LOQ). Solutions of 2.5 µg/ml and 0.25 µg/ml were already prepared for linearity and it showed acceptable detection (Figures 4.2 - 4.3). Upon analysis, a 0.025 µg/ml solution no longer showed acceptable detection of baclofen (Figure 4.4). For the purpose of this study a LOD/LOQ concentration of 0.25 µg/ml was thus applied.

**Figure 4.2:** Chromatogram obtained for baclofen solution at a concentration of 2.5 µg/ml

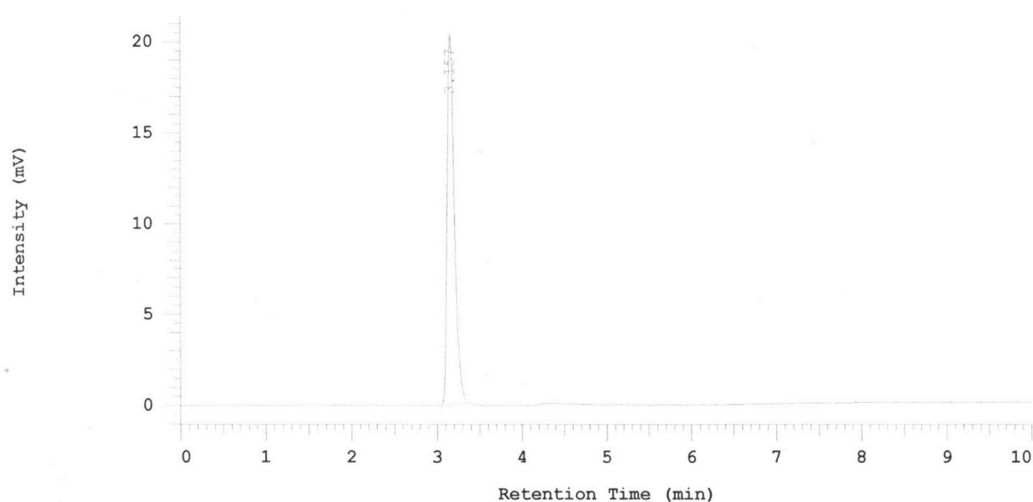


Figure 4.3: Chromatogram obtained for baclofen solution at a concentration of 0.25 µg/ml

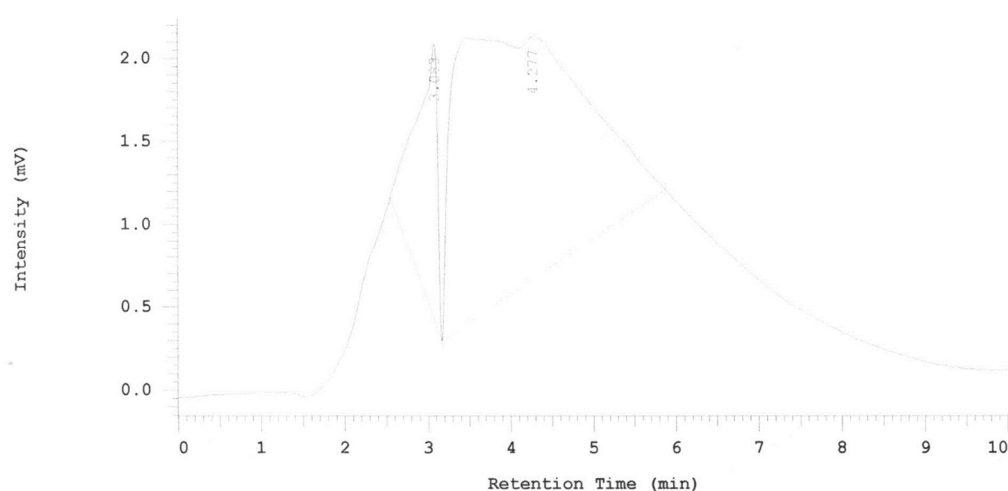


Figure 4.4: Chromatogram obtained for baclofen solution at a concentration of 0.025 µg/ml

The percentage recovery for this method was determined to be $100.42 \pm 3.81\%$ and the repeatability determined with the solution with a theoretical concentration of 200 µg/ml was calculated to be 0.32%. The method verification process revealed that the analytical method will be accurate and sensitive enough to allow quantification of baclofen throughout this study.

4.3 Solid-state form screening

In order to conduct proper solid-state form screening it is necessary to characterise the bulk material or start-out material in terms of physico-chemical properties. The next few paragraphs will discuss the data obtained during basic physical and chemical characterisation of the purchased baclofen bulk material. These results were then further used as the control data and to identify any solid-state form alteration that could occur throughout this study.

4.3.1 Basic physico-chemical characterisation of purchased baclofen bulk material

This study aimed at investigating whether different solid-state forms of baclofen do indeed exist and if so what the influence on the solubility, dissolution and permeability thereof will be. Physico-chemical characterisation was done by means of differential scanning calorimetry (DSC), thermogravimetric analysis (TGA), thermal microscopy (TM), scanning electron microscopy (SEM), Fourier-transform infrared spectroscopy (FT-IR), X-ray powder diffraction (XRPD), and vapour sorption.

4.3.1.1 Differential Scanning Calorimetry (DSC)

The thermogram obtained for baclofen compared well with that reported in literature. During the course of this study, the thermal peak temperatures were used rather than the onset or endset temperatures. According to Abdelkader *et al.* (2008), baclofen was heated at a rate of 10°C/min and has an endothermic peak at 210°C and Jivania *et al.* (2010) reported it should show a melting endothermic peak at 218.87°C with a heating rate of 20°C/min. Figure 4.5 illustrates an endotherm with a peak at 213.93°C and a melting endset temperature of about 218.28°C that correlates with the data reported in literature. According to Mirza *et al.* (2007), the monohydrate solid-state form of baclofen dehydrates at $\cong 67^{\circ}\text{C}$ with subsequent melting of the anhydrate at a temperature of $\cong 212^{\circ}\text{C}$. Therefore, it was deduced that the purchased baclofen raw material is the anhydrate solid-state form of baclofen. To corroborate this, further thermal testing was pursued.

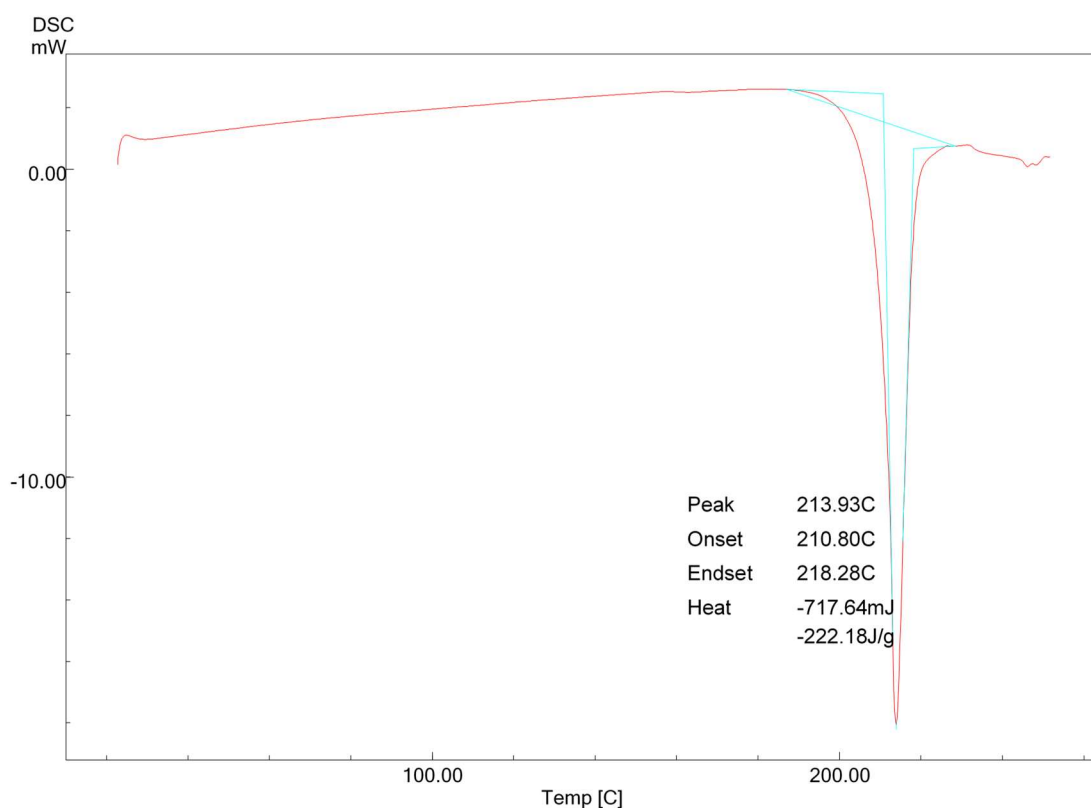


Figure 4.5: DSC thermogram obtained for baclofen purchased bulk material at a heating rate of 10°C/min.

4.3.1.2 Thermo-gravimetric analysis (TGA)

Due to the fact that Mirza *et al.* (2007) reported that baclofen may also exist as a monohydrate, it was imperative to investigate any moisture loss during heating of the raw material, especially since no dehydration was evident in the thermogram depicted in Figure 4.5. Any weight loss from the bulk material upon heating was tested by means of thermo-gravimetric analysis as described in Chapter 3, paragraph 3.3.2.2. The weight loss measured over the temperature range of 25°C to 200°C was 1.0% (Figure 4.6). After 200°C up to a final heating temperature of 300°C a complete weight loss of 99.0 % was obtained.

By applying the following equation:

$$\% \text{ Weight loss} = \frac{\text{Molecular weight}_{\text{solvent}}}{\text{Molecular weight}_{\text{solvent}} + \text{Molecular weight}_{\text{baclofen}}} \times 100 \quad (4.1)$$

it was possible to calculate the hydration level that a moisture loss of 1.0% would indicate. If baclofen would exist as the monohydrate, a percentage (%) weight loss of 7.8% would've occurred, thus meaning that since a weight loss percentage of only 1.0% was measured, it was concluded that the baclofen raw material exists in the anhydrous state.

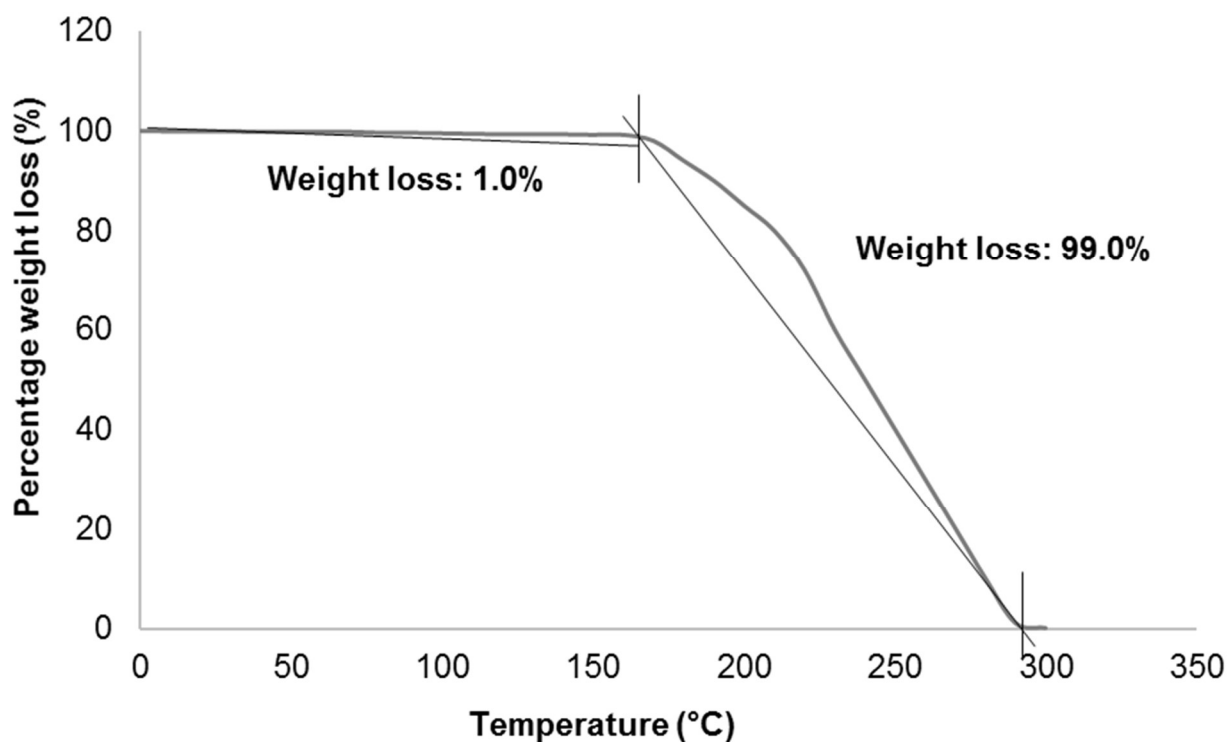


Figure 4.6: TGA thermogram obtained for baclofen purchased bulk material (i.e. anhydrate), using a heating rate of 10°C/min, heating from ambient to 300°C

4.3.1.3 Hot-stage microscopy (HSM)

At $215 \pm 1^\circ\text{C}$, apparent moisture droplets started to form on the surface of the cover slip (Figure 4.7 (b)) and at $223 \pm 1^\circ\text{C}$ baclofen anhydrate melted completely (Figure 4.7 (c)). Figure 4.7 (d) illustrates a clear observation of the start of sublimation of baclofen anhydrate at approximately $210 \pm 1^\circ\text{C}$. As seen from Figure 4.7 (c), the sublimate melted together with the bulk of the baclofen raw material that was present on the microscope slide. It may also be possible that the sublimate dissolved in the molten, liquefied baclofen on the microscope slide.

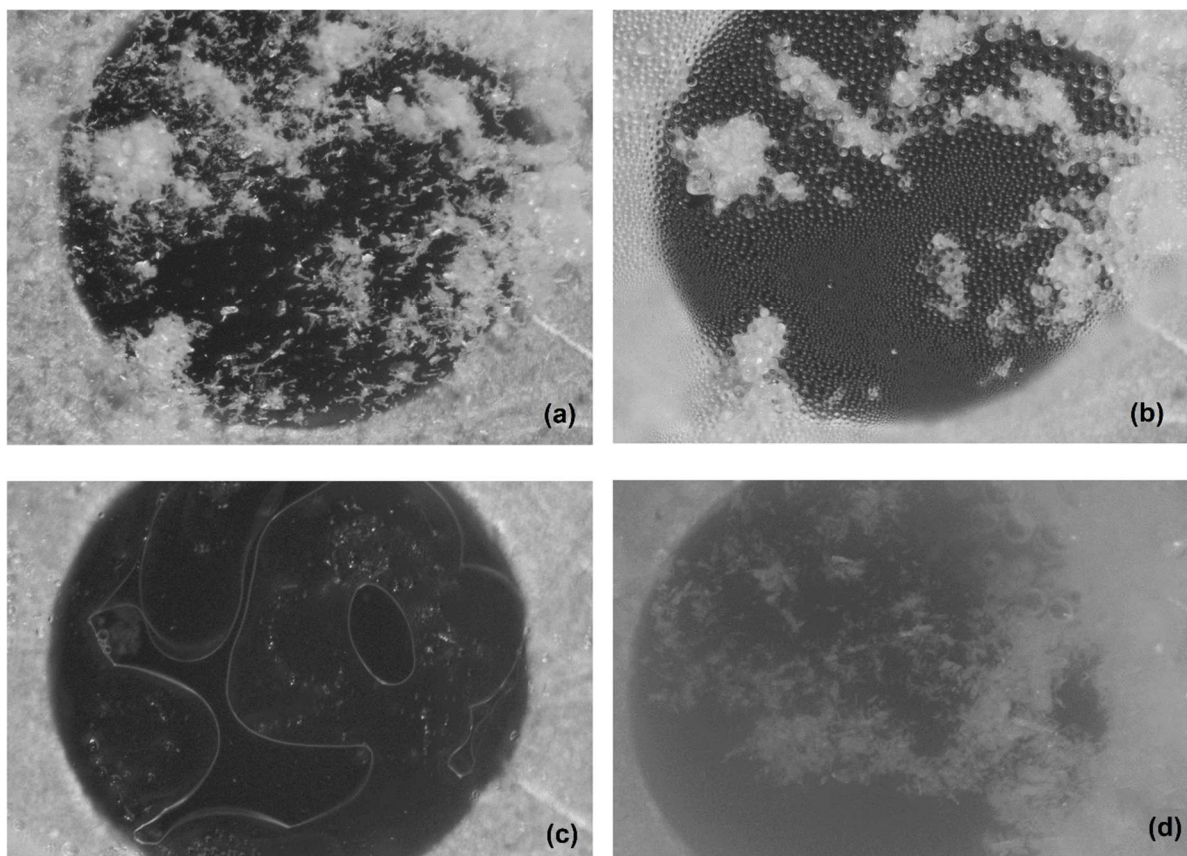


Figure 4.7: Hot stage micrographs obtained for (a) baclofen purchased bulk material (i.e. anhydrate) at ambient temperature ($25^{\circ}\text{C} \pm 1^{\circ}\text{C}$), (b) formation of what seemed to be moisture on the surface of the cover slip at 215°C , (c) complete melting of baclofen anhydrate at 223°C and (d) clear observation of the start of sublimation of baclofen anhydrate at approximately 210°C

4.3.1.4 Scanning electron microscopy (SEM)

The crystal habit of baclofen anhydrate in the SEM micrograph displayed in Figure 4.8 shows a striated appearance. It appears to form clumps of crystalline material which are layered on top of one another.

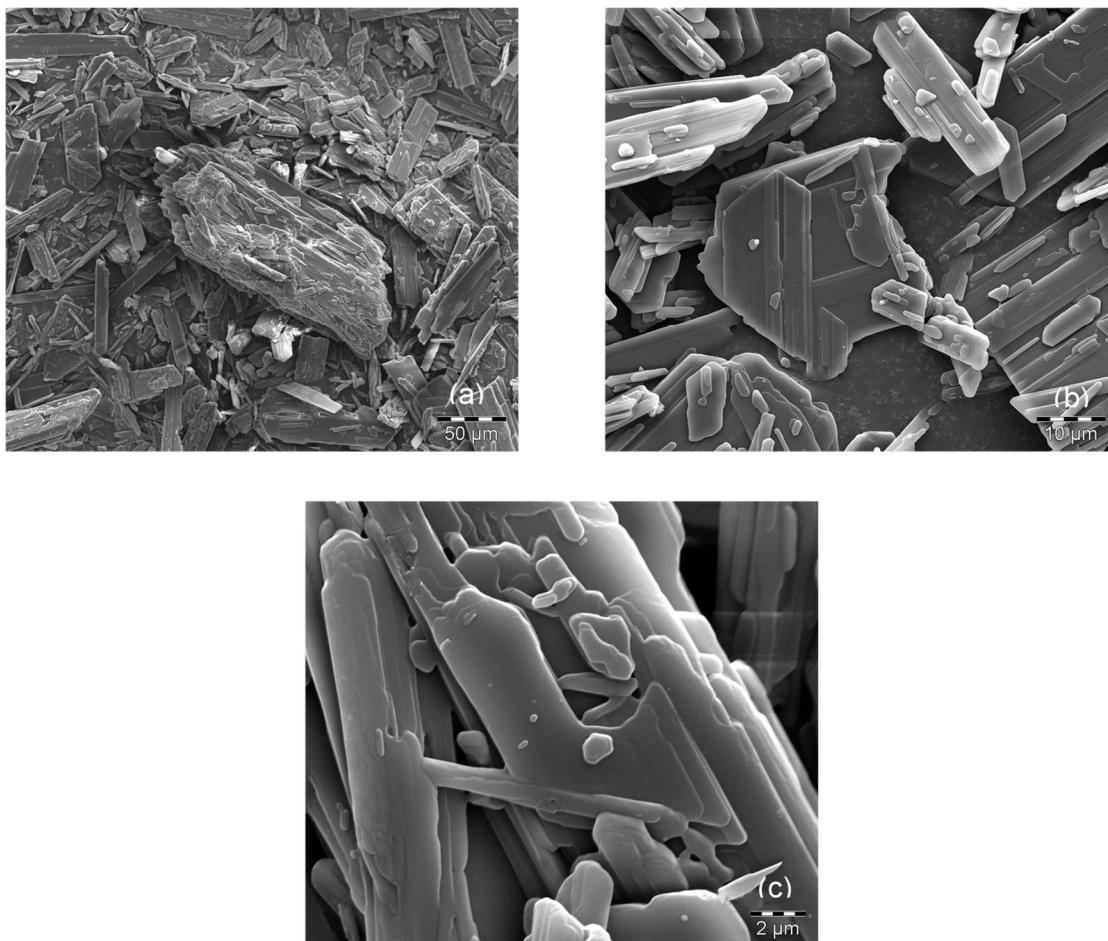


Figure 4.8: SEM micrographs obtained for baclofen purchased bulk material (i.e. anhydrate) with (a) captured at a 50 μm scale, (b) captured at a larger magnification of 10 μm scale and (c) captured at 2 μm scale

4.3.1.5 Fourier-Transform infrared spectroscopy (FT-IR)

Major peaks of baclofen due to its functional groups ($-\text{C}-\text{Cl}$, $-\text{COOH}$, and $-\text{NH}_2$) are visible at 1100, 1530, and 1610 cm^{-1} (Jivania *et al.*, 2010) that corresponds with the IR spectrum of baclofen (see Figure 4.9 and Table 4.2). Baclofen also showed major peaks in the wavenumber areas of 1900 cm^{-1} ($-\text{C}=\text{C}$ in the aromatic ring) and 2150 cm^{-1} . The absence of $-\text{OH}$ groups in the wavenumber region between 3600-3200 cm^{-1} can indicate that water molecules does not form a part of the molecule structure and confirms the anhydrous form.

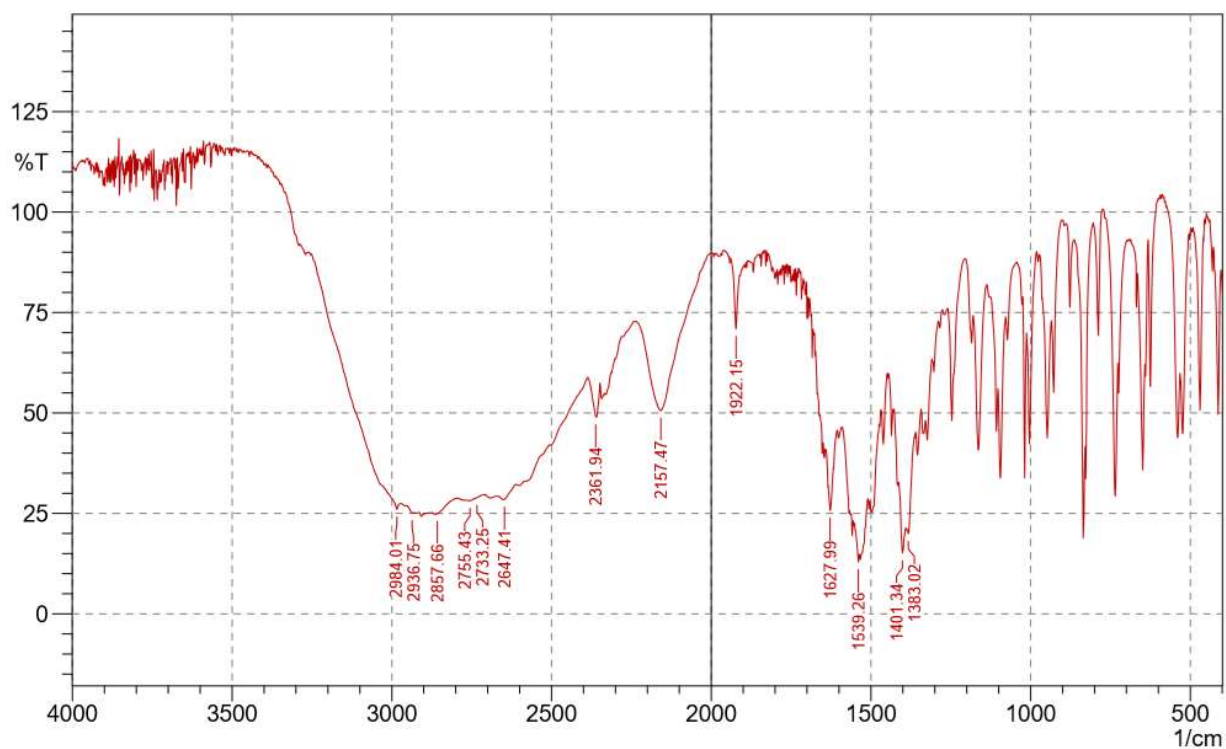


Figure 4.9: FT-IR spectrum obtained for baclofen purchased bulk material (i.e. anhydrate)

Table 4.2: FT-IR peak listing reported for baclofen purchased bulk material (i.e. anhydrate)

	Wavenumber (cm ⁻¹)		
No:	Primary wavenumbers for baclofen (Jivania et al., 2010; Moffat et al., 2011)	Baclofen anhydrate (Figure 4.9)	Functional groups
1	835	835.00	-CH
2	1095	1095.00	-C-Cl
3	-	1383.02	-α-CH ₃
4	1495	1401.34	-α-CH ₂
5	1527 - 1574	1539.26 – 1574.00	-COOH
7	1624	1627.99	-NH ₂
8	-	1922.15	-C=C
9	-	2157.47	-C≡C

4.3.1.6 X-Ray powder diffraction (XRPD)

The X-ray diffractogram for baclofen purchased bulk material (i.e. anhydrate) (Figure 4.10) correlates with that reported by Mirza *et al.*, 2007 for baclofen anhydrate. A summary of the most prominent diffraction peaks is listed in Table 4.3.

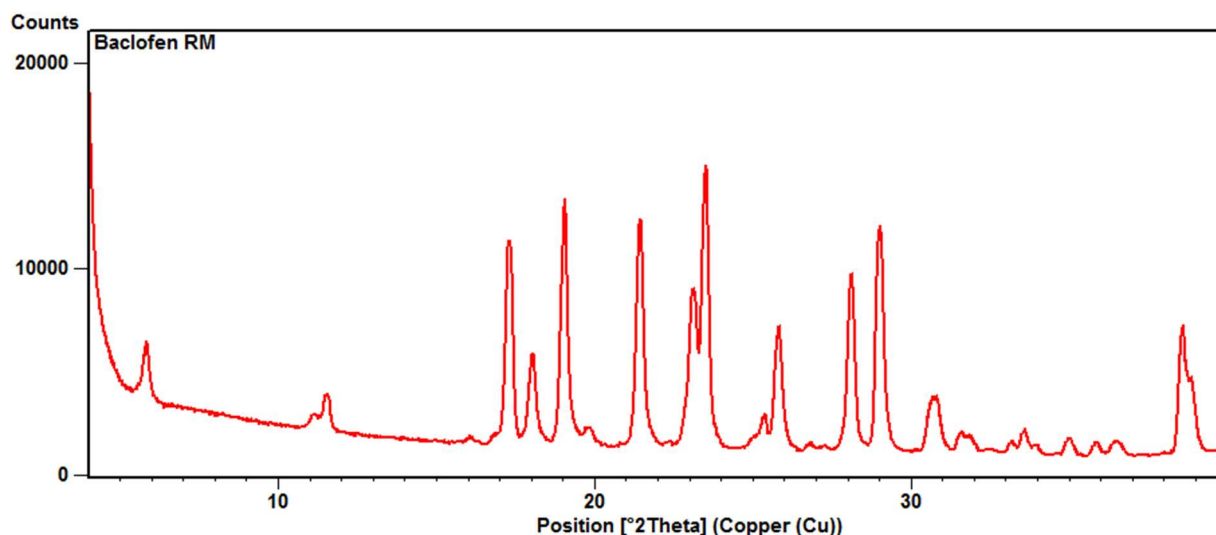


Figure 4.10: XRPD diffractogram obtained for baclofen purchased bulk material (i.e. anhydrate) at ambient temperature

Table 4.3: XRPD peak listing reported for baclofen anhydrate

Baclofen anhydrate			
Literature source	Experimentally determined		
Position [°2Th.] reported by Mirza <i>et al.</i> , 2007	Position [°2Th.]	d-Spacing [Å]	Relative Peak Intensity [%]
5.8	5.88	15.04	18.37
-	17.25	5.14	66.35
17.5	17.41	5.09	56.80
-	18.07	4.91	33.23
-	19.08	4.65	86.81
-	21.48	4.14	81.01
-	23.07	3.86	54.16
-	23.20	3.83	54.91

Table 4.3 continued: XRPD peak listing reported for baclofen anhydrate

Baclofen anhydrate			
Literature source	Experimentally determined		
Position [°2Th.] reported by Mirza <i>et al.</i>, 2007	Position [°2Th.]	d-Spacing [Å]	Relative Peak Intensity [%]
23.4	23.55	3.78	100.00
-	25.85	3.45	45.17
-	28.15	3.17	65.25
-	28.91	3.09	53.99
29.4	29.08	3.07	76.18
-	30.65	2.92	18.69
-	30.84	2.89	19.26
-	38.59	2.33	47.26
-	38.87	2.32	28.83

4.3.1.7 Vapour sorption of baclofen anhydrate

Different solid-state forms of a compound usually display different absorption and desorption behaviour (Mirza *et al.*, 2007). From vapour sorption data it is also possible to deduce if a phase transformation such as solvent-mediated transformation might occur upon exposure to high relative humidity conditions. Figure 4.11 illustrates the vapour sorption isotherms obtained for baclofen purchased bulk material (i.e. anhydrate) at ambient temperature but varying relative humidity percentages. No weight loss was measured over the humidity range of 0% RH to 30% RH. A significant amount of weight loss (6%) was measured over the %RH range of 35 - 75%RH. This observed weight loss could be due to recrystallisation (phase transformation) of anhydrous baclofen (Burnett *et al.*, 1999). After the recrystallisation, the sample had a much lower moisture sorption capacity indicating the solubility will be lower. The lower moisture sorption capacity may be dominated by surface adsorption, allowing water absorption into the structure of baclofen (Burnett *et al.*, 1999).

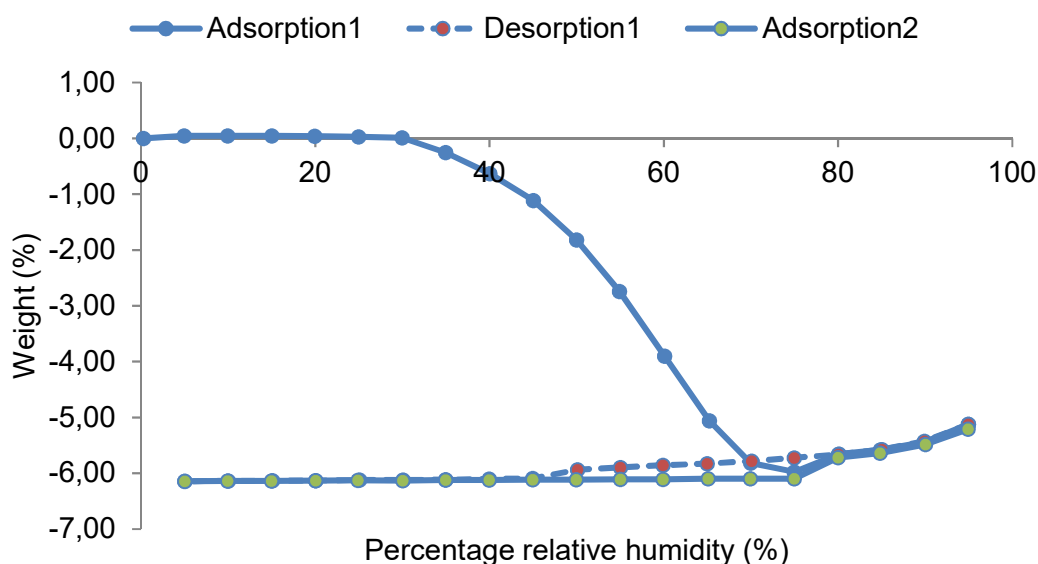


Figure 4.11: Vapour sorption isotherm obtained for baclofen purchased bulk material (i.e. anhydrate). The isotherms were obtained at $25 \pm 0.5^\circ\text{C}$ with humidity variation of 0 - 95% (Adsorption 1), 95 - 5% (Desorption 1) and 5 - 95% RH (Adsorption 2)

4.3.1.8 Conclusion

The physico-chemical properties of baclofen anhydrate was investigated in terms of melting point, loss of moisture upon heating, water content, crystallinity and vapour sorption isotherms. From the thermal data discussed in paragraphs 4.3.1.1 to 4.3.1.3, it was concluded that the melting peak temperature determined by DSC of baclofen anhydrate was at 213.93°C and complete melting of baclofen anhydrate was observed with HSM at $223 \pm 1^\circ\text{C}$. A weight loss of 99% between 200°C up to the final heating temperature of 300°C was determined by TGA that is a result of the sublimation upon heating that can be seen in Figure 4.7. FT-IR and XRPD results correlated with that reported in literature for baclofen anhydrate, whilst vapour sorption studies showed that anhydrous baclofen recrystallises at a very low relative humidity of 35% RH. Further investigation into this phenomenon was therefore necessary.

4.4 Screening for different solid-state forms after recrystallisation

From the data published by Mirza *et al.* (2007) it is clear that baclofen may exist in the monohydrate form, however, no other forms of baclofen have been reported in literature. That does, however, not exclude the possibility that other forms of baclofen may exist.

4.4.1 Recrystallisation using distilled water

From the data presented in section 4.3.1.7 in addition to the data published by Mirza *et al.* (2007), it became evident that baclofen anhydrate has the ability to recrystallise to another form namely

a monohydrate. Subsequently, the recrystallisation of baclofen using distilled water was investigated according to the method provided in Chapter 3, paragraph 3.2.1. Characterisation of the recrystallised baclofen was done by means of DSC, TGA, TM, SEM, FT-IR and XRPD as described in Chapter 3, paragraphs 3.3.2.1- 3.3.2.6.

4.4.1.1 Differential scanning calorimetry (DSC)

The DSC thermogram obtained for baclofen recrystallised in water can be observed in Figure 4.12 and is characterised by two peaks. The first peak (exothermic) was observed at 154°C and the second endothermic peak at 206.03°C. Mirza *et al.* (2007) reported the DSC thermogram of the monohydrate having two endothermic events, dehydration, where the first peak was observed at 67.18°C and the second at 211.88°C. The second peak on Figure 4.12 as well as reported by Mirza *et al.* (2007) is the same as the endothermic peak for baclofen anhydrate at 213°C (Figure 4.5). Observing the DSC data presented in Figure 4.12, it is also clear that some form of dehydration is possibly occurring from ambient temperature already, due to the fact that no baseline is visible on the thermogram in the temperature range of 25°C to 100°C.

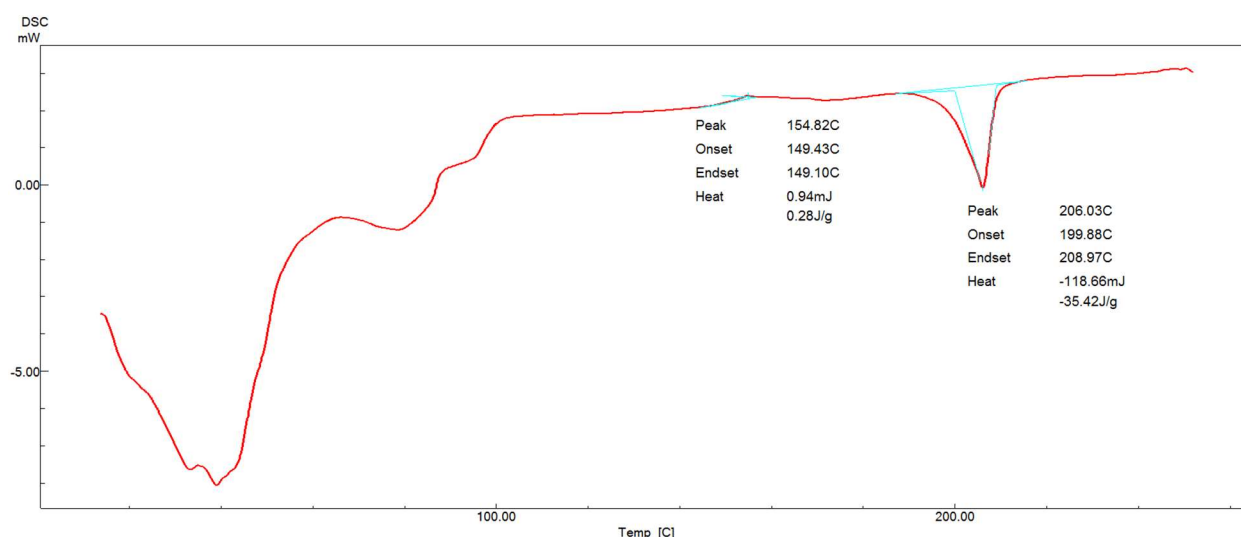


Figure 4.12: DSC thermogram obtained for baclofen recrystallised in water at heating rate of 10°C/min

4.4.1.2 Thermo-gravimetric analysis (TGA)

A TGA thermogram of baclofen recrystallised in water can be observed in Figure 4.13. The weight loss of the recrystallised baclofen measured over the temperature range of 25°C to 100°C was measured to be 33.61%, while Mirza *et al.* (2007) reported a weight loss of 7.5% over the temperature range of 40 – 80°C. It was very challenging to analyse the recrystallised baclofen product using TGA, because the recrystallised product was not well defined crystals, but rather a slurry-like mass. When this mass was placed on filter paper for drying purposes it was observed that the crystals were very fine and small and in some instances were absorbed into the filter

paper, leaving almost no powder sample. Drying of sample on a solid surface would've provided more dried sample, but also more dehydrated sample. The reason for using filter paper was to get rid of the bulk water rapidly in order to quickly start TG analysis. This led to the situation where getting a suitable sample of the monohydrate form for TGA was almost impossible. Sample for DSC analysis was easier to obtain since the sample was directly weighed into the sample pan and once a relative degree of weight stability was obtained the pan was tightly sealed with a lid which prevented further dehydration. The sample preparation for TG-analysis didn't allow this due to the fact that the analytical technique makes use of open sample pans whereby water evaporation can occur very easily.

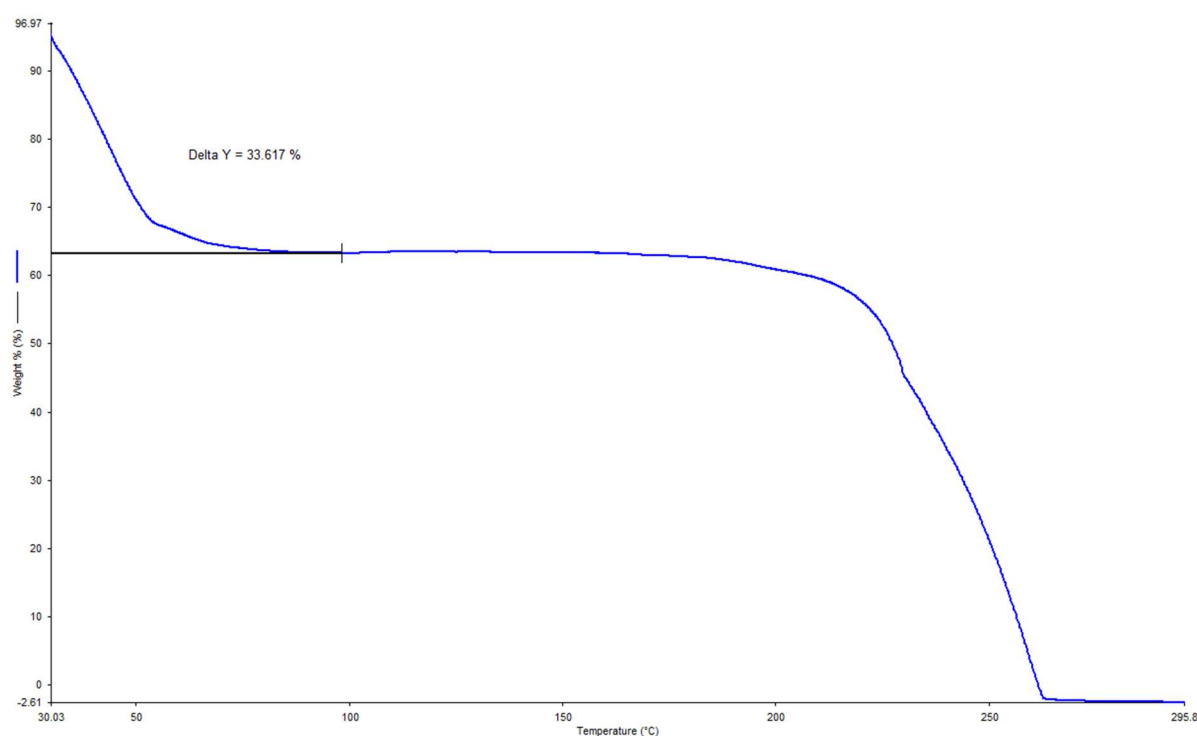


Figure 4.13: TGA thermogram obtained for baclofen recrystallised in water, using a heating rate of 10°C/min, heating from ambient temperature to 300°C

4.4.1.3 Hot-stage microscopy (HSM)

During HSM analysis, the heating of baclofen recrystallised in water started at an ambient temperature of 20°C ± 1°C (Figure 4.14 (a)) at a heating rate of 10°C/min. This makes it difficult to get the crystals on a single layer, leading to clusters of the recrystallised baclofen on the microscope slide. Figure 4.14 (b) clearly illustrates the release of water vapour as gas bubbles in the temperature range of 70°C – 125°C where the recrystallised baclofen dehydrated. Figure 4.14 (c) illustrates a sublimate of the baclofen which formed on the cover slip.

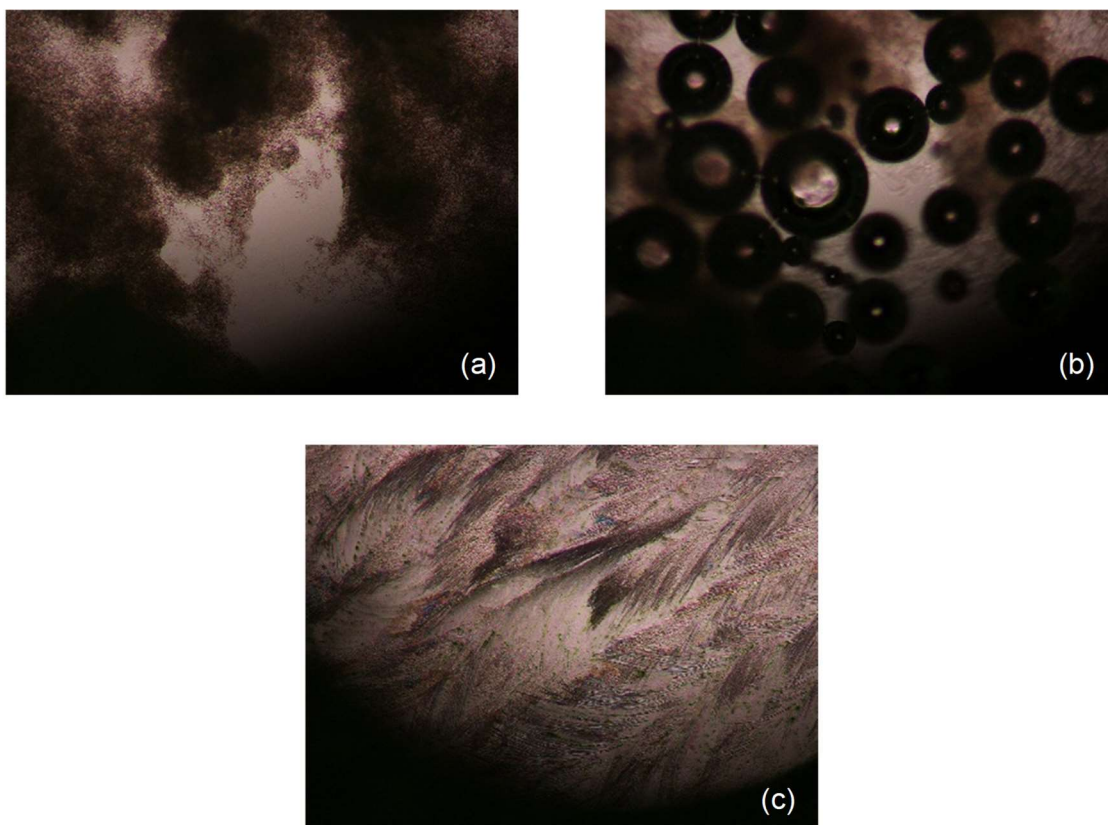


Figure 4.14: Photomicrographs obtained for baclofen recrystallised from water at 20°C (a), development of water bubbles (b) and the sublimate of baclofen at 20°C(c)

4.4.1.4 Scanning electron microscopy (SEM)

The baclofen anhydrate illustrated a striated appearance (Figure 4.8), whereas the recrystallised baclofen (as illustrated in Figure 4.15) does not exhibit a well-defined crystal structure. The crystals appear to be very fine, soft and flexible.

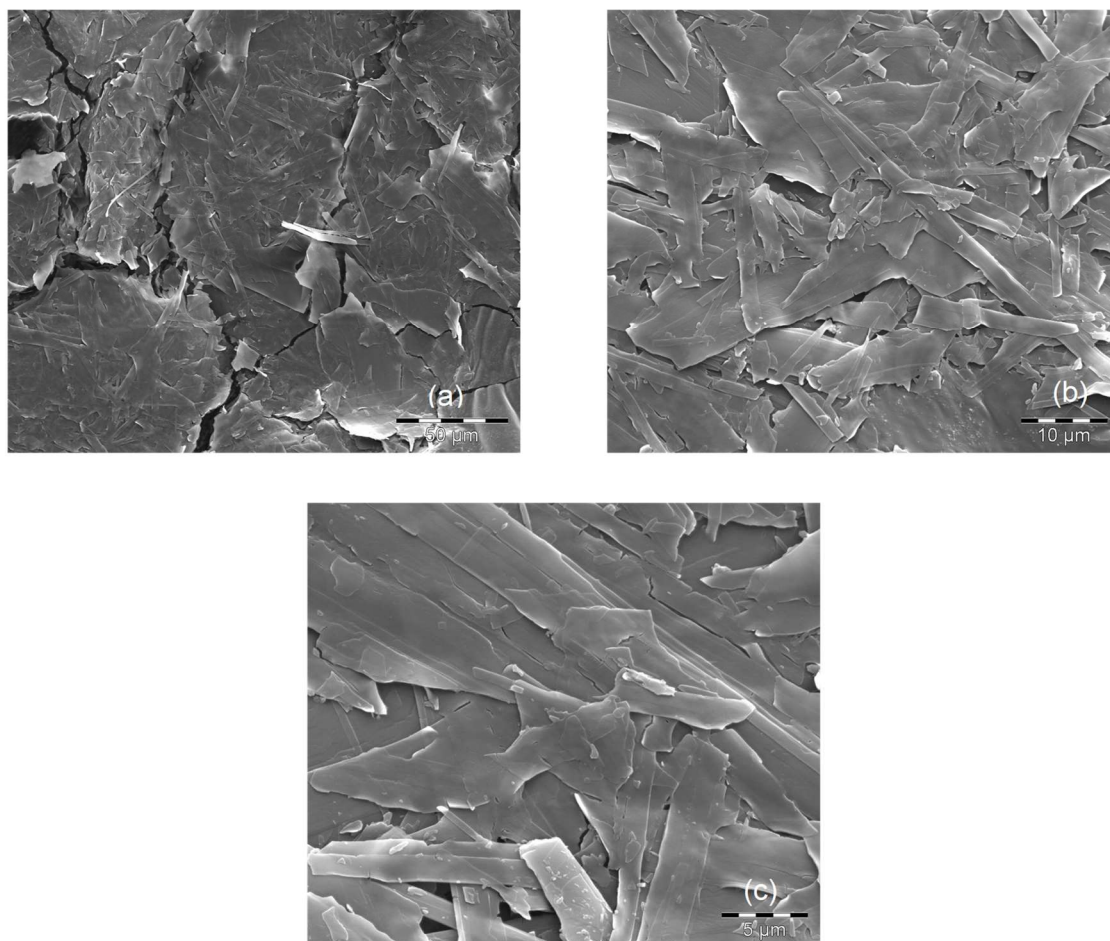


Figure 4.15: SEM micrographs obtained for baclofen recrystallised in water with (a) captured at a 50 μm scale, (b) captured at a larger magnification of 10 μm scale and (c) captured at 5 μm scale.

Comparison of the SEM micrographs obtained for the monohydrate (Figure 4.15) and anhydrate (Figure 4.8) leads to the conclusion that the monohydrate actually exists as a slurry, making it very difficult to characterise it as a proper solid-state form. Since this solid-state form was already characterised and discussed in Mirza *et al.*, (2007), it was decided to investigate the properties of this form even more in-depth.

4.4.1.5 Fourier-transform infrared spectroscopy (FT-IR)

The major peaks of the monohydrate can be observed at 742, 793, 951, 1074, 1093, 1190, 1235, 1327, 1407, 1437 and 1598 cm^{-1} . The main differences between anhydrous baclofen and the baclofen recrystallised with water were observed in the region between 700 and 1600 cm^{-1} and 3334.10 cm^{-1} (Mirza *et al.*, 2007). The 3334.10 cm^{-1} peaks indicate the presence of water (-OH groups) in the structure possibly indicating the existence of the monohydrate form.

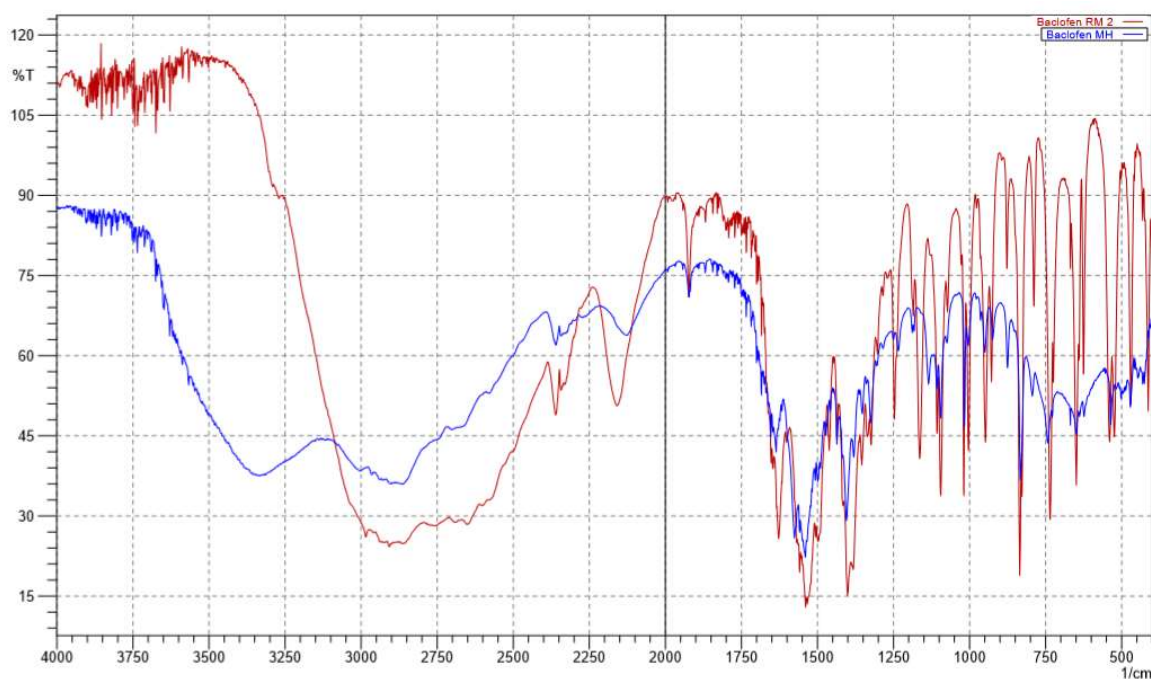


Figure 4.16: An overlay of the FT-IR spectra obtained for baclofen anhydrate (red) and recrystallised with distilled water baclofen (blue)

Table 4.4: FT-IR peak listing reported for baclofen recrystallised with distilled water

	Wavenumber (cm ⁻¹)		
No:	Baclofen anhydrate	Recrystallised baclofen	Functional groups
1	1383.02	-	-α-CH ₃
2	1401.34	1405.20	-α-CH ₂
3	1539.26	1539.26	-COOH
4	1627.99	1635.71	-NH ₂
5	1922.15	1923.11	-C=C
6	2157.47	2127.58	-C≡C
7	-	3334.10	-OH

4.4.1.6 X-Ray powder diffraction (XRPD)

The XRPD for the baclofen recrystallisation (Figure 4.17) shows the position of the most observed diffraction peaks at 10.7, 16.1 and 21.5 (Mirza *et al.*, 2007) that corresponds with the XRPD data showed in Table 4.5.

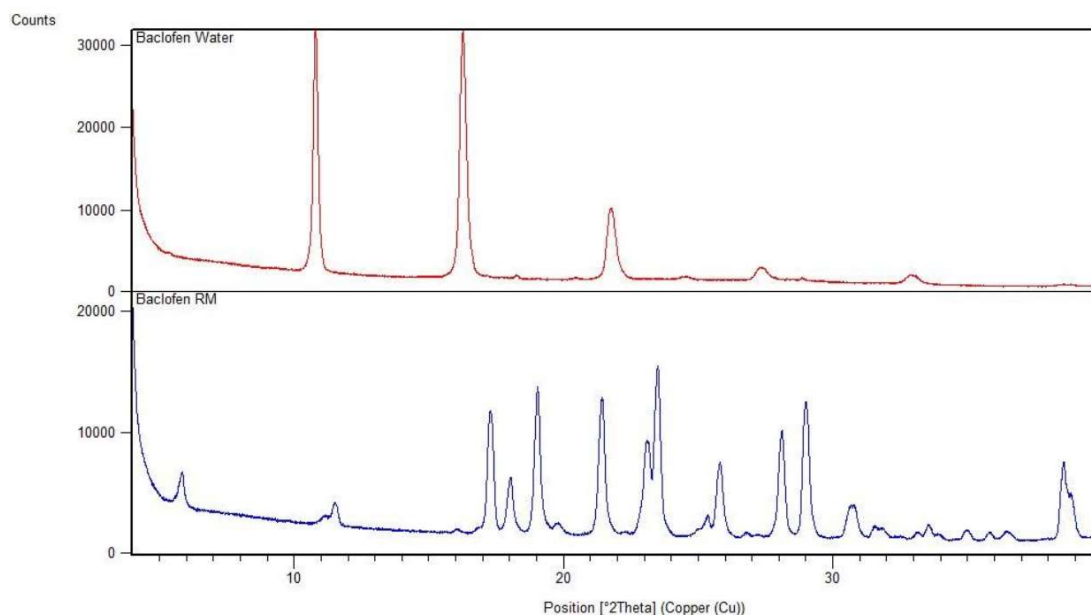


Figure 4.17: XRPD diffractograms obtained for baclofen anhydrate (blue) and recrystallised baclofen (red).

Table 4.5: XRPD peak listings reported for baclofen anhydrate and recrystallised baclofen

Baclofen anhydrate			Recrystallised baclofen		
Position [°2Th.]	d-Spacing [Å]	Relative Peak Intensity [%]	Position [°2Th.]	d-Spacing [Å]	Relative Peak Intensity [%]
5.88	15.04	18.37	-	-	-
-	-	-	10.79	8.19	96.54
-	-	-	16.27	5.45	100.00
17.25	5.14	66.35	-	-	-
17.41	5.09	56.80	-	-	-
18.07	4.91	33.23	-	-	-
19.08	4.65	86.81	-	-	-
21.48	4.14	81.01	-	-	-
-	-	-	21.73	4.09	27.69
23.07	3.86	54.16	-	-	-
23.20	3.83	54.91	-	-	-
23.55	3.78	100.00	-	-	-

Table 4.5 continued: XRPD peak listings reported for baclofen anhydrate and recrystallised baclofen

Baclofen anhydrate			Recrystallised baclofen		
Position [°2Th.]	d-Spacing [Å]	Relative Peak Intensity [%]	Position [°2Th.]	d-Spacing [Å]	Relative Peak Intensity [%]
25.85	3.45	45.17	-	-	-
28.15	3.17	65.25	-	-	-
28.91	3.09	53.99	-	-	-
29.08	3.07	76.18	-	-	-
30.65	2.92	18.69	-	-	-
30.84	2.89	19.26	-	-	-
38.59	2.33	47.26	-	-	-
38.87	2.32	28.83	-	-	-

In order to investigate the crystallisation of baclofen anhydrate when exposed to sufficient water, which would facilitate the crystallisation of baclofen monohydrate, a continuous XRPD analysis was performed. This was done by placing a sufficient quantity of baclofen anhydrate on a zero background sample holder. Distilled water was added to the powder sample in such a manner that it produced a thick slurry, thus the initial scan, as provided in Figure 4.18, produced an almost amorphous ‘halo’-like diffraction pattern. XRPD data was collected continuously over a period of 80 minutes (Figure 4.18). The diffraction peak at $16.2^{\circ}2\theta$ was considered as a clearly distinguishable peak relating to the monohydrate. The relative intensity of this peak was calculated with reference to the peak obtained during the single XRPD scan, as presented in Figure 4.17. The relative intensity was plotted against the time interval at which the scan was obtained. From this, the graph as presented in Figure 4.19 was obtained. During this experimental setup, it took approximately 72 min for the recrystallisation of the monohydrate to reach completion. After 72 min, the relative intensity of the peak at $16.2^{\circ}2\theta$ started to diminish, thereby suggesting that when water starts to evaporate the monohydrate reverts back to the anhydrate form. After 80 min, the diffraction collection was stopped, sample removed and inspected. The sample appeared still wet to the touch. Complete dehydration could have been observed if the continuous scan continued for a longer period of time, however, due to experimentation limitations it was not possible. The same can be observed in Figure 4.20 where the recrystallised baclofen was investigated through HSM. The sample started to dehydrate at 50°C where bubbles started to form and complete dehydration could be observed at 90°C .

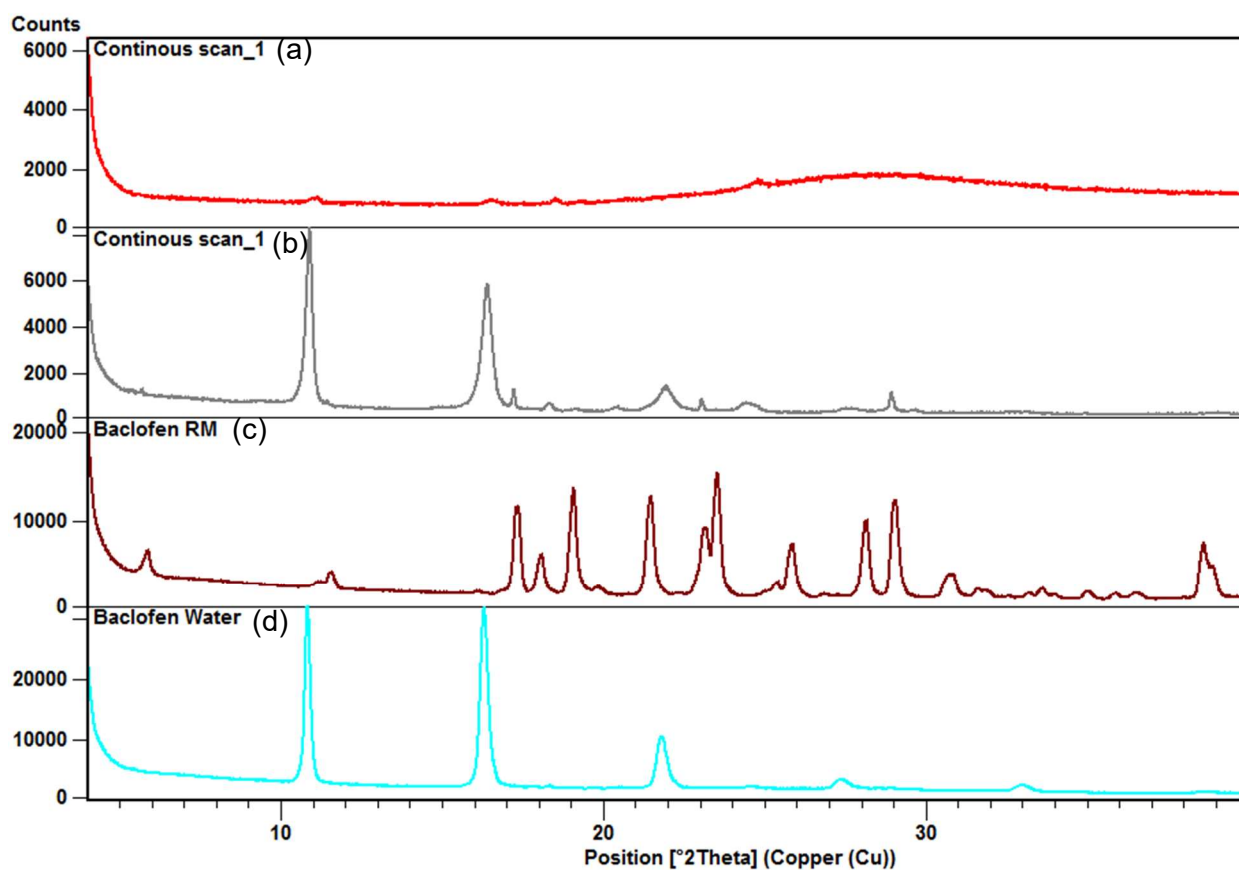


Figure 4.18: XRPD continuous scan diffractograms obtained during the investigation of the crystallisation of the monohydrate when baclofen anhydrate is exposed to sufficient water to create a thick slurry. Where (a) is the initial scan of baclofen anhydrate immediately after the distilled water was added, (b) is the diffraction pattern obtained after 72 minutes, (c) diffraction pattern of baclofen anhydrate and (d) diffraction pattern for baclofen monohydrate

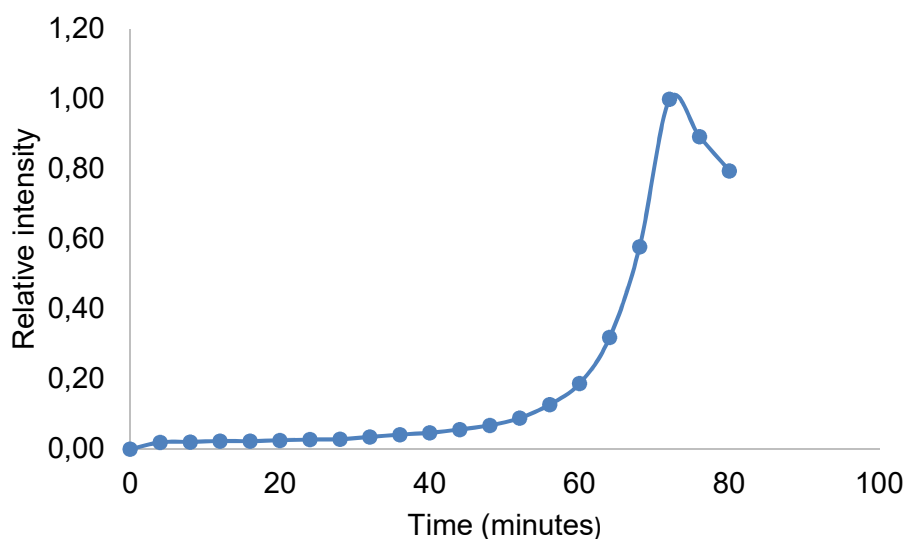


Figure 4.19: Graph plotted using the calculated relative intensity of the diffraction peak at $16.2^\circ 2\theta$ for baclofen monohydrate over a period of 80 minutes. The sample temperature was maintained at ambient conditions during the collection of data and diffraction data was collected every 5 minutes.

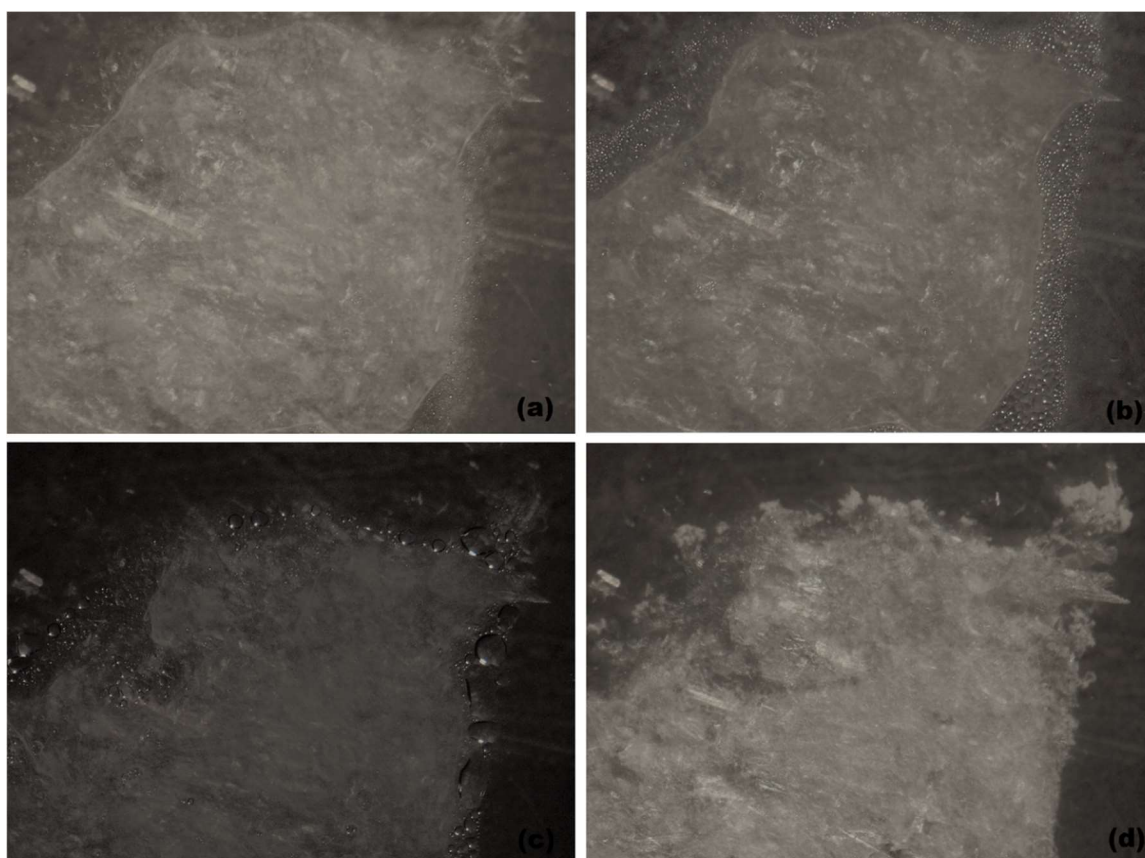


Figure 4.20: Photomicrographs obtained for baclofen recrystallised from water at 25°C (a), development of water bubbles 50°C (b) the continuation of water bubbles forming at 60°C (c) and (d) complete dehydration of the sample at 90°C .

4.4.1.7 Conclusion

The goal was to investigate the impact of recrystallisation with distilled water on baclofen and to illustrate the effect of recrystallisation on the physico-chemical properties of this form. Hot-stage microscopy illustrated the release of water vapour as gas bubbles during heating of the sample and FT-IR spectrum indicated the presence of water in the molecule through the -OH stretch at 3334.10 cm^{-1} . This can indicate that a monohydrate form of baclofen may exist, however, the powder mass was difficult to work with and the fast dehydration of the monohydrate leads to the conclusion that the recrystallised baclofen cannot be used meaningful and therefore no solubility studies and dissolutions were done further in this study using baclofen monohydrate. It was concluded that baclofen monohydrate is a transient solid-state form and will only exist in an environment where water is present. Once water started to evaporate from the environment, the solid-state form also started to transform to the anhydrate. Furthermore, by scrutinising all presented data it might be hypothesised that the described monohydrate is not truly a different solid-state form, but merely an intermediate product obtained when the anhydrate is mixed with water or when it is exposed to humidity conditions. This led to investigating whether the monohydrate or any other solid-state form might be obtained when different organic solvents are used as recrystallising solvents.

4.4.2 Behaviour of baclofen anhydrate in various organic solvents

From the data presented in section 4.4.1, it became evident that baclofen may also exist in the monohydrate form, even though it is an intermediate product in the presence of water. The possibility was explored that baclofen may exist in other solid-state forms and that the different forms may lead to different physico-chemical properties than that of baclofen anhydrate. The possibility that baclofen monohydrate, as described in literature, might be prepared using recrystallisation from organic solvents were therefore investigated. Especially since the data obtained in this study with water as recrystallisation solvent showed the monohydrate to be a very unstable, transient solid-state form. Recrystallisation of baclofen was attempted by using various solvents including acetone, 1-butanol, 2-butanol, ethanol, methanol, 1-propanol and 2-propanol. However, the recrystallisation was unsuccessful, with no crystals even forming through slow solvent evaporation. During these recrystallisation studies, it was observed that the solubility of baclofen in the organic solvents is very low. No data was obtained that could give more insight into the solubility of baclofen in organic solvents and therefore equilibrium solubility studies were performed.

4.5 Equilibrium solubility in solvents

During the course of this study the equilibrium solubilities of baclofen raw material were determined in acetone, 1-butanol, 2-butanol, ethanol, methanol, 1-propanol and 2-propanol.

4.5.1 Acetone

Solubility results obtained for baclofen in acetone are displayed in Figure 4.21. Baclofen reached a concentration of 3.21 ± 0.11 mg/ml in acetone after 24 h. What appeared to be a phase transition of baclofen in the acetone occurred after 1 h with a measured dissolved concentration of 4.02 ± 0.04 mg/ml dropping to a measured dissolved concentration of 3.82 ± 0.5 mg/ml. DSC, FT-IR and XPRD was done at 1 h, 4 h and 24 h intervals of the excess baclofen that was not in solution in the acetone to examine possible solid-state changes. DSC performed on the excess baclofen within acetone at 1 h, 4 h and 24 h showed a peak melting temperature of 208.60°C , 209.90°C and 209.10°C respectively, displayed in Figure 4.22, that correlates with baclofen raw material with a peak temperature of 213.93°C (Figure 4.5) where no dehydration or desolvation was observed from the DSC thermogram. FT-IR performed on the excess baclofen in acetone at 1 h and 24 h and the absorbance peaks (Table 4.6) of the excess baclofen correlate with the peaks of baclofen raw material (Figure 4.9). The XRPD peaks of the excess baclofen (Figure 4.23) correlate with those of the baclofen anhydrate.

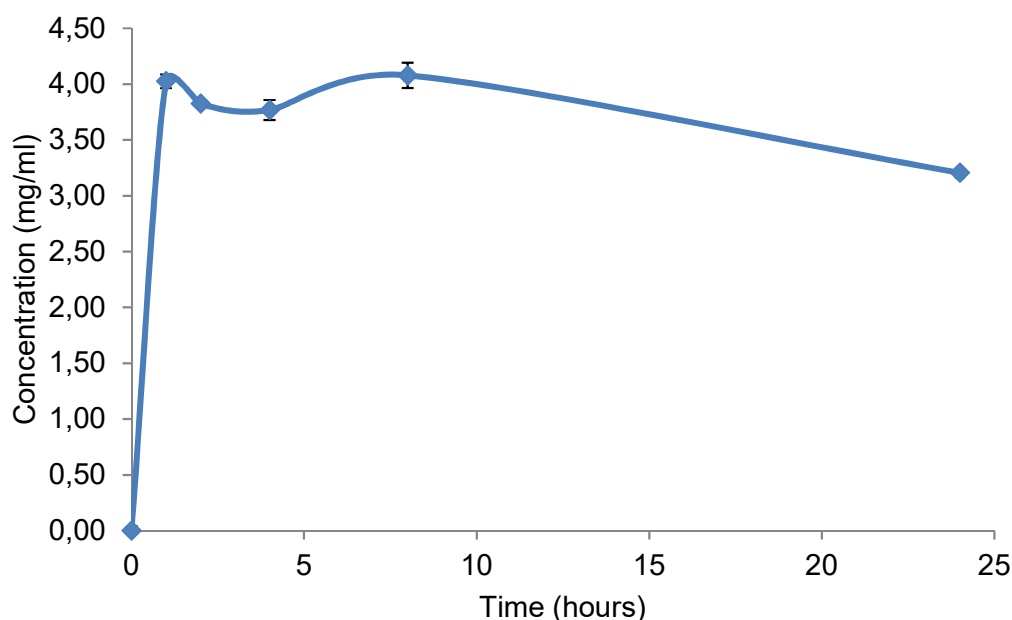


Figure 4.21: The solubility profile obtained for baclofen anhydrate in acetone over a period of 24 h at $37^{\circ}\text{C} \pm 0.5^{\circ}\text{C}$

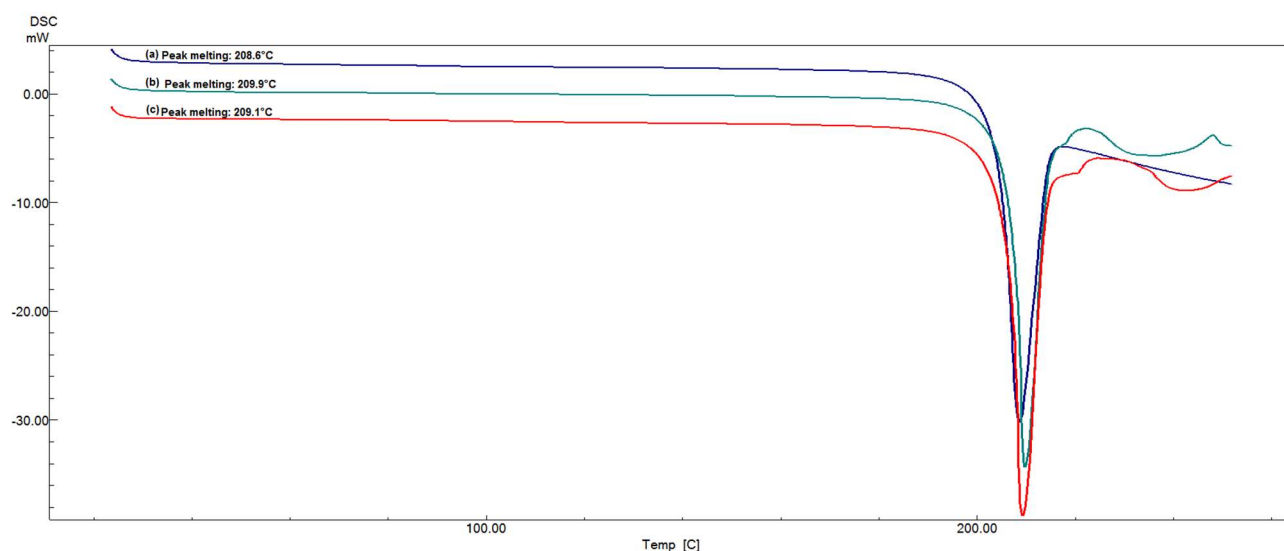


Figure 4.22: An overlay of the DSC thermogram obtained for baclofen in acetone at 1 h (blue), 4 h (green) and 24 h (red) at heating rate 10°C/min

Table 4.6: FT-IR peak listing reported for baclofen in acetone

No:	Wavenumber (cm ⁻¹)			Functional groups
	Baclofen anhydrate	Baclofen excess 1 h	Baclofen excess 24 h	
1	1383.02	1383.02	1383.02	-α-CH ₃
2	1401.34	1401.34	1401.34	-α-CH ₂
3	1539.26	1534.44	1534.44	-COOH
4	1627.99	1627.99	1627.99	-NH ₂
5	1922.15	1922.15	-	-C=C
6	2157.47	2157.47	2157.47	-C≡C
7	2647.41 – 2755.43	2649.34 – 2755.43	2649.34 – 2755.43	-C-H (aldehyde C-H)
8	2857.66 – 2984.01	2846.09 – 2984.01	2853.81 – 2984.01	-CH (alkyl)

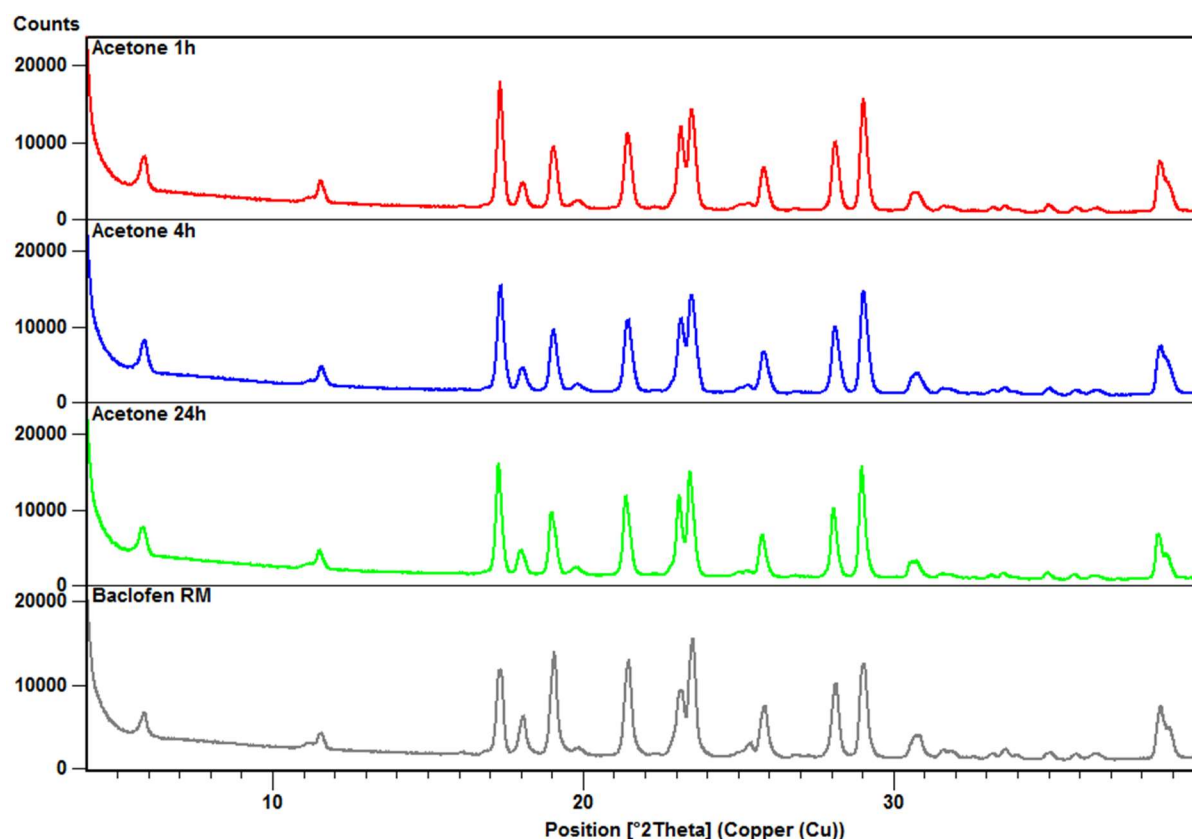


Figure 4.23: XRPD diffractograms obtained for baclofen in acetone at 1h (red), 4 h (blue), 24 h (green) and baclofen anhydrate (grey)

The significance of the decreased solubility concentration at the 24 h time interval (Figure 4.21) was determined via the Grubbs test and this indicated that there was not a significant outlier ($P > 0.05$). The reason for this could be clearer if more withdrawals were performed closer to the 24 h time interval, this could, however, not be done due to experimental limitations. It could have been overcome with the use of an automated withdrawal system. FT-IR, DSC and XRPD, however indicated no differences for baclofen in acetone.

4.5.2 1-Butanol

Solubility results obtained for baclofen in 1-butanol are displayed in Figure 4.24. Baclofen reached a concentration of 0.05 ± 0.003 mg/ml after 24 h. DSC, FT-IR and XRPD were done at 1 h and 24 h intervals of the excess baclofen in the 1-butanol to examine if any solid-state changes occurred. DSC results showed peak melting temperatures of 210.35°C (1 h) and 210.35°C (24 h), displayed in Figure 4.25. This correlates with the DSC data obtained with baclofen raw material (Figure 4.5). FT-IR absorbance peaks obtained for 1 h and 24 h samples displayed similar absorbance peaks (Table 4.7) as with baclofen raw material (Figure 4.9). The XRPD peaks of the excess baclofen (Figure 4.26) correlate with those of the baclofen raw material.

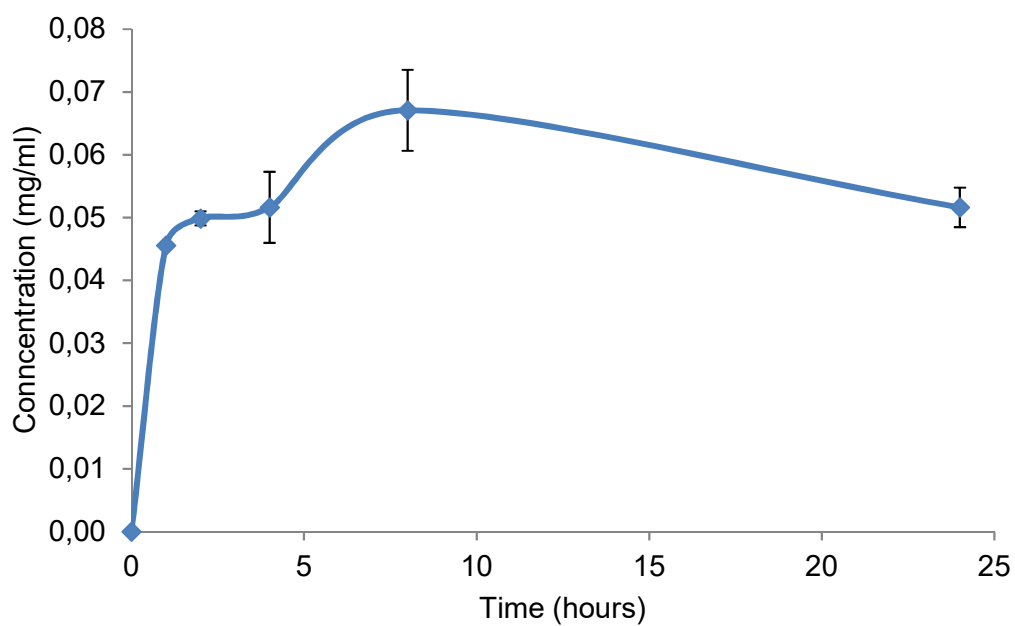


Figure 4.24: The solubility profile obtained for baclofen anhydrate 1-butanol over a period of 24 h at $37^{\circ}\text{C} \pm 0.5^{\circ}\text{C}$

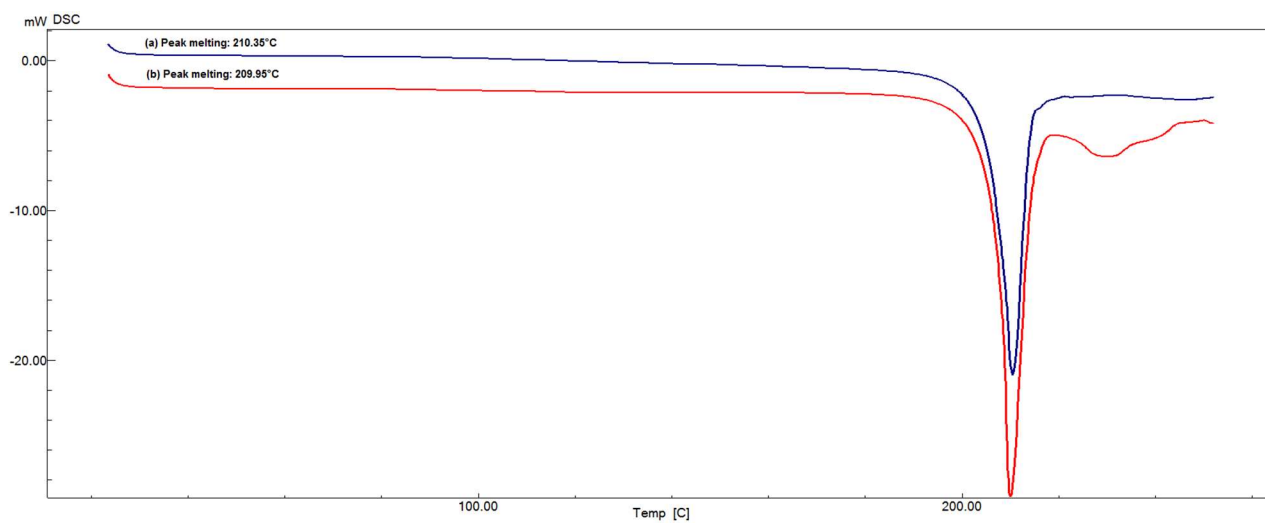
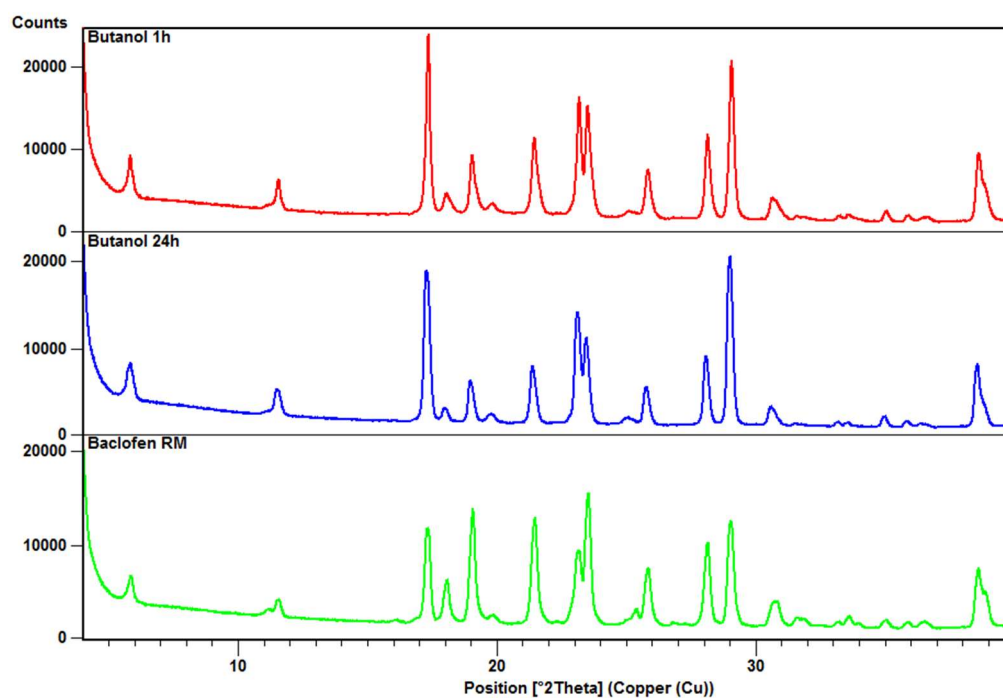


Figure 4.25: An overlay of the DSC thermogram obtained for baclofen in 1-butanol at 1 h (blue) and 24 h (red) at heating rate $10^{\circ}\text{C}/\text{min}$

Table 4.7: FT-IR peak listing reported for baclofen in 1-butanol

No:	Wavenumber (cm ⁻¹)			Functional groups
	Baclofen anhydrate	Baclofen excess 1 h	Baclofen excess 24 h	
1	-	523.7 – 539.13	523.7 – 539.13	C-Br
2	-	649.07	649.07	C-Cl
3	-	734.91 – 1094.65	734.91 – 1094.65	=C-H
4	1383.02	1383.02	1383.02	-α-CH ₃
5	1401.34	1400.38	1400.38	-α-CH ₂
6	1539.26	1534.44	1534.44	-COOH
7	1627.99	1627.99	1627.99	-NH ₂
8	1922.15	1922.15	1922.15	-C=C
9	2157.47	2157.47	2157.47	-C≡C
10	-	2500.82 – 2600	2500.82 – 2600	OH
11	2647.41	2645.48 - 2750.61	2647.41 - 2755.43	-C-H (aldehyde C-H)
12	2857.66	2857.66 - 2984.97	2857.66 - 2984.97	-CH (alkyl)

**Figure 4.26:** XRPD diffractograms obtained for baclofen in 1-butanol at 1 h (red), 4 h (blue) and baclofen anhydrate (green)

The baclofen concentration increase at the 8 h time interval was tested for an outlier using the Grubbs test and it was found that the increase was insignificant. FT-IR, DSC and XRPD, indicated no solid-state differences for baclofen in 1-butanol and therefore confirms that no solid-state transformation occurred.

4.5.3 2-Butanol

Solubility results obtained for baclofen in 2-butanol are displayed in Figure 4.27. Baclofen reached a concentration of 0.11 ± 0.004 mg/ml after 24 h. DSC, FT-IR and XPRD was done at 1 h and 24 h of the excess baclofen in the 2-butanol to examine the possibility of any crystallisation to another solid-state form. DSC results showed peak melting temperatures of 210.32°C (1 h) and 209.86°C (24 h) respectively, displayed in Figure 4.28, being similar to that of baclofen anhydrate. FT-IR performed on the excess baclofen in 2-butanol at 1 h and 24 h time intervals displayed no difference in absorbance peaks (Table 4.8). The XRPD peaks of the excess baclofen (Figure 4.29) correlates with those of the baclofen raw material.

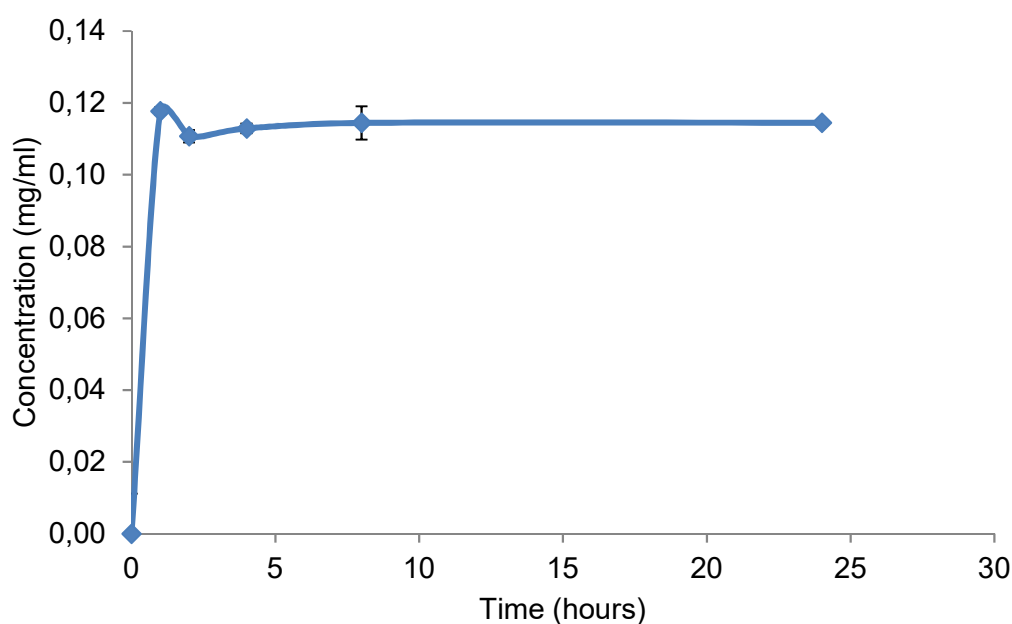


Figure 4.27: The solubility profile obtained for baclofen anhydrate in 2-butanol over a period of 24 h at $37^{\circ}\text{C} \pm 0.5^{\circ}\text{C}$

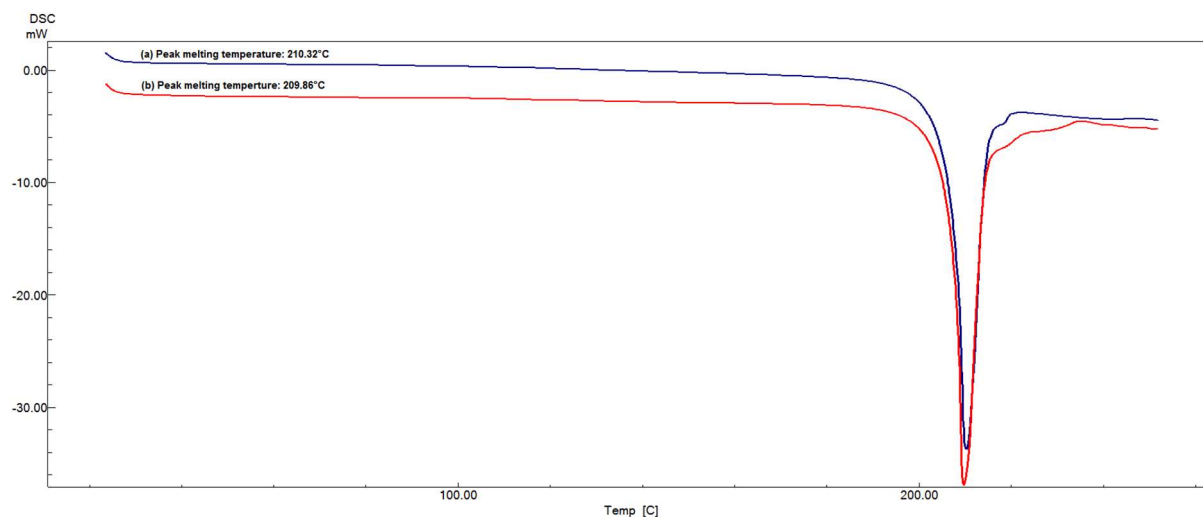


Figure 4.28: An overlay of the DSC thermogram obtained for baclofen in 2-butanol at 1 h (blue) and 24 h (red) at heating rate 10°C/min

Table 4.8: FT-IR peak listing reported for baclofen in 2-butanol

Wavenumber (cm ⁻¹)				
No:	Baclofen anhydrate	Baclofen excess 1 h	Baclofen excess 24 h	Functional groups
1	1383.02	1383.02	1383.02	-α-CH ₃
2	1401.34	1401.34	1400.38	-α-CH ₂
3	1539.26	1532.51	1532.51	-COOH
4	1627.99	1627.99	1627.99	-NH ₂
5	1922.15	1922.15	1922.15	-C=C
6	2157.47	2157.47	2157.47	-C≡C
7	2647.41 – 2755.43	2647.41 – 2755.43	2647.41 – 2755.43	-C-H (aldehyde C-H)
8	2857.66 – 2984.01	2857.66 – 2984.01	2857.66 – 2984.01	-CH (alkyl)

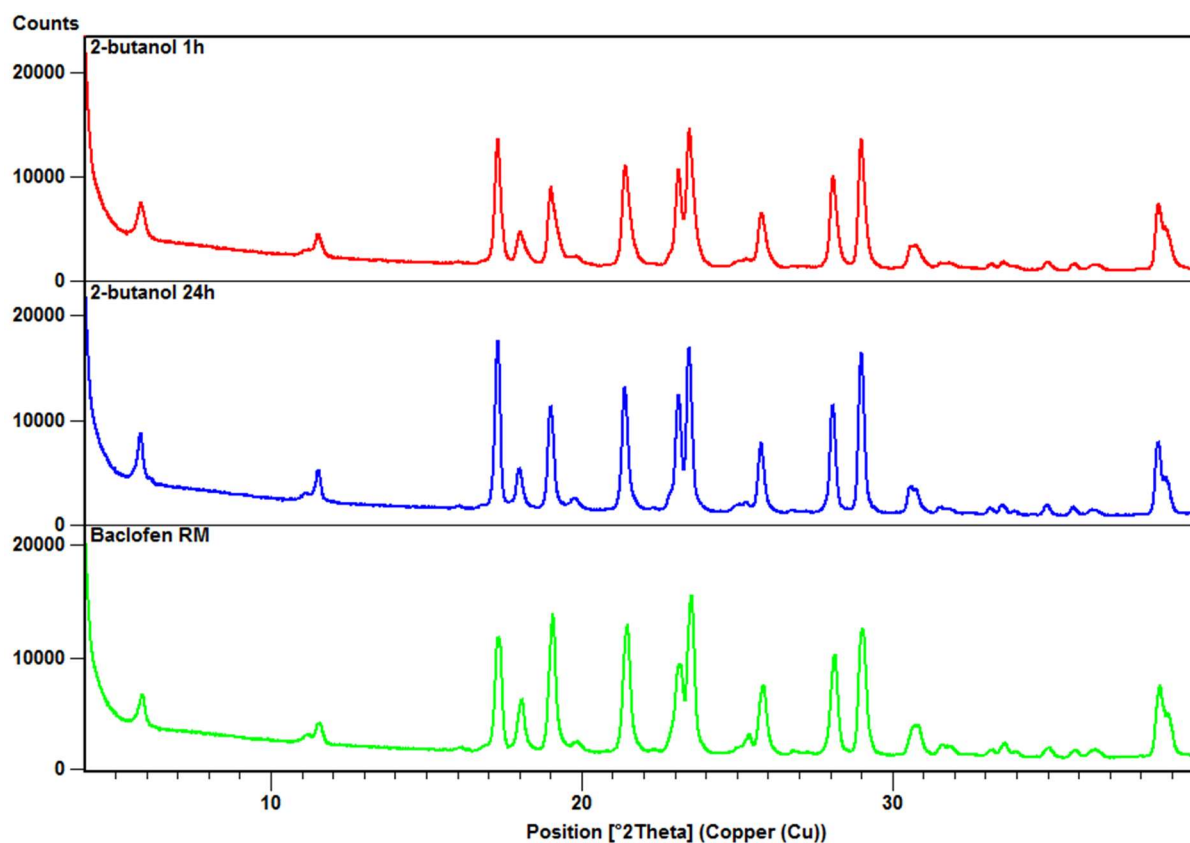


Figure 4.29: XRPD diffractograms obtained for baclofen in 2-butanol at 1 h (red), 4 h (blue) and baclofen anhydrate (green)

4.5.4 Ethanol

Solubility results obtained for baclofen in ethanol are displayed in Figure 4.30. Baclofen reached a dissolved concentration of 0.11 ± 0.0002 mg/ml after 24 h. DSC, FT-IR and XRPD was done at 1 h and 24 h of the excess baclofen in the ethanol to examine the changes that occurred. The results are displayed in Figures 4.30 – 4.32 and Table 4.9 and indicated no differences for baclofen in ethanol.

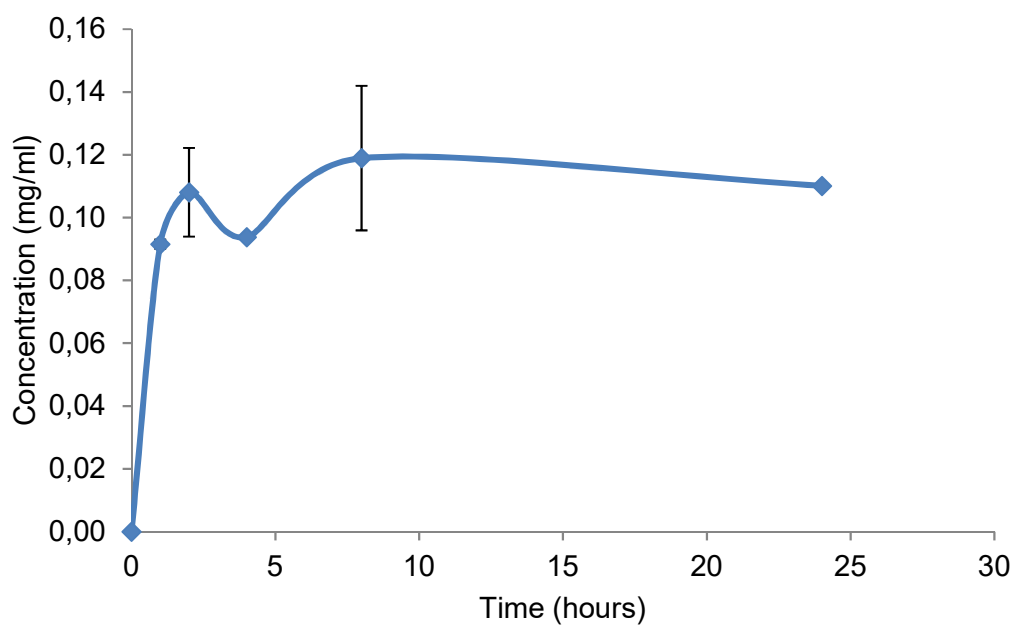


Figure 4.30: The solubility profile obtained for baclofen anhydrate in ethanol over a period of 24 h at $37^{\circ}\text{C} \pm 0.5^{\circ}\text{C}$

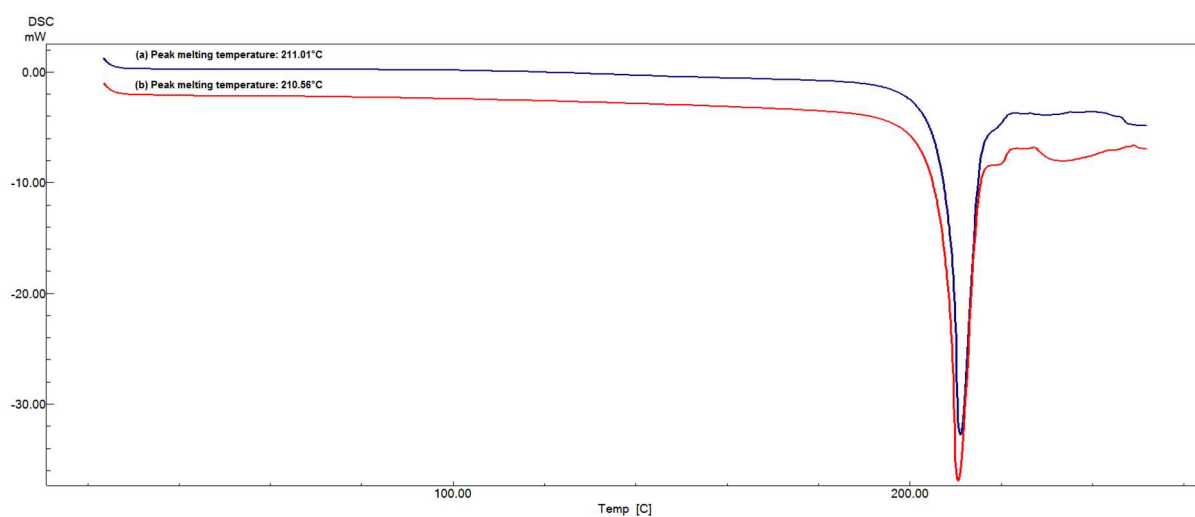


Figure 4.31: An overlay of the DSC thermogram obtained for baclofen in ethanol at 1 h (blue) and 24 h (red) at heating rate $10^{\circ}\text{C}/\text{min}$

Table 4.9: FT-IR peak listing reported for baclofen in ethanol

No:	Wavenumber (cm ⁻¹)			Functional groups
	Baclofen anhydrate	Baclofen excess 1 h	Baclofen excess 24 h	
1	1383.02	1383.02	1383.02	-α-CH ₃
2	1401.34	1400.38	1401.34	-α-CH ₂
3	1539.26	1533.47	1533.47	-COOH
4	1627.99	1627.99	1627.99	-NH ₂
5	1922.15	1922.15	1922.15	-C=C
6	2157.47	2157.47	2157.47	-C≡C
7	2647.41 - 2755.43	2647.41 - 2755.43	2647.41 - 2755.43	-C-H (aldehyde C-H)
8	2857.66 - 2984.01	2862.49 - 2984.97	2862.49 - 2984.97	-CH (alkyl)

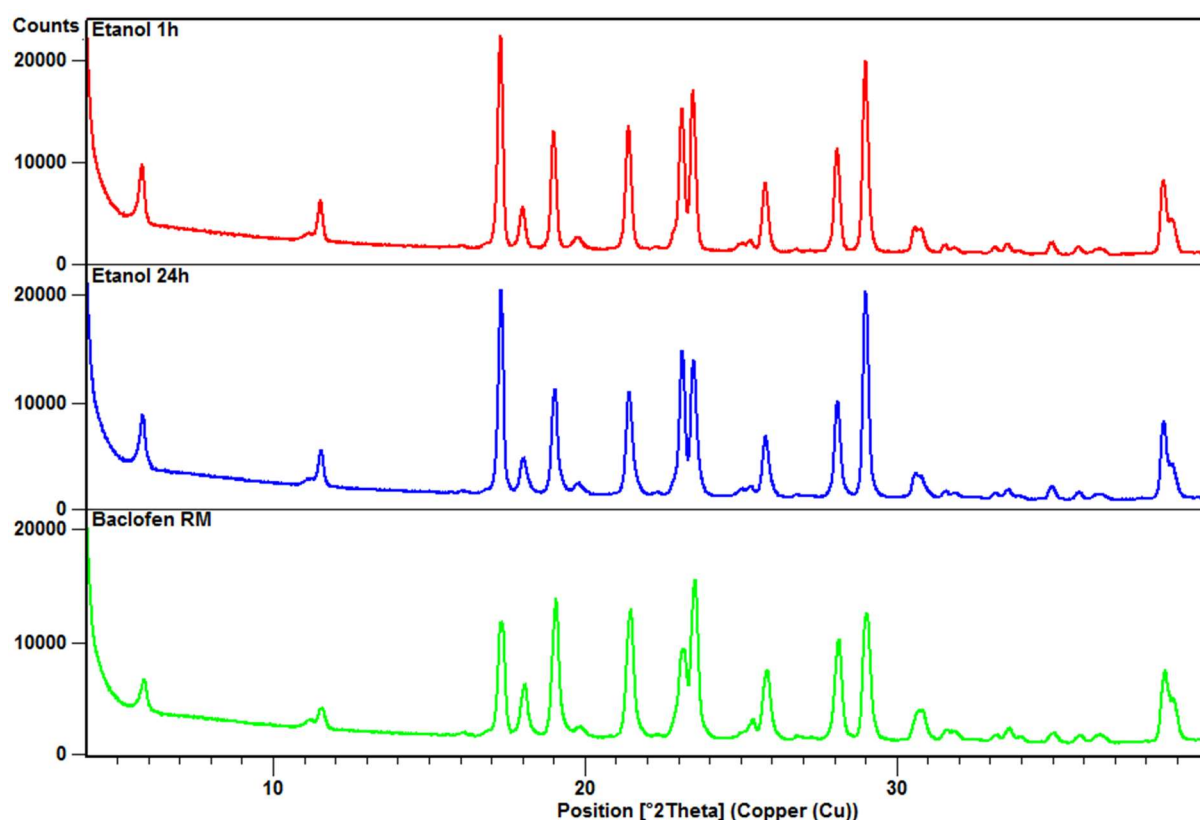


Figure 4.32: XRPD diffractograms obtained for baclofen in ethanol at 1 h (red), 4 h (blue) and baclofen anhydrate (green)

4.5.5 Methanol

Solubility results obtained for baclofen in methanol are displayed in Figure 4.33. Baclofen reached a concentration of 0.20 ± 0.01 mg/ml after 24 h. DSC, FT-IR and XPRD was done at 1 h and 24 h of the excess baclofen in the methanol. The results are presented in Figures 4.34 and 4.35 as well as Table 4.10 and correlates with that of baclofen anhydrate.

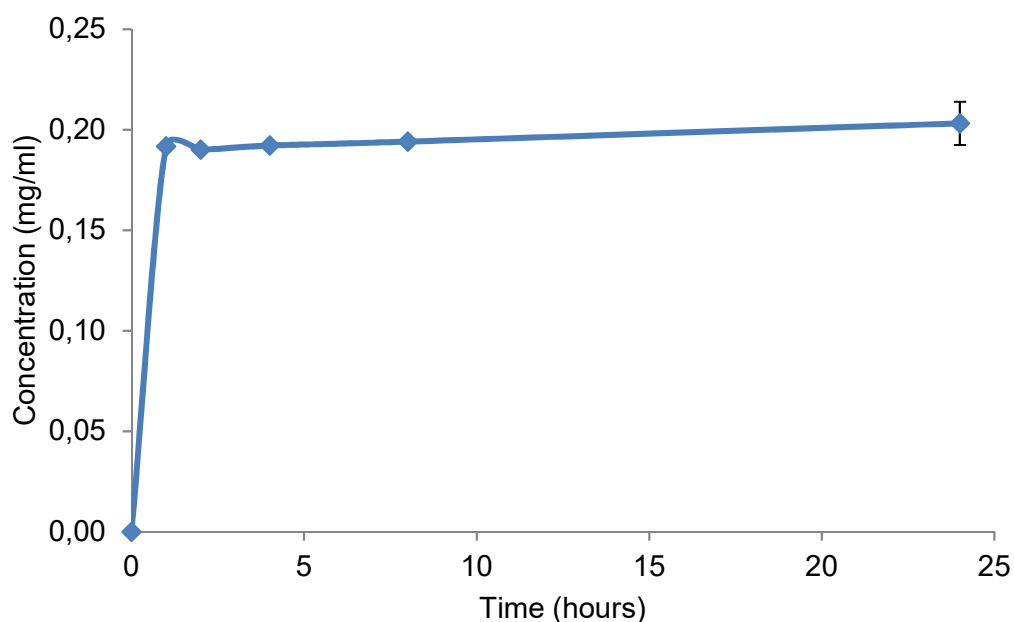


Figure 4.33: The solubility profile obtained for baclofen anhydrate methanol over a period of 24 h at $37^{\circ}\text{C} \pm 0.5^{\circ}\text{C}$

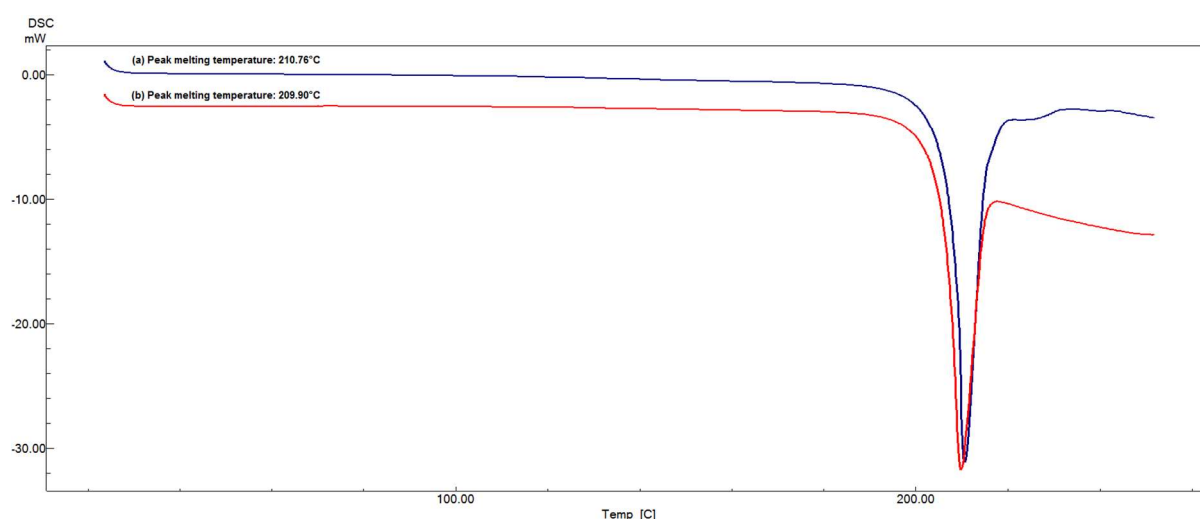


Figure 4.34: An overlay of the DSC thermogram obtained for baclofen in methanol at 1 h (blue) and 24 h (red) at heating rate $10^{\circ}\text{C}/\text{min}$

Table 4.10: FT-IR peak listing reported for baclofen in methanol

No:	Wavenumber (cm ⁻¹)			Functional groups
	Baclofen anhydrate	Baclofen excess 1 h	Baclofen excess 24 h	
1	1383.02	1383.02	1383.02	-α-CH ₃
2	1401.34	1400.38	1401.34	-α-CH ₂
3	1539.26	1533.47	1533.47	-COOH
4	1627.99	1627.99	1627.99	-NH ₂
5	1922.15	1922.15	1922.15	-C=C
6	2157.47	2157.47	2157.47	-C≡C
7	2647.41 - 2755.43	2647.41 - 2755.43	2647.41 - 2755.43	-C-H (aldehyde C-H)
8	2857.66 - 2984.01	2846.09 - 2984.97	2846.09 - 2984.97	-CH (alkyl)

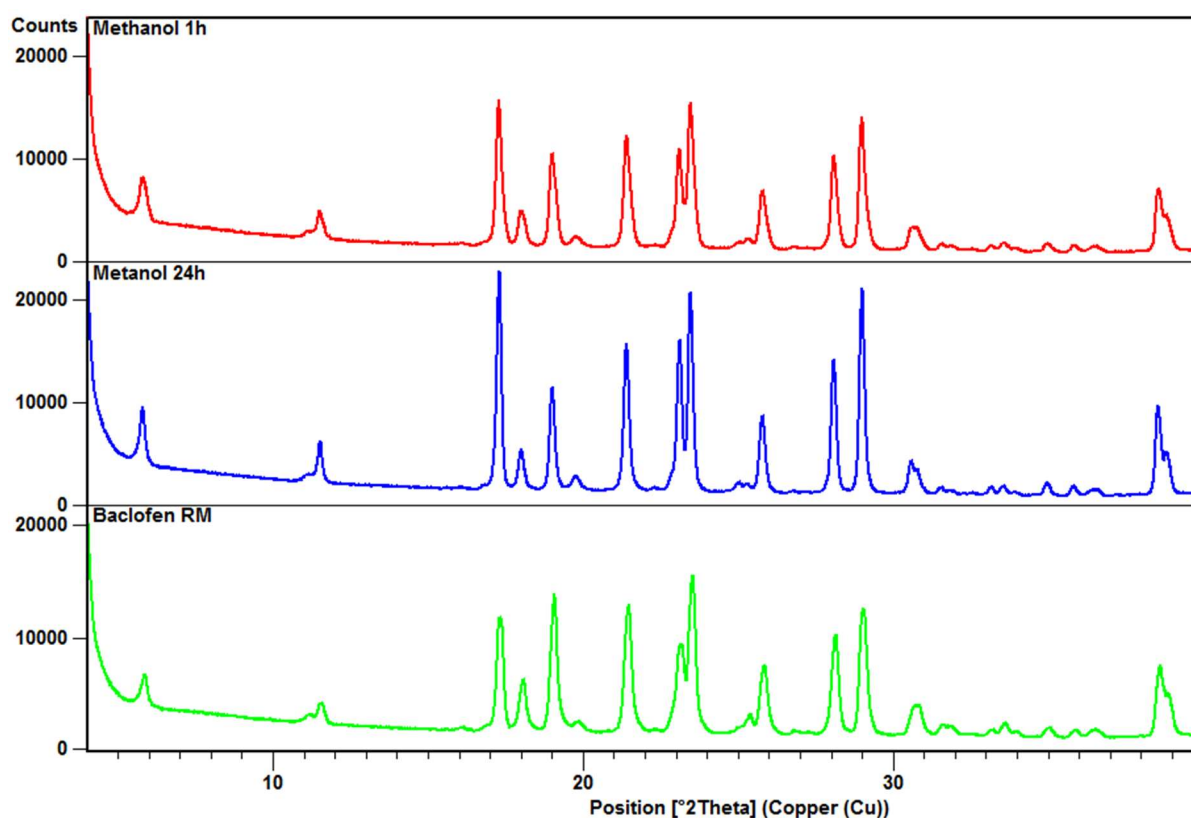


Figure 4.35: XRPD diffractograms obtained for baclofen in methanol at 1 h (red), 4 h (blue) and baclofen anhydrate (green)

4.5.6 1-Propanol

Solubility results obtained for baclofen in 1-propanol are displayed in Figure 4.36. Baclofen reached a concentration of 0.06 ± 0.001 mg/ml after 24 h. DSC, FT-IR and XPRD was done at 1 h and 24 h of the excess baclofen in the 1-propanol (Figures 4.37 – 4.38 and Table 4.11).

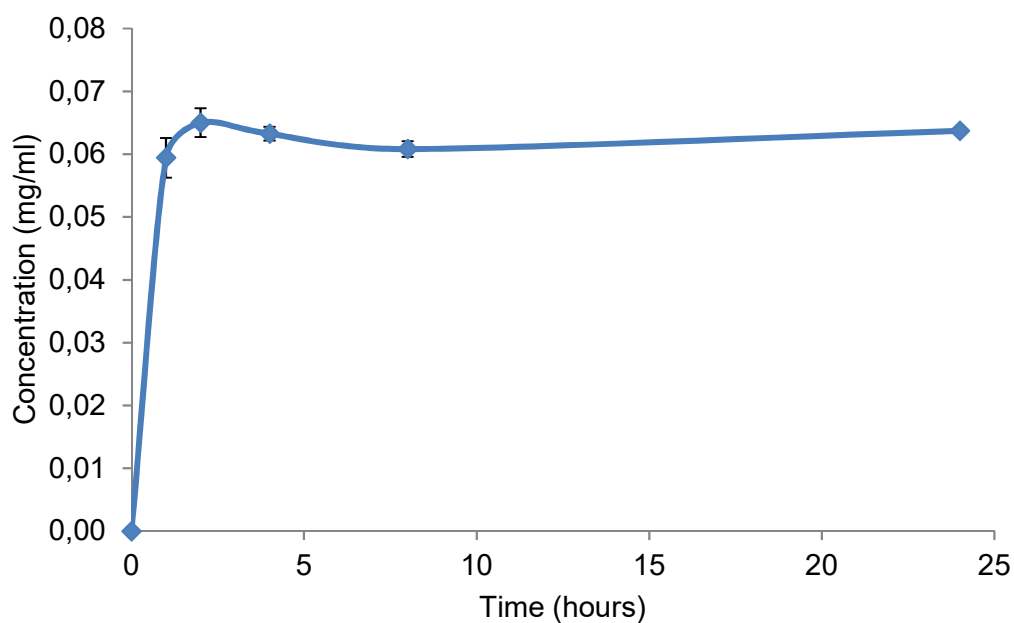


Figure 4.36: The solubility profile obtained for baclofen anhydrate in 1-propanol over a period of 24 h at $37^{\circ}\text{C} \pm 0.5^{\circ}\text{C}$

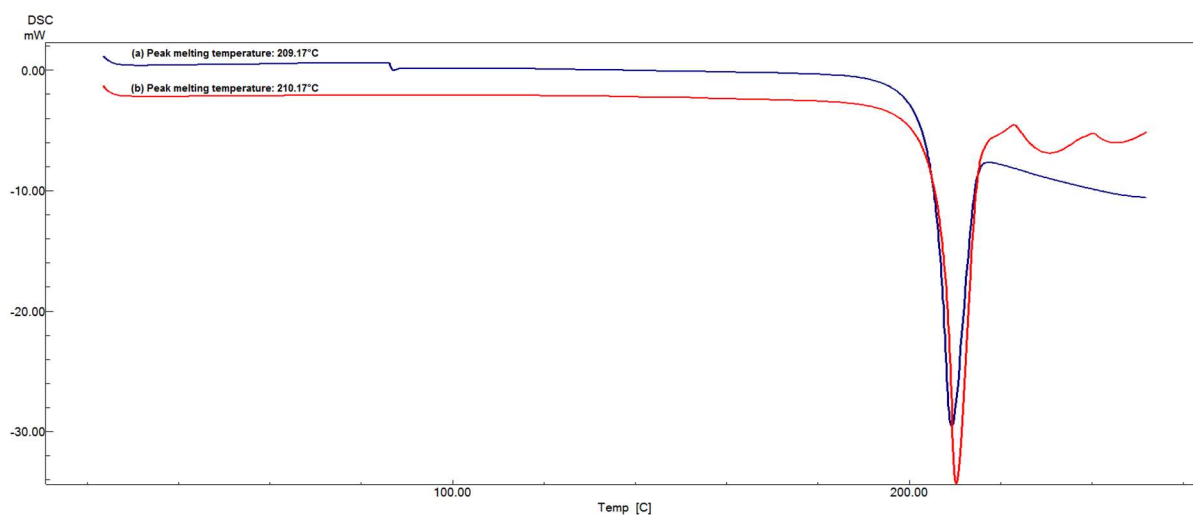


Figure 4.37: An overlay of the DSC thermogram obtained for baclofen in 1-propanol at 1 h (blue) and 24 h (red) at heating rate $10^{\circ}\text{C}/\text{min}$

Table 4.11: FT-IR peak listing reported for baclofen in 1-propanol

No:	Wavenumber (cm ⁻¹)			Functional groups
	Baclofen anhydrate	Baclofen excess 1 h	Baclofen excess 24 h	
1	1383.02	1383.02	1383.02	-α-CH ₃
2	1401.34	1400.38	1401.34	-α-CH ₂
3	1539.26	1533.47	1533.47	-COOH
4	1627.99	1627.99	1627.99	-NH ₂
5	1922.15	1922.15	1922.15	-C=C
6	2157.47	2157.47	2157.47	-C≡C
7	2647.41 - 2755.43	2647.41 - 2755.43	2647.41 - 2755.43	-C-H (aldehyde C-H)
8	2857.66 - 2984.01	2857.66 - 2984.01	2857.66 - 2984.01	-CH (alkyl)

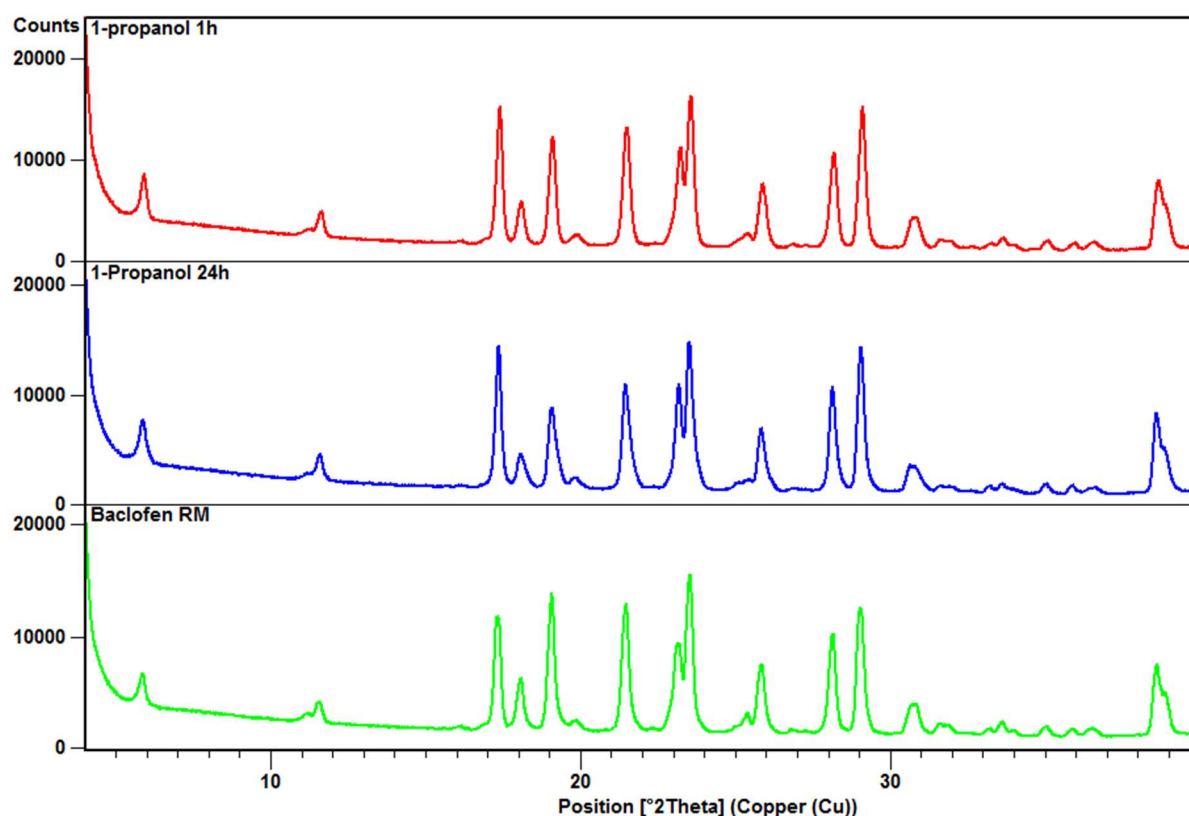


Figure 4.38: XRPD diffractograms obtained for baclofen in 1-propanol at 1h (red), 4 h (blue) and baclofen anhydrate (green)

4.5.7 2-Propanol

Solubility results obtained for baclofen in 2-propanol are displayed in Figure 4.39. Baclofen reached a concentration of 0.03 ± 0.0005 mg/ml after 24 h. DSC, FT-IR (Table 4.12) and XPRD was done at 1 h and 24 h of the excess baclofen in the 2-propanol (Figures 4.40 – 4.41).

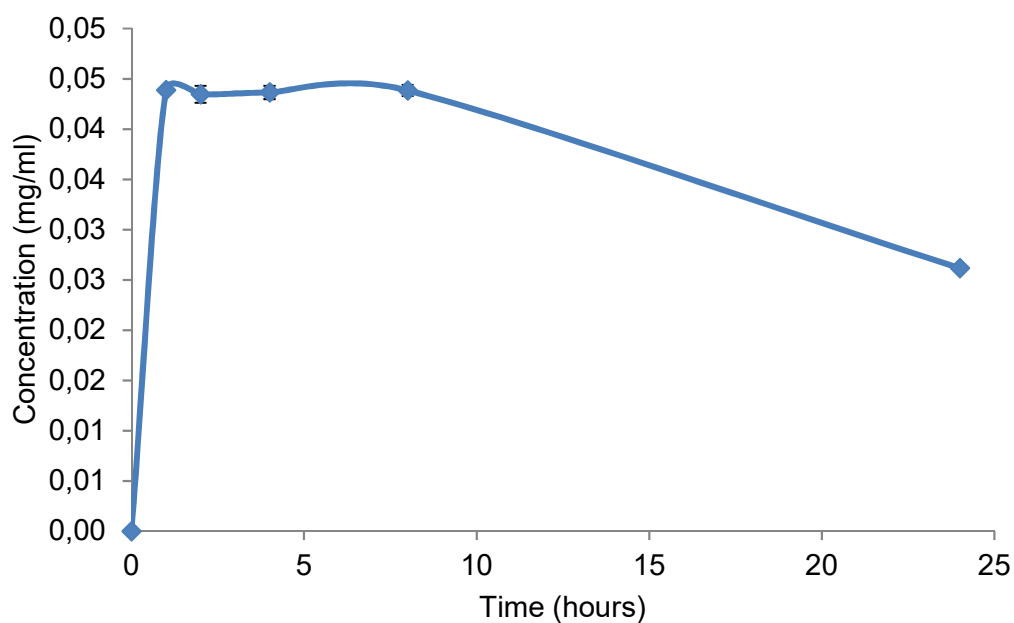


Figure 4.39: The solubility profile obtained for baclofen anhydrate in 2-propanol over a period of 24 h at 37°C

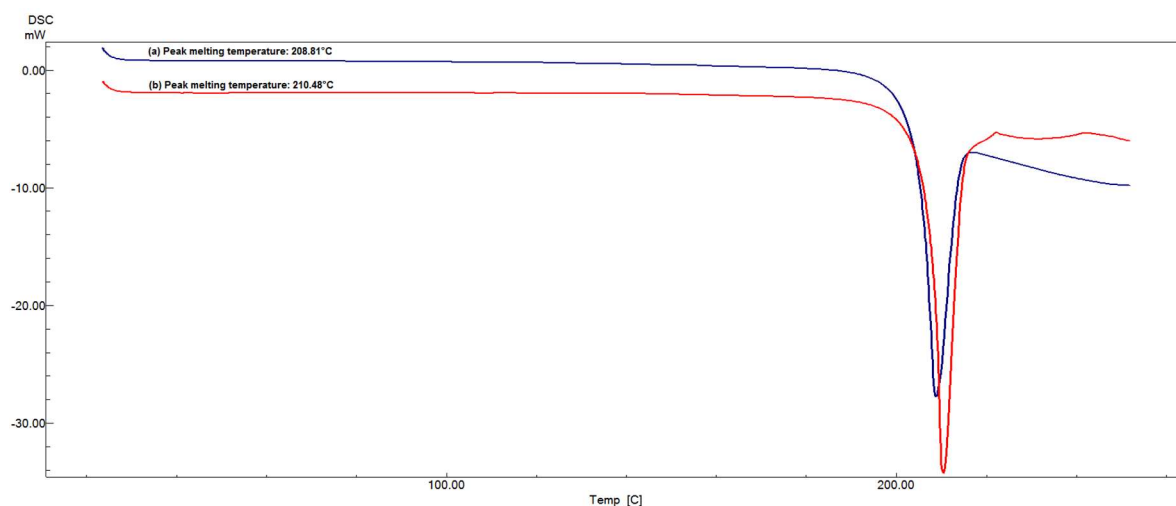
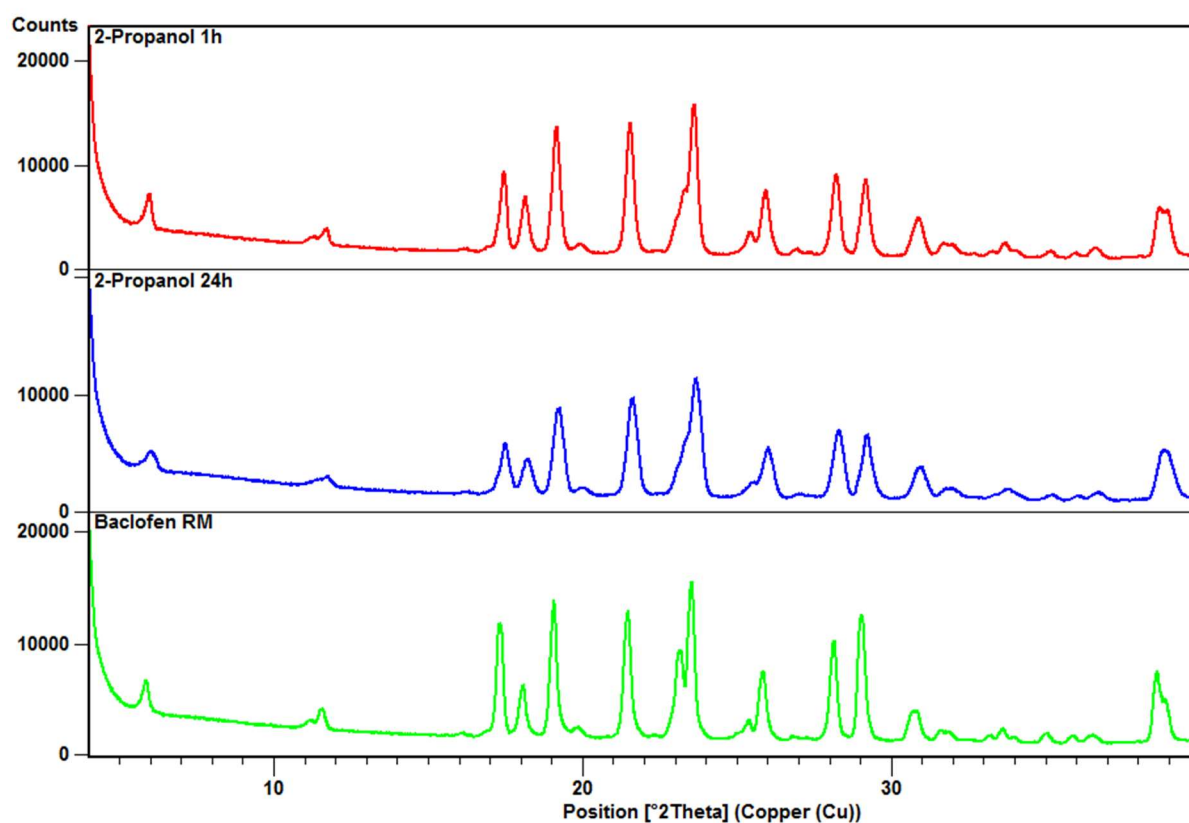


Figure 4.40: An overlay of the DSC thermogram obtained for baclofen in 2-propanol at 1 h (blue) and 24 h (red) at heating rate 10°C/min.

Table 4.12: FT-IR peak listing reported for baclofen in 2-propanol

No:	Wavenumber (cm ⁻¹)			Functional groups
	Baclofen anhydrate	Baclofen excess 1 h	Baclofen excess 24 h	
1	1383.02	1383.02	1383.02	-α-CH ₃
2	1401.34	1400.38	1401.34	-α-CH ₂
3	1539.26	1533.47	1533.47	-COOH
4	1627.99	1627.99	1627.99	-NH ₂
5	1922.15	1922.15	1922.15	-C=C
6	2157.47	2157.47	2157.47	-C≡C
7	2647.41 - 2755.43	2647.41 - 2755.43	2647.41 - 2755.43	-C-H (aldehyde C-H)
8	2857.66 - 2984.01	2856.70 - 2984.97	2836.45 - 2984.97	-CH (alkyl)

**Figure 4.41:** XRPD diffractograms obtained for baclofen in 2-propanol at 1 h (red), 4 h (blue) and baclofen anhydrate (green)

The Grubbs test indicated the 24 h time interval concentration as a significant outlier $P < 0.05$. This could show a possibility of degradation or recrystallisation product, however, the FT-IR, XRPD and DSC results indicated that no solid-state transformation occurred.

4.5.9 Conclusion

Baclofen anhydrate is slightly soluble in acetone, very slightly soluble in 2-butanol, ethanol and methanol and practically insoluble in 1-butanol, 1-propanol and 2-propanol (Figure 4.42 and Table 4.13). Acetone, 2-butanol and ethanol had what appeared to be phase transitions, however, after the excess powder was examined through DSC, FT-IR and XRPD it was observed the excess powder had the same physico-chemical properties as baclofen raw material (anhydrate).

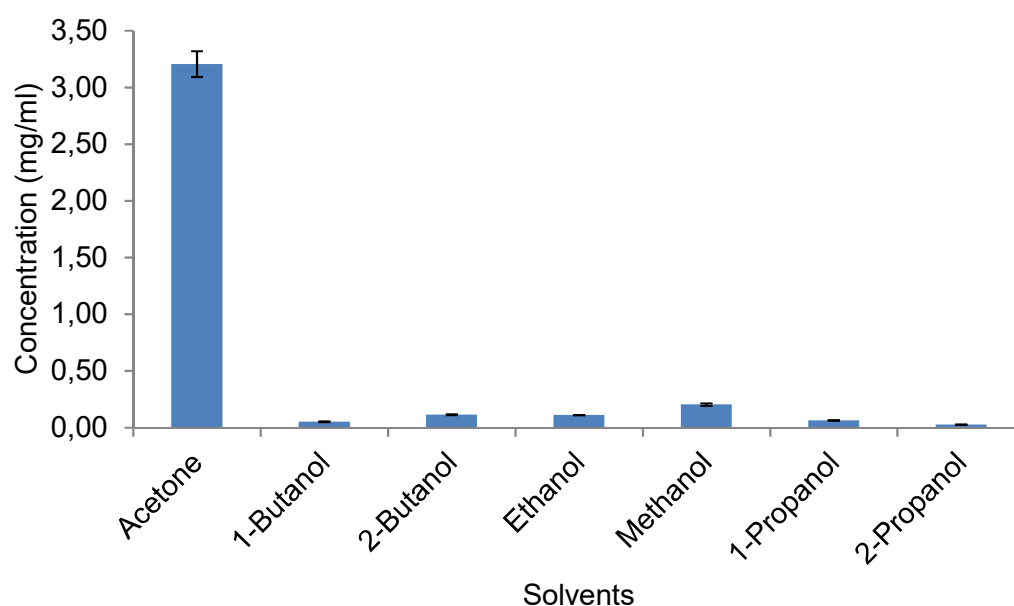


Figure 4.42: Summary of solubilities of baclofen in the different organic solvents

Table 4.13: Presentation of the concentrations obtained for the different solvents

Solvent	Concentration (mg/ml)
Acetone	3.21 ± 0.11
1-butanol	0.05 ± 0.003
2-butanol	0.11 ± 0.004
Ethanol	0.11 ± 0.0002
Methanol	0.20 ± 0.01
1-propanol	0.06 ± 0.001
2-propanol	0.03 ± 0.005

4.6 Quench cooling

Since none of the recrystallisation efforts resulted in new solid-state forms, the method of quench cooling of the melt was used as a last endeavour. Quench cooling of baclofen raw material was performed according to the method provided in Chapter 3, paragraph 3.3.1. This method did not render baclofen in an amorphous solid-state form. Upon quench cooling the molten baclofen recrystallised rapidly. Characterisation of the recrystallised baclofen upon quench cooling was done by means of TM, FT-IR and XRPD.

4.6.1 Hot-state microscopy (HSM)

Heating of the quench cooled baclofen started at an ambient temperature of 20.5°C (Figure 4.43 (a)) at a heating rate of 10°C/min. Melting was observed at 122°C (Figure 4.43 (b)) and upon cooling of the molten sample the same recrystallised sample was obtained (Figure 4.43 (c)).

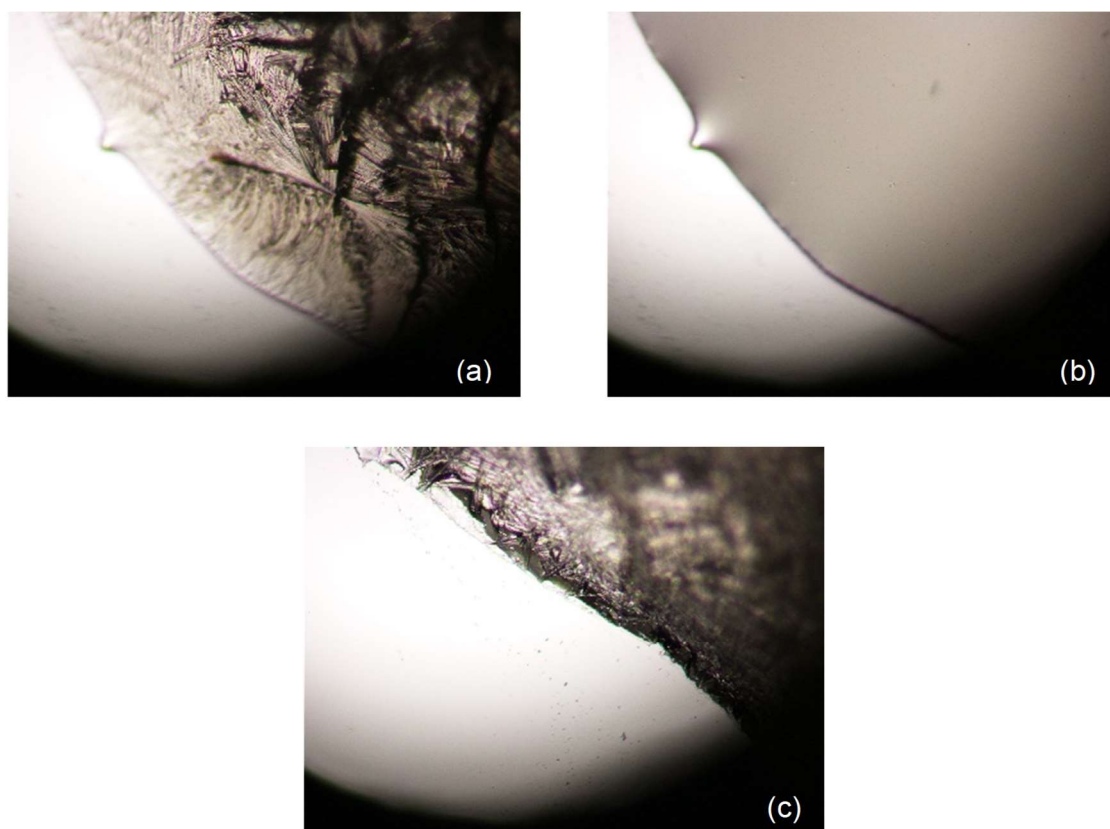


Figure 4.43: Photomicrographs obtained for recrystallised baclofen obtained after quench cooling of molten baclofen at 20.5°C (a), the recrystallised baclofen melted at 122°C (b) and the recrystallisation of the melt upon subsequent cooling 20.5°C (c)

4.6.2 Fourier-Transform infrared spectroscopy (FT-IR)

Major peaks of the monohydrate can be observed at 809.17, 1014.60, 1090.79, 1260.54, 1348.30, 1494.90, 1699.36, 1895.14, 2130.47, 2517.21, 2879.85, 3094.92 and 3194.26 cm^{-1} . The main differences between baclofen anhydrate and the melt quench cooled baclofen were observed in the region between 800 and 1300 cm^{-1} . This includes functional groups such as -C-H, -C-O and -C=O which indicates that the quenched cooled baclofen differs from baclofen anhydrate. The recrystallised baclofen also doesn't have the -OH groups that the monohydrate has. This indicates that there is no water in the structure.

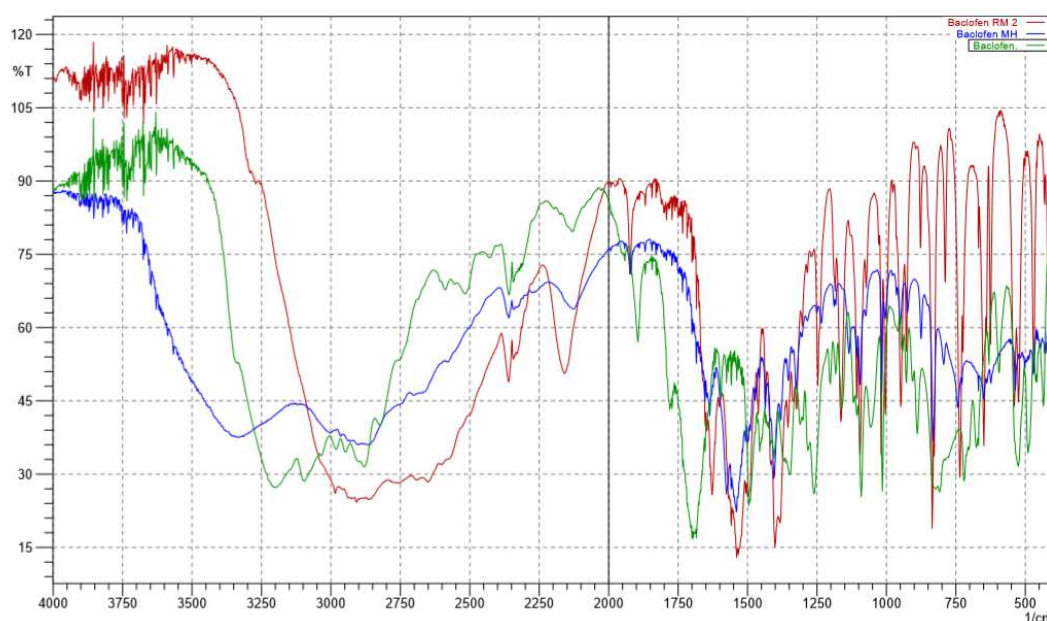


Figure 4.44: An overlay of the FT-IR spectra obtained for baclofen anhydrate (red), monohydrate (blue) and melt recrystallised baclofen (green)

Table 4.14: FT-IR peak listing reported for melt recrystallised baclofen

	Wavenumber (cm^{-1})		
No:	Baclofen anhydrate	Baclofen melt recrystallisation	Functional groups
1	-	809.17	-C-H
2	-	1014.60 – 1260.54	-C-O
3	1383.02	1348.30	- α -CH ₃
4	1401.34	1494.90	- α -CH ₂
5	1539.26	-	-COOH
6	1627.99	1699.36	-NH ₂

Table 4.14 continued: FT-IR peak listing reported for melt recrystallised baclofen

No:	Wavenumber (cm ⁻¹)		
	Baclofen anhydrate	Baclofen melt recrystallisation	Functional groups
7	-	1895.14	-C=O
8	1922.15	-	-C=C
9	2157.47	2130.47	-C≡C
10	2647.41 – 2755.43	2517.21	-C-H (aldehyde C-H)
11	2857.66 – 2984.01	2879.85	-CH (alkyl)
12	-	3094.92	=C-H & =CH ₂ (usually sharp)
13	-	3194.26	=C-H & =CH ₂ (usually sharp)

4.6.3 X-Ray powder diffraction (XRPD)

The XRPD for the quenched cooled baclofen (Figure 4.45) shows the position of the most observed diffraction peaks at 20.21, 22.28, 23.99 and 31.40°2θ while it has been reported by Mirza *et al.*, 2007 that the major peaks in baclofen can be observed at 5.8, 17,5 23.4 and 29.4 indicating that the quenched cooled form differs from baclofen.

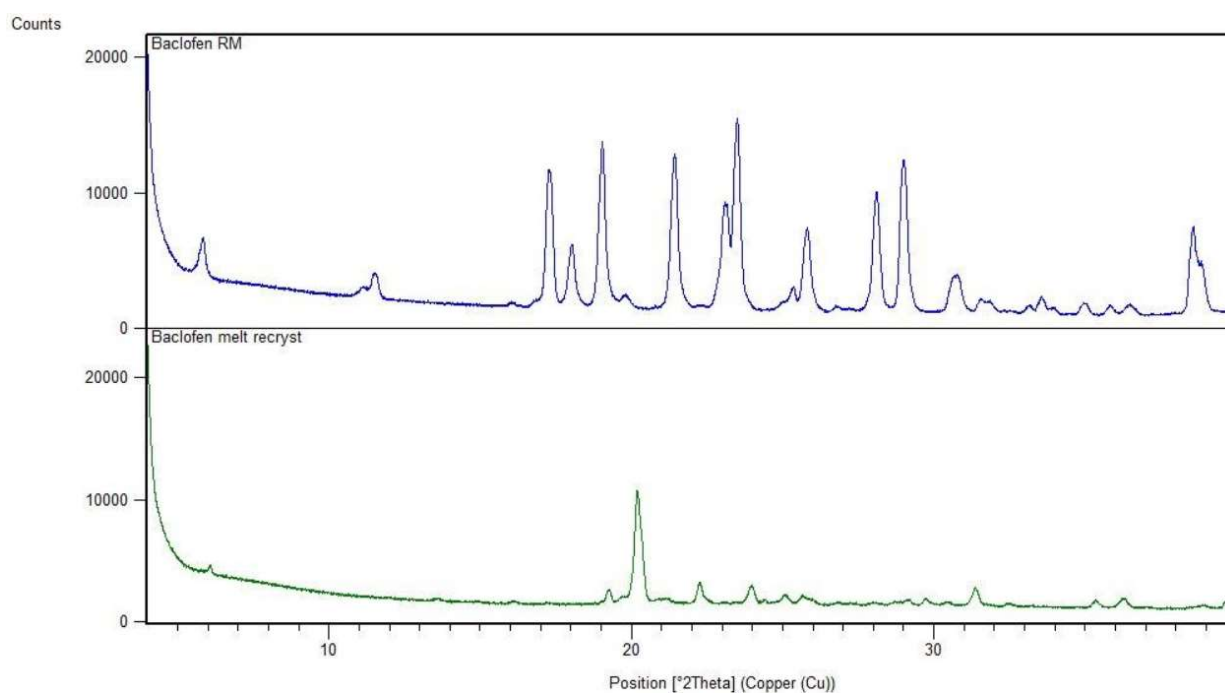


Figure 4.45: XRPD diffractograms obtained for baclofen anhydrate and melt recrystallised baclofen

Table 4.15: XRPD peak listing reported for melt recrystallised baclofen

Baclofen anhydrate			Baclofen melt recrystallisation		
Position [°2Th.]	d-Spacing [Å]	Relative Peak Intensity [%]	Position [°2Th.]	d-Spacing [Å]	Relative Peak Intensity [%]
5.88	15.04	18.37	-	-	-
17.25	5.14	66.35	-	-	-
17.41	5.09	56.80	-	-	-
18.07	4.91	33.23	-	-	-
19.08	4.65	86.81	-	-	-
-	-	-	20.21	4.39	100.00
21.48	4.14	81.01	-	-	-
-	-	-	22.28	3.99	20.01
23.07	3.86	54.16	-	-	-
23.20	3.83	54.91	-	-	-
23.55	3.78	100.00	-	-	-
-	-	-	23.99	3.71	17.26
25.85	3.45	45.17	-	-	-
28.15	3.17	65.25	-	-	-
28.91	3.09	53.99	-	-	-
29.08	3.07	76.18	-	-	-
30.65	2.92	18.69	-	-	-
30.84	2.89	19.26	-	-	-
-	-	-	31.40	2.85	16.99
38.59	2.33	47.26	-	-	-
38.87	2.32	28.83	-	-	-

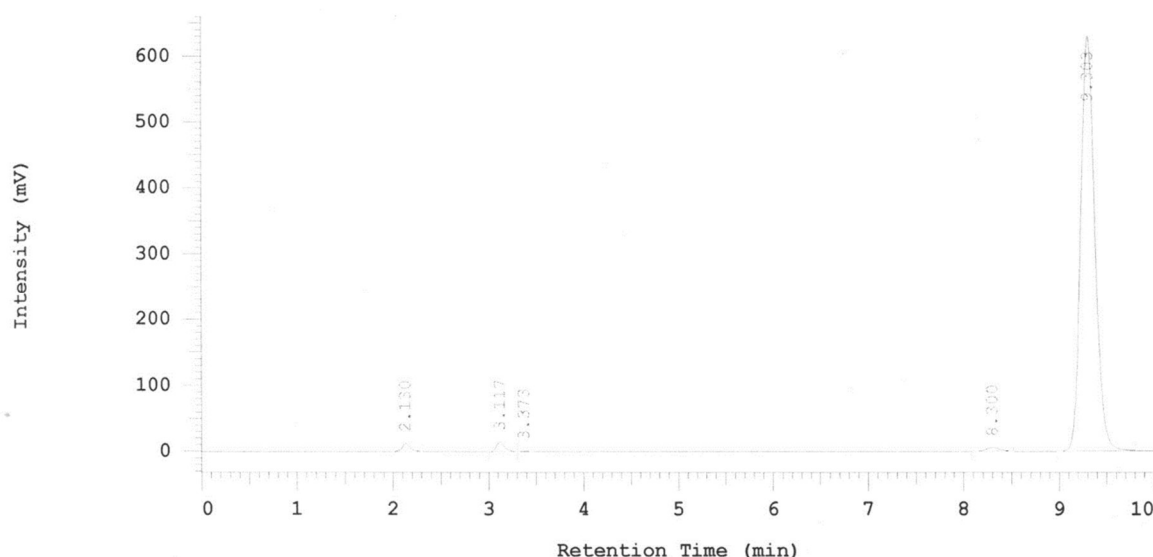


Figure 4.46: Chromatogram obtained for melt recrystallised baclofen

4.6.4 Conclusion

The goal was to investigate if different solid-state forms of baclofen exist. The method of quench cooling of the melt at first indicated a new crystallised solid-state form. However, on further investigation the purity test, using HPLC, indicated that it was not a different solid-state form for baclofen but rather a related product (Figure 4.46).

Overall, it can be concluded that baclofen can exist only as an anhydrate and a monohydrate, with the monohydrate being a very unstable, transient solid-state form that can only exist either in a supersaturated solution or in an environment where sufficient water is available. The fact that baclofen anhydrate starts to recrystallise to baclofen monohydrate at a relative humidity of 35% is quite troublesome. Thus meaning that raw material as well as dosage form manufacturers of baclofen should be aware of the possible solvent-mediated phase transformation.

References

- Abdelkader, H., Youssef Abdalla, O. & Salem, H. 2008. Formulation of Controlled-Release Baclofen Matrix Tablets II: Influence of Some Hydrophobic Excipients on the Release Rate and In Vitro Evaluation. *AAPS PharmSciTech*, 9(2):675-683.
- Aucamp, M., Stieger, N., Barnard, N. & Liebenberg, W. 2013. Solution-mediated phase transformation of different roxithromycin solid-state forms: Implications on dissolution and solubility. *International journal of pharmaceutics*, 449(1-2):18-27.
- Burnett, D.J., Thielmann, F. & Booth, J. 2004. Determining the critical relative humidity for moisture-induced phase transitions. *International journal of pharmaceutics*, 287(1-2):123-133.
- Jivania, R.R., Patelb, C.N., Patelb, D.M. & Jivania, N.P. 2010. Development of a novel floating *in-situ* gelling system for stomach specific drug delivery of the narrow absorption window drug baclofen. *Iranian journal of pharmaceutical research*, 9(4):359-368.
- Magnusson, B and Örnemark, U. 2014. A laboratory guide to method validation and related topics. (Eurachem guide. Second edition: The fitness for purpose of analytical methods).
- Mirza, S., Miroshnyk, I., Rantanen, J., Aalonen, J., Harjula, P., Kiljunen, E., Heinämäki, J. & Yliruusi, J. 2007. Solid-state properties and relationship between anhydrate and monohydrate of baclofen. *Journal of pharmaceutical sciences*, 96(9):2399-2408.
- Moffat, A., Osselton, M., Widdop, B. & Watts, J. 2011. Monographs (Clarke's analysis of drugs and poisons. 14th ed. London: Pharmaceutical Press. P. 809-2262).
- Ymén, I. 2011. Introduction to the solid state-physical properties and processes. (In Storey, R.A. & Ymén, I. *ed.* Solid state characterization of pharmaceuticals. West Sussex, United Kingdom: Wiley. p. 1-34).

CHAPTER 5

SOLUBILITY, DISSOLUTION AND PERMEABILITY STUDIES OF BACLOFEN

5.1 Introduction

From the previous chapter it was concluded that baclofen can exist in only two solid-state forms, namely the anhydrate and the monohydrate. The monohydrate was characterised as a very unstable, transient solid-state form of baclofen. The data indicated that the monohydrate dehydrates very easily and for that reason it was decided to examine how easily and quickly the dehydration and hydration can occur. Further it is important to determine if this phase transition will have any influence on the solubility or dissolution in the different bio-relevant media.

5.2 Equilibrium solubility in bio-relevant media

Hydrates, in general, will be less soluble than the anhydrate form in water because the hydrated form already has water-hydrogen bonds and the free energy that are released upon further bonding with the solvent water molecules is less than from the anhydrated form and there are fewer sites on the molecule available for interaction (Babu & Nangia, 2011; Censi & Di Martino, 2015; Khankari & Grant, 1994). This leads to the hydrated form being less soluble than the anhydrated form (Babu & Nangia, 2011; Khankari & Grant, 1994). The physical stability of the anhydrate and hydrate forms will depend on the relative humidity and/or the temperature of the environment (Censi & Di Martino, 2015). There is no solubility data available in literature of baclofen in any organic solutions and this was also considered a reliable method to identify if any other solid-state forms may form when the solution is near supersaturation.

Solubility of baclofen anhydrate in bio-relevant media was performed according to the method provided in Chapter 3, paragraph 3.3.2.9. During the course of this study the equilibrium solubilities of baclofen raw material were determined in distilled water and different bio-relevant media since the pH solubility profile may influence the dissolution and permeability of baclofen (Bock *et al.*, 2003).

5.2.1 Distilled water

The solubility results obtained for baclofen in distilled water are displayed in Figure 5.1. Baclofen reached a concentration of 3.71 ± 0.03 mg/ml at 37°C, which is lower than the solubility of baclofen in distilled water reported in literature at 6 mg/ml at ambient temperature (Cruaud *et al.*, 1999). FT-IR and XPRD was done at 1h, 4h and 24h and DSC was done at 1h and 24h of the excess baclofen in the distilled water to examine if any phase transformation to the monohydrate occurred. The results are provided in Figures 5.2 – 5.4. DSC was performed on excess baclofen within distilled water at 1h and 24h with a peak melting temperature of 206.6°C and 203.9°C

respectively, displayed in Figure 5.2. These melting temperatures do not correlate with baclofen raw material with a peak temperature of 213.93°C but rather that of the reported baclofen monohydrate (Figure 4.12) this can indicate that hydration of baclofen took place leading to the formation of the monohydrate in a supersaturated solution. FT-IR performed on the excess baclofen in distilled water at 1 h and 24 h displayed in Figure 5.3 and Table 5.1 showed correlation with the peaks of baclofen anhydrate (Figure 4.9). The XRPD peaks of the excess baclofen (Figure 5.3) also correlates with those of baclofen anhydrate (Figure 4.10).

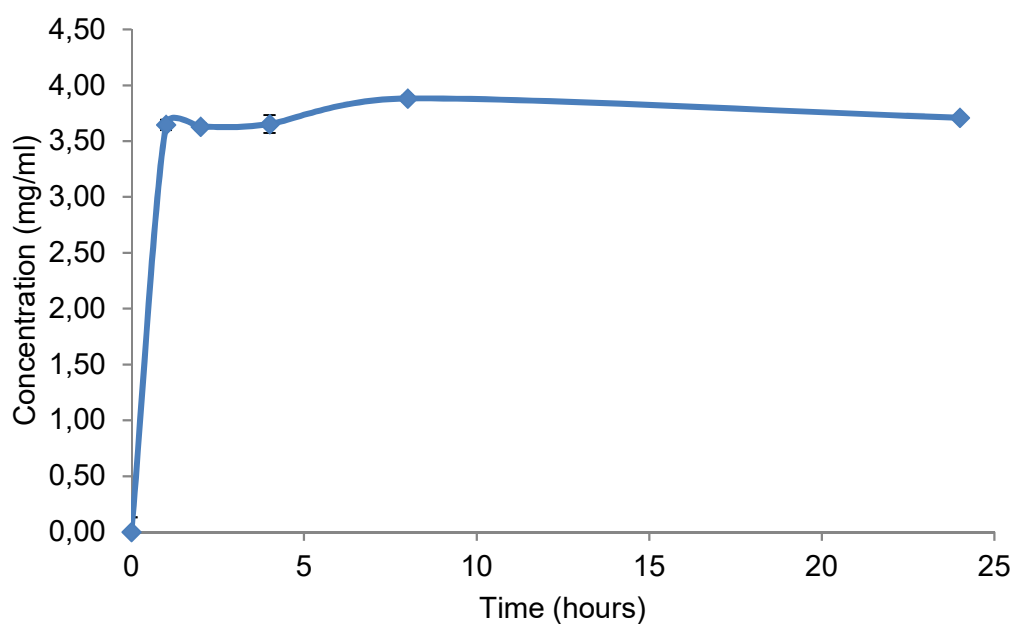


Figure 5.1: The solubility profile obtained for baclofen anhydrate in distilled water over a period of 24 h at 37°C ± 0.5°C

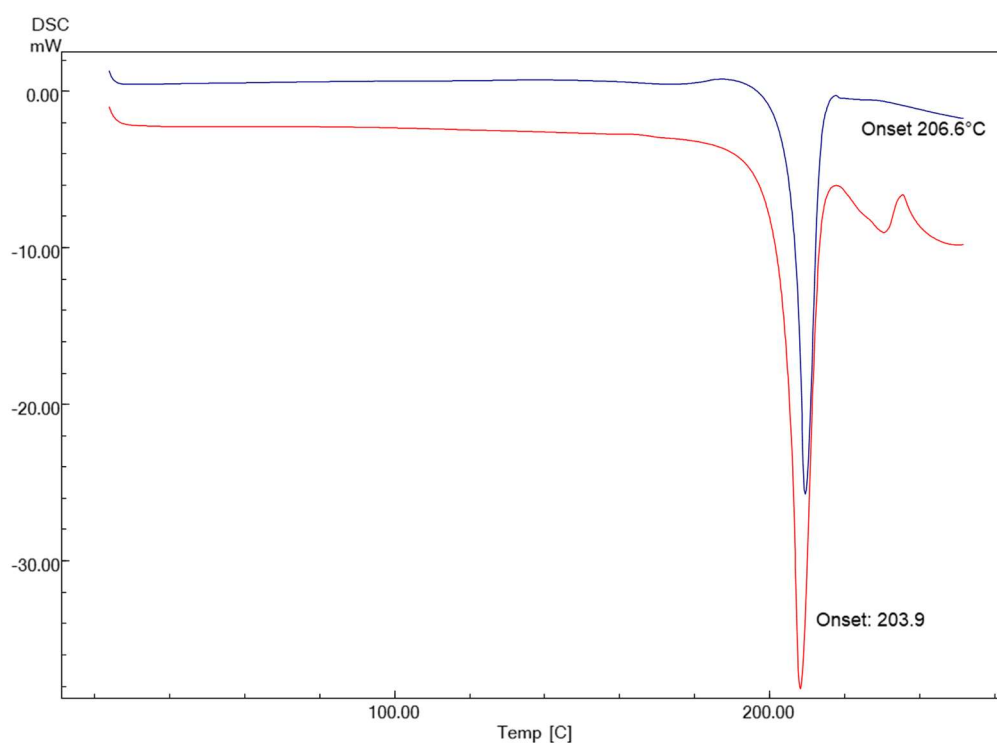


Figure 5.2: The DSC thermogram obtained for baclofen in distilled water at 1 h (blue) and 24 h (red) with a heating rate 10°C/min

Table 5.1: FT-IR peak listing reported for baclofen in distilled water

No:	Wavenumber (cm ⁻¹)			
	Baclofen anhydrate	Baclofen excess 1 h	Baclofen excess 24 h	Functional groups
1	-	649.07 - 948.05	649.07 - 948.05	=C-H
2	-	1003.03 - 1163.13	1003.03 - 1163.13	-C-O
3	1383.02	1383.02	1383.02	-α-CH ₃
4	1401.34	1400.38	1400.38	-α-CH ₂
5	1539.26	1529.62	1529.62	-COOH
6	1627.99	1627.99	1627.99	-NH ₂
7	1922.15	1922.15	1922.15	-C=C
8	2157.47	2157.47	2157.47	-C≡C
9	2647.41 - 2755.43	2649.34 - 2751.57	2652.24 - 2751.57	-C-H (aldehyde C-H)
10	2857.66 - 2984.01	2845.13 - 2984.97	2846.09 - 29841.97	-CH (alkyl)

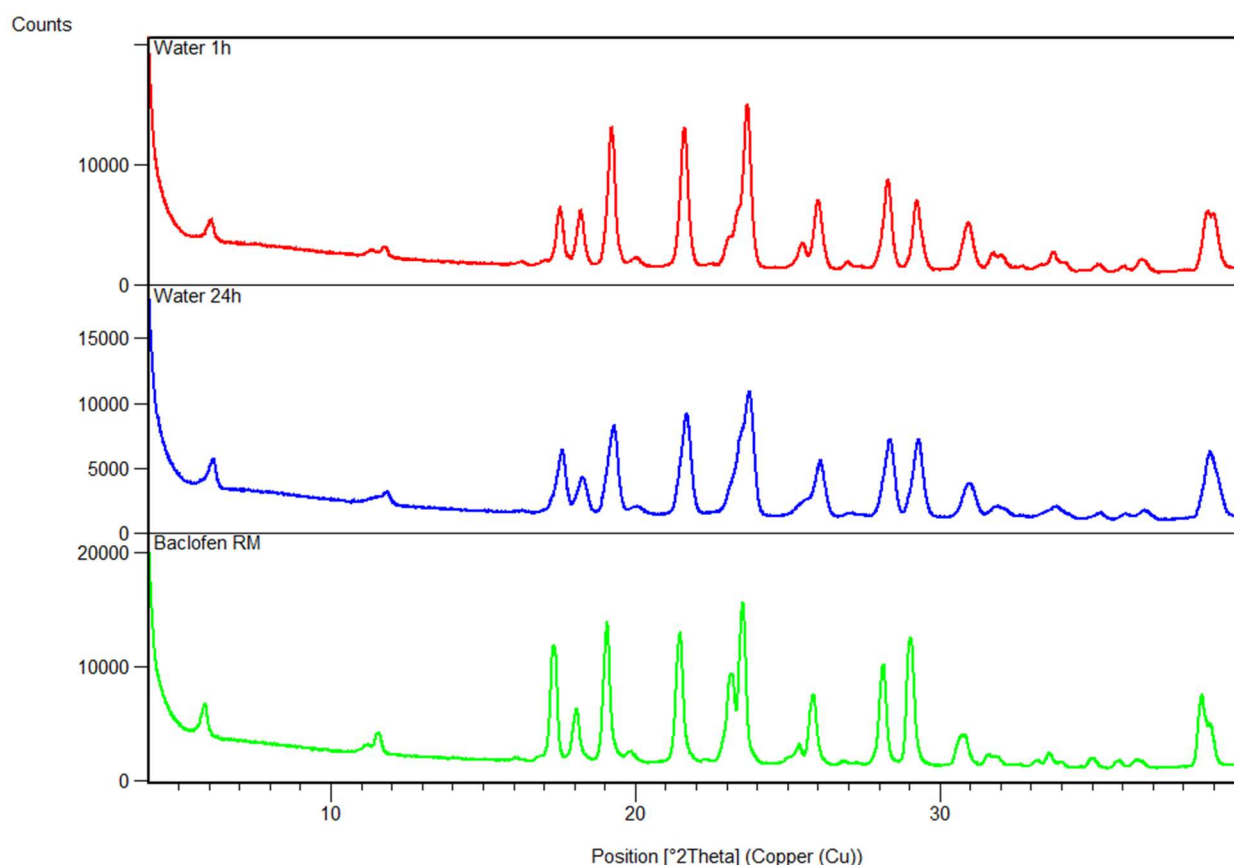


Figure 5.3: XRPD diffractograms obtained for baclofen in distilled water at 1 h (red), 24 h (blue) and baclofen anhydrate (green)

The fact that the monohydrate solid-state form was detected by means of DSC analysis and not through XRPD or FT-IR analyses can be ascribed to the time lapse between the withdrawals and when the analyses were performed. The DSC analysis was done first followed by FT-IR analysis and lastly XRPD. From Chapter 4 it became apparent that the monohydrate is a highly unstable solid-state form which dehydrates very easily. Therefore any storage that could allow evaporation of water will trigger the transformation back to the anhydrate.

5.2.2 0.1 M Hydrochloric acid buffer (HCl)

The solubility results obtained for baclofen in HCl buffer solution, containing 50 ml potassium chloride and 85 ml 0.2 M HCl to produce 200 ml of 0.1 M HCl, are displayed in Figure 5.4. Baclofen reached a concentration of 20.84 ± 2.59 mg/ml at 37°C in 0.1 M HCl buffer, which is lower than the concentration of 26 mg/ml at 37°C reported in literature (Abdelkader *et al.*, 2007; Vekariya *et al.*, 2012), however, a solubility concentration of 15 mg/ml was also reported (Ranpise *et al.*, 2013), where the temperature was not specified. Figure 5.4 and Table 5.3 illustrates that baclofen is very sensitive to small differences in pH. The solubility of baclofen in a pH 1.0 HCl solution indicated a concentration of 26.50 ± 0.5 mg/ml, while a pH 1.6 had a concentration of 10.42 ± 0.5 mg/ml. The total difference in concentration from pH 1.0 to pH 1.6 was 16.08 mg/ml

and this could also explain the differences in solubility from literature and the data reported below, i.e. a different pH may have been used to determine the solubility leading to different concentrations of baclofen in HCl. What appeared to be a phase transition of baclofen in the HCl (pH 1.2) occurred after 1 h with a dissolved concentration difference of 3.3 mg/ml. This was considered a significant difference and therefore DSC, FT-IR and XPRD were done at 1 h, 4 h and 24 h of the excess baclofen in the HCl buffer solution to examine the changes, if any that occurred. DSC results showed a peak melting temperature of 188.51°C (1 h sample) and 196.77°C (24 h) respectively, displayed in Figure 5.5 that does not correlate with baclofen anhydrate with a peak temperature of 213.93°C. This difference could be an indication of possible salt formation or complexation of baclofen with chloride ions. FT-IR was determined with the excess baclofen in HCl at 1 h and 24 h displayed Table 5.2 and it correlates with the peaks of baclofen anhydrate. The same applies to the XRPD, results, Figure 5.6.

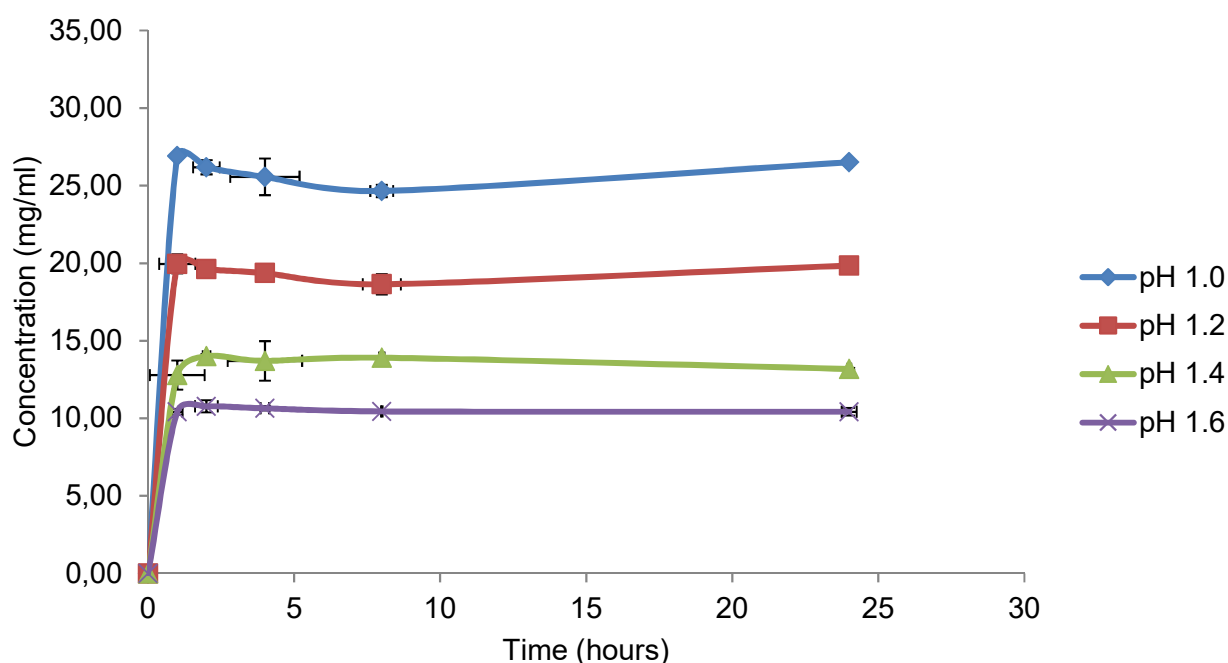


Figure 5.4: Solubility profile of baclofen raw material in different pH level HCl buffer solution concentrations at 37°C ± 0.5°C

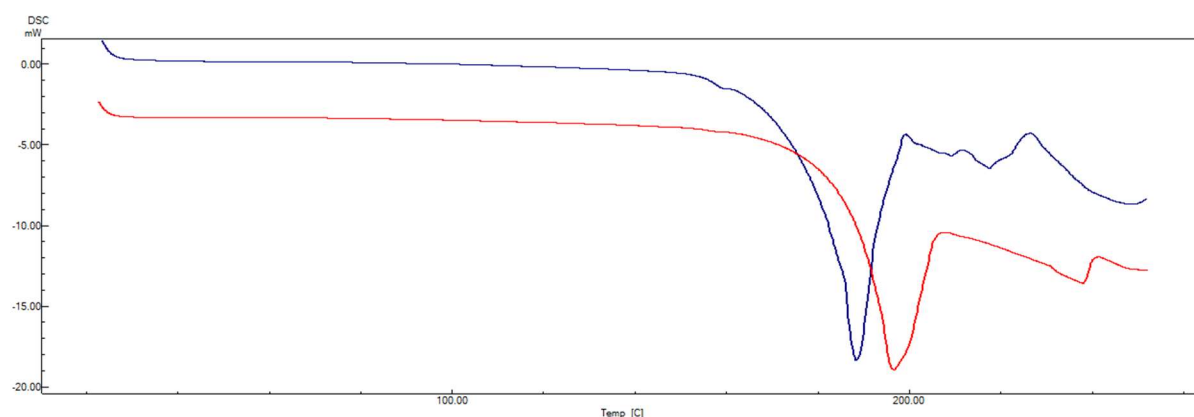


Figure 5.5: The DSC thermogram obtained for baclofen in HCl buffer solution 1 h (blue) and 24 h (red) with heating rate 10°C/min

Table 5.2: FT-IR peak listing reported for baclofen in HCl buffer solution

No:	Wavenumber (cm ⁻¹)			
	Baclofen anhydrate	Baclofen excess 1 h	Baclofen excess 24 h	Functional groups
1	-	649.07 - 948.05	649.07 - 948.05	=C-H
2	-	1003.03 - 1164.09	1003.03 - 1164.09	-C-O
3	1383.02	1383.02	1383.02	-α-CH ₃
4	1401.34	1401.34	1401.34	-α-CH ₂
5	1539.26	1533.47	1534.44	-COOH
6	1627.99	1627.03	1627.03	-NH ₂
7	1922.15	1922.15	1922.15	-C=C
8	2157.47	2157.47	2157.47	-C≡C
9	2647.41 - 2755.43	2651.27 - 2755.43	2651.27 - 2755.43	-C-H (aldehyde C-H)
10	2857.66 - 2984.01	2846.09 - 2984.97	2846.09 - 2984.97	-CH (alkyl)

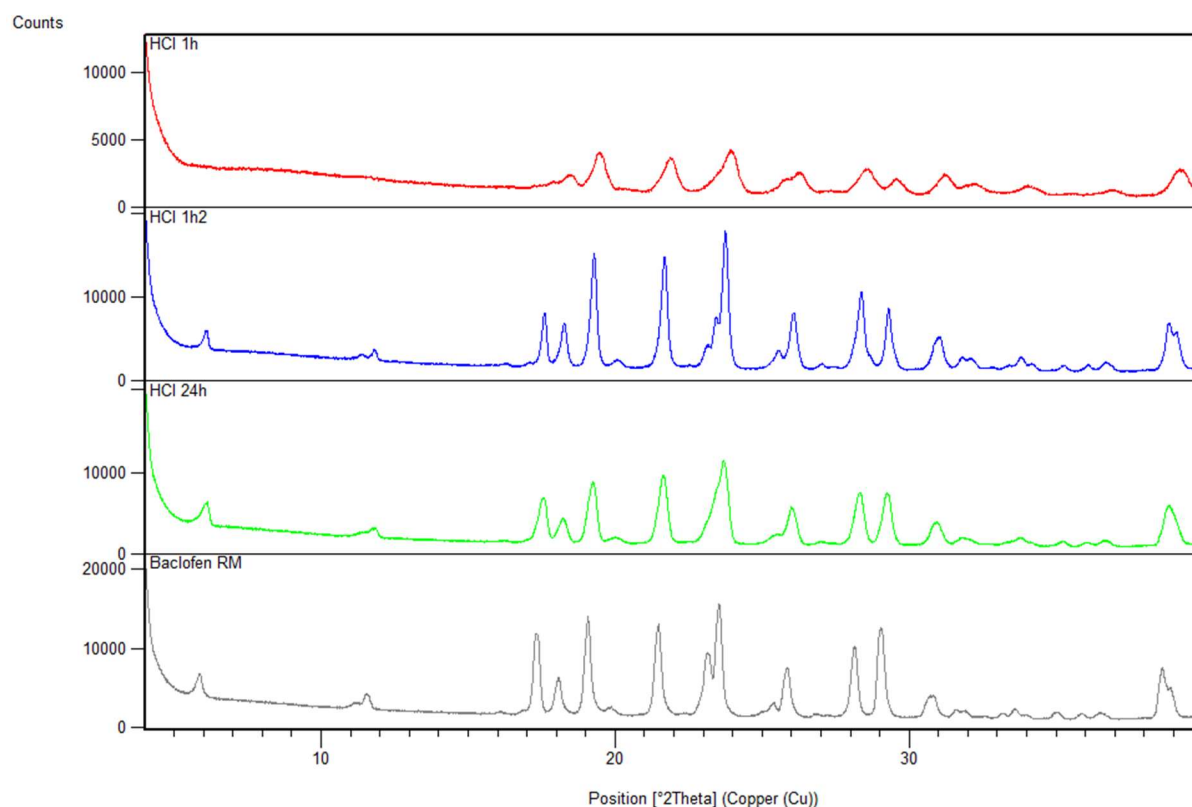


Figure 5.6: XRPD diffractograms obtained for baclofen in HCL buffer solution at 1 h (red), 2 h (blue), 24 h (green) and baclofen anhydrate (grey)

Table 5.3: Solubility concentrations of baclofen in different HCl buffer solutions with differing pH values

pH	Baclofen concentration (mg/ml) at 1 h (\pm STDEV)	Baclofen concentration (mg/ml) at 24 h (\pm STDEV)
1.0	26.91 \pm 0.11	26.50 \pm 0.09
1.2	19.96 \pm 0.62	19.85 \pm 0.04
1.4	12.79 \pm 0.94	13.81 \pm 0.06
1.6	10.42 \pm 0.18	10.42 \pm 0.25

5.2.3 Citrate buffer solution (pH 4.5)

The solubility results obtained for baclofen in citrate buffer solution, containing 2.101 g citric acid in 100 ml water and 2.941 g of sodium citrate in 100 ml water to produce 200 ml of citrate buffer, are displayed in Figure 5.7. Baclofen reached a concentration of 4.82 ± 0.41 mg/ml citrate buffer, which is lower than the solubility of baclofen in acetate buffer solution (pH 4.5) reported in literature at a concentration of 8 mg/ml (Ranpise *et al.*, 2013), solubility temperature not reported. What appeared to be a phase transition of baclofen occurred after 1 h with a measured dissolved

concentration of 5.18 ± 0.05 mg/ml and 4 h with a measured dissolved concentration of 5.07 ± 0.13 mg/ml. DSC, FT-IR and XPRD were done at 1 h, 4 h and 24 h of the excess baclofen in the citrate buffer solution. DSC results of the 1 h, 4h and 24 h samples showed peak melting temperatures of 192.90°C , 200.05°C and 201.81°C respectively, displayed in Figure 5.8. These melting points are significantly lower than that of baclofen anhydrate (213.93°C). Once again this might be an indication of possible salt formation or complexation with citrate salt. FT-IR data (Table 5.3) and XRPD diffraction data of the excess baclofen (Figure 5.9) correlates with those of the baclofen anhydrate.

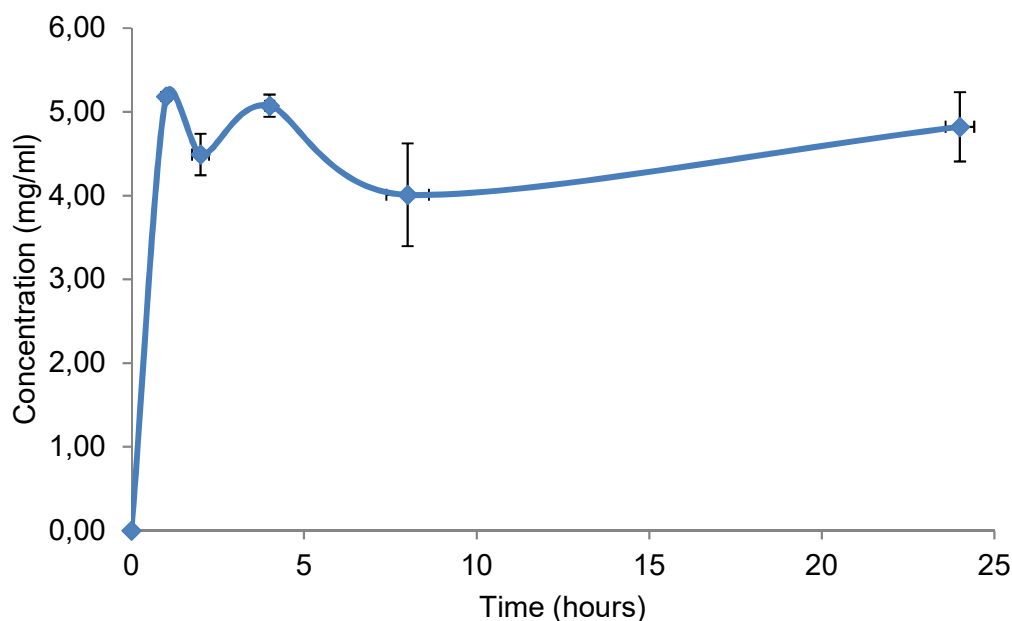


Figure 5.7: The solubility profile obtained for baclofen anhydrate in citrate buffer solution over a period of 24 h at $37^{\circ}\text{C} \pm 0.5^{\circ}\text{C}$

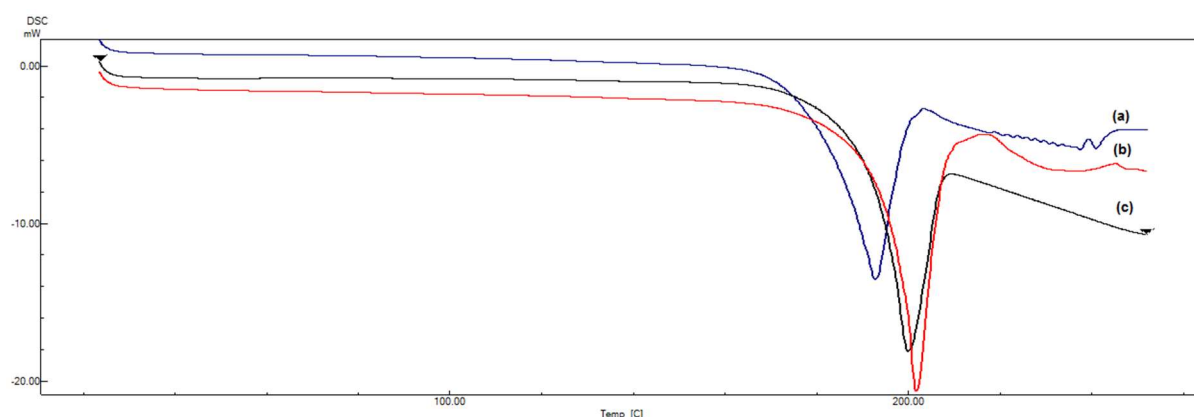


Figure 5.8: The DSC thermogram obtained for excess baclofen in citrate buffer solution (a) 1 h, (b) 4 h and (c) 24 h with heating rate $10^{\circ}\text{C}/\text{min}$

Table 5.4: FT-IR peak listing reported for excess baclofen in citrate buffer solution

	Wavenumber (cm ⁻¹)					
No:	Baclofen anhydrate	Baclofen excess 1 h	Baclofen excess 2 h	Baclofen excess 4 h	Baclofen excess 24 h	Functional groups
1	-	649.07 - 948.05	649.07 - 948.05	649.07 - 948.05	649.07 - 948.05	=C-H
2	-	1003.03 - 1164.09	1003.03 - 1164.09	1003.03 - 1164.09	1003.03 - 1164.09	-C-O
3	1383.02	1383.02	1383.02	1383.02	1383.02	-α-CH ₃
4	1401.34	1400.38	1401.34	1401.34	1401.34	-α-CH ₂
5	1539.26	1533.47	1533.47	1533.47	1534.44	-COOH
6	1627.99	1627.03	1627.03	1627.03	1627.99	-NH ₂
7	1922.15	1922.15	1922.15	1922.15	1922.15	-C=C
8	2157.47	2157.47	2157.47	2157.47	2157.47	-C≡C
9	2647.41 - 2755.43	2646.45 - 2753.5	2646.45 - 2753.5	2646.45 - 2753.5	2646.45 - 2753.5	-C-H (aldehyde C-H)
10	2857.66 - 2984.01	2848.98 - 2984.97	2848.98 - 2984.97	2848.98 - 2984.97	2844.16 - 2984.97	-CH (alkyl)

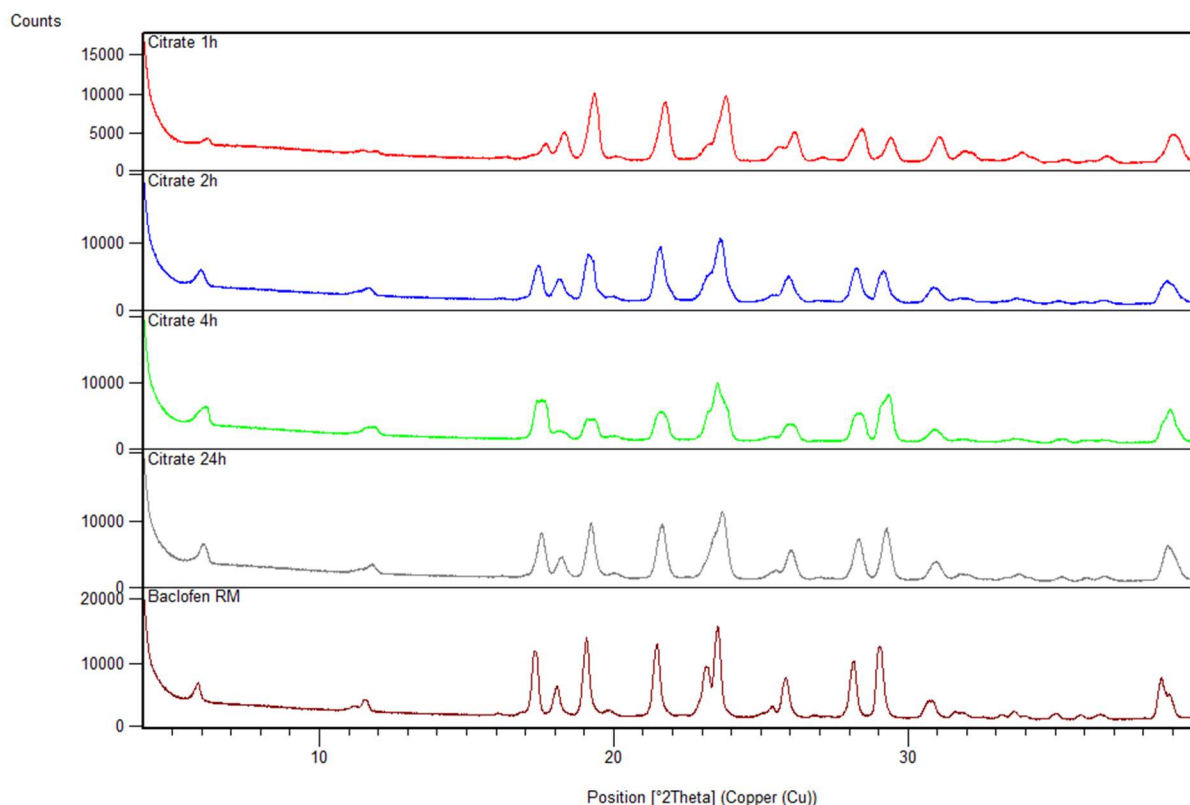


Figure 5.9: XRPD diffractograms obtained for baclofen in citrate buffer solution at 1 h (red), 2 h (blue), 4 h (green), 24 h (grey) and baclofen anhydrate (brown)

5.2.4 Phosphate buffer solution (pH 6.8)

The solubility results obtained for baclofen in phosphate buffer solution containing 50 ml of monobasic potassium phosphate and 22.4 ml 0.2 M NaOH to produce 200 ml of phosphate buffer solution, are displayed in Figure 5.10. Baclofen reached a concentration of 4.71 ± 0.003 mg/ml, which is slightly lower than the solubility of baclofen in phosphate buffer solution reported in literature at a concentration of 5 - 5.2 mg/ml at 37°C (Ranpise et al., 2013; Vekariya et al., 2012). DSC, FT-IR and XRPD were done at 1 h and 24 h on the excess baclofen in the phosphate buffer solution. DSC was performed on excess baclofen within phosphate buffer solution at 1 h and 24 h and peak melting temperatures of 208.37°C and 210.17°C respectively (Figure 5.11). FT-IR (Table 5.4) and XRPD (Figure 5.12) data also showed that the solid-state form correlates with baclofen anhydrate.

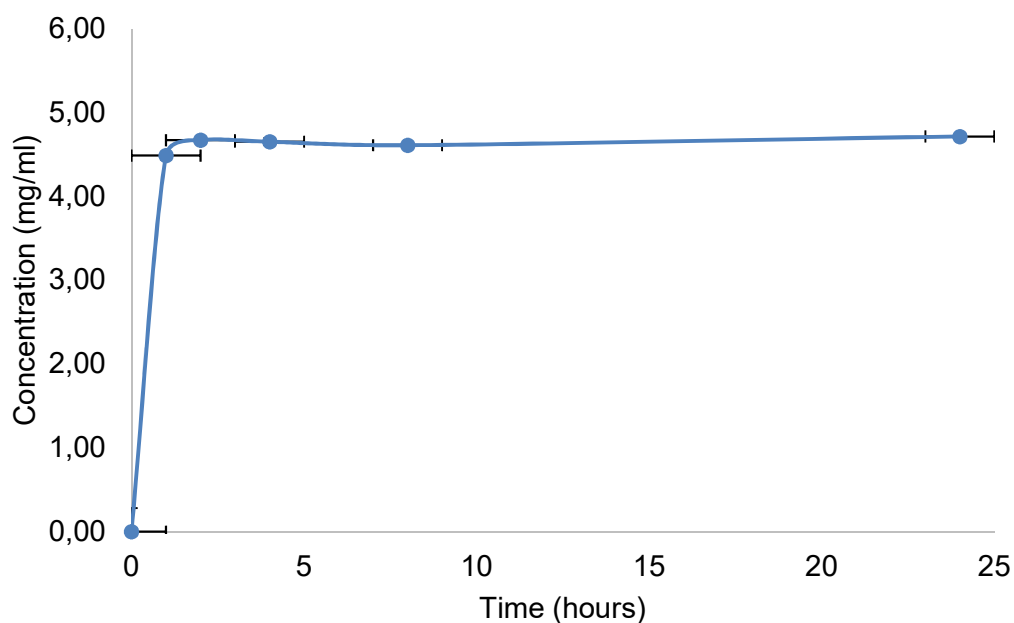


Figure 5.10: The solubility profile obtained for baclofen anhydrate in phosphate buffer solution over a period of 24 h at $37^{\circ}\text{C} \pm 0.5^{\circ}\text{C}$

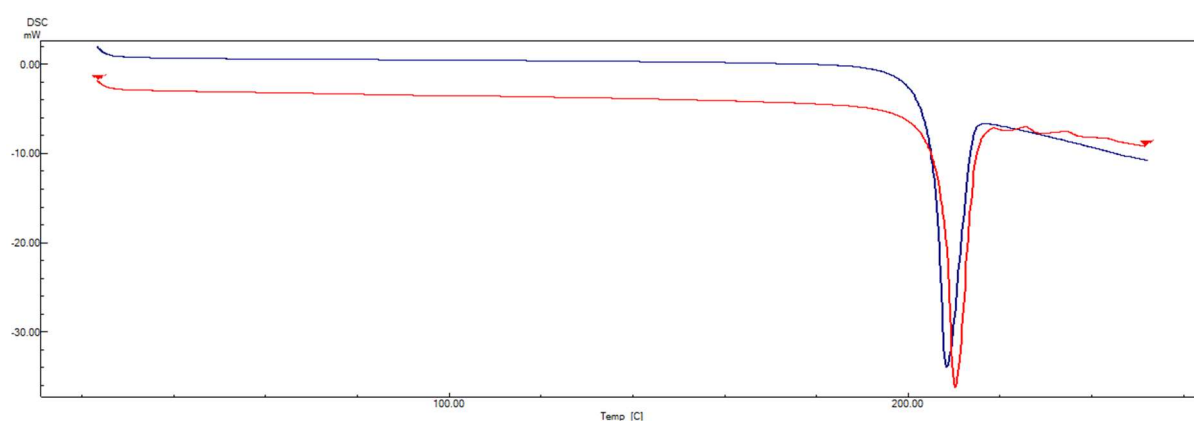


Figure 5.11: The DSC thermogram obtained for baclofen in phosphate buffer solution at 1 h (blue) and 24 h (red) with heating rate $10^{\circ}\text{C}/\text{min}$.

Table 5.5: FTIR peak listing reported for excess baclofen in phosphate buffer solution

Wavenumber (cm^{-1})				
No:	Baclofen anhydrate	Baclofen excess 1 h	Baclofen excess 24 h	Functional groups
1	-	624.96 - 948.05	624.96 - 948.05	=C-H
2	-	1003.03 - 1163.13	1003.03 - 1163.13	-C-O
3	1383.02	1383.02	1383.02	$-\alpha\text{-CH}_3$

Table 5.5 continued: FTIR peak listing reported for excess baclofen in phosphate buffer solution

Wavenumber (cm ⁻¹)				
No:	Baclofen anhydrate	Baclofen excess 1 h	Baclofen excess 24 h	Functional groups
4	1401.34	1400.38	1401.34	-α-CH ₂
5	1539.26	1528.65	1534.44	-COOH
6	1627.99	1627.99	1627.99	-NH ₂
7	1922.15	1922.15	1922.15	-C=C
8	2157.47	2157.47	2157.47	--C≡C
9	2361.94	2361.94	2361.94	-C-H (aldehyde C-H)
10	2857.66 - 2984.01	2857.66 - 2984.01	2857.66 - 2984.01	-CH (alkyl)

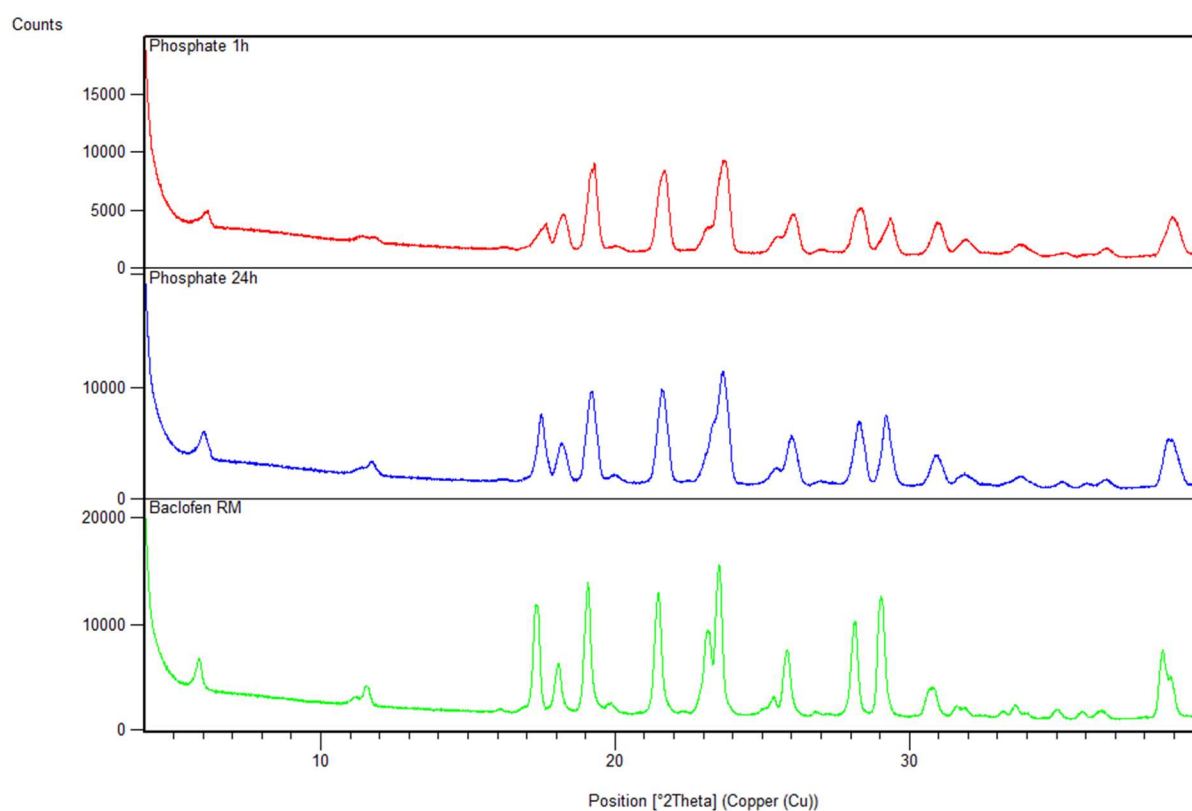


Figure 5.12: XRPD diffractograms obtained for baclofen in phosphate buffer solution at 1 h (red), 4 h (blue) and baclofen anhydrate (green)

5.2.5 Conclusion

The solubility of baclofen anhydrate in distilled water, citrate and phosphate buffer solutions were notably lower in comparison to that in hydrochloric acid buffer with pH 1.2. The pH values of those three bio-relevant media are closer to the isoelectric point (pH 7) with zwitterions as the predominant form. Baclofen in HCl buffer solution showed the highest solubility concentration, which can be ascribed to rapid protonation (pK_{a1} 9.6) of the amino group with ammonium ions as the predominant form (Vekariya *et al.*, 2012). Possible solid-state transformation of baclofen in HCl- and citrate buffer solutions were observed through DSC analyses, however, FT-IR and XRPD analyses didn't reveal the same phenomena. This could, however, be explained by longer waiting periods between the withdrawal and the actual analysis of the sample. More in-depth research into the possibility of baclofen to form salts should be pursued.

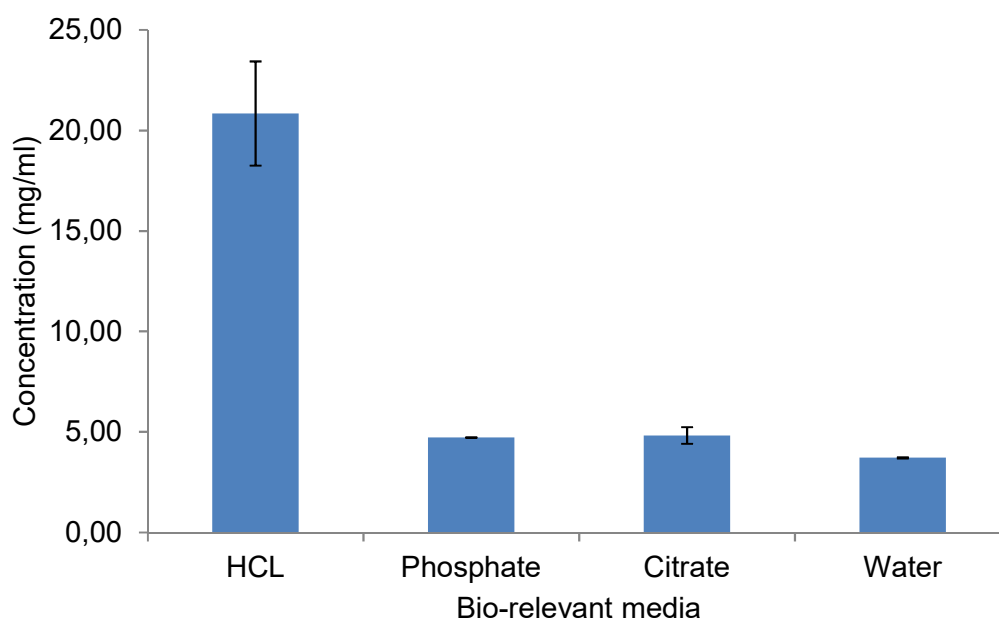


Figure 5.13: Summary of solubilities of baclofen in the different bio-relevant media obtained at $37^{\circ}\text{C} \pm 0.5^{\circ}\text{C}$

Table 5.6: Presentation of the concentrations obtained for the different bio-relevant media

Bio-relevant medium	Concentration (mg/ml)
Distilled water	3.71 ± 0.02
0.1 M Hydrochloride buffer solution (pH 1.2)	20.84 ± 2.58
Citrate buffer solution (pH 4.5)	4.82 ± 0.41
Phosphate buffer solution (pH 6.8)	4.71 ± 0.003

5.3 Powder dissolution results

Dissolution of baclofen anhydrate was performed according to the method provided in Chapter 3, paragraph 3.3.2.10. During the course of this study the dissolution of baclofen anhydrate was determined in the same bio-relevant media in which equilibrium solubility was determined in a saturated solution and 25 mg. Dissolution in a saturated solution was calculated from the equilibrium solubility data to determine if possible solution-mediated phase transformations can occur and the 25 mg of baclofen was used since this correlates with the highest dose of a baclofen tablet currently on the South African market.

5.3.1 Distilled water

Powder dissolution profiles of baclofen anhydrate using different weights, 2 g in 500 ml and 25 mg in 900 ml, in distilled water are displayed in Figure 5.14. An amount of 2 g of baclofen was used to prepare a saturated solution for the dissolution study in accordance with the solubility data reported in section 5.2.1. The higher amount (2 g) baclofen anhydrate achieved a $102.10 \pm 2.06\%$ dissolution after 180 min whilst 25 mg baclofen anhydrate achieved a $108.21 \pm 5.89\%$ dissolution after 180 min.

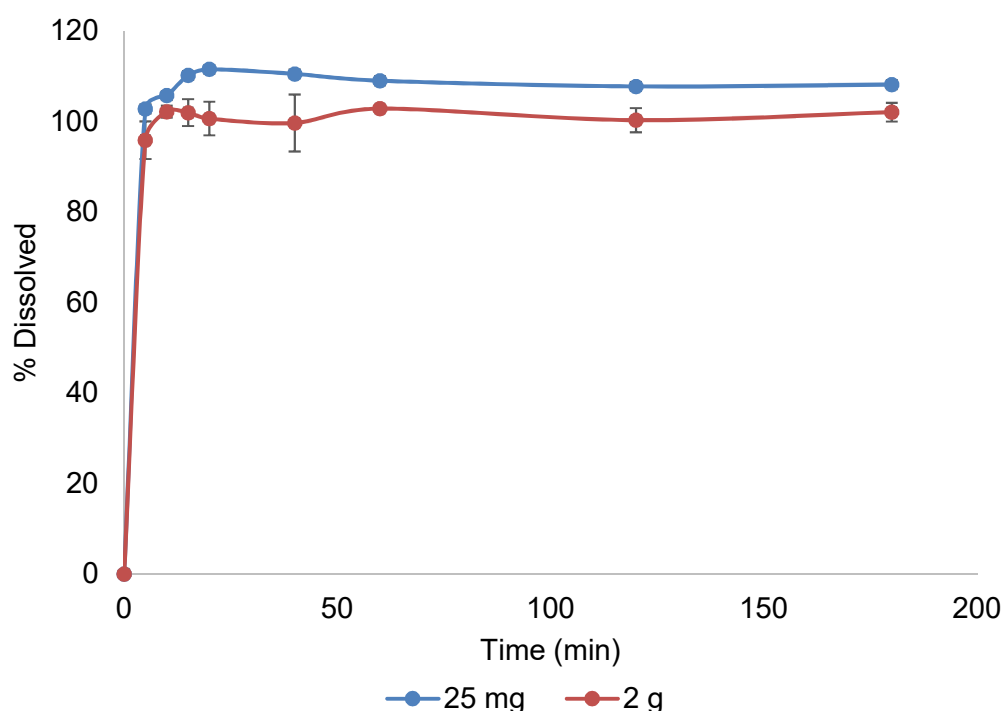


Figure 5.14: The dissolution profile obtained for 2 g and 25 mg baclofen in distilled water at $37 \pm 0.5^\circ\text{C}$ and 100 rpm paddle stirring speed

5.3.2 0.1 M Hydrochloric acid (HCl) – pH 1.2

Dissolution profiles of baclofen with different weights 4 g in 500 ml and 25 mg in 900 ml in HCl are displayed in Figure 5.15. An amount of 4 g of baclofen was used to obtain a saturated solution during the dissolution testing was not in accordance with the solubility data reported in section 5.2.2. According to the solubility data 18 g of baclofen were needed to prepare a saturated solution. This is a very large sample size to fit into a standard dissolution vessel. It was then decided that 18 g was unpractical to use. The maximum amount of powder that could be added to the dissolution vessel to ensure that the powder gets mixed completely was found to be 4 g. For the 4 g dissolution of baclofen anhydrate, a dissolved percentage of $73.63 \pm 28.97\%$ was obtained after 180 min. The tablet dose quantity of 25 mg achieved a $59.75 \pm 0.99\%$ dissolution percentage within the specified time. The dissolution data don't correlate with the equilibrium solubility results of baclofen in HCl buffer solution. According to the dissolution data obtained, approximately 3.27 mg/ml baclofen dissolved, which is about 7 mg/ml less than that obtained during equilibrium solubility testing. It is hypothesised that the pH of the HCl dissolution medium was even higher than pH 1.6. The experimental design lacked in the sense that the pH of the medium was not measured after the completion of the dissolution. Another reason that might explain the results is the wettability of the baclofen powder. The stirring dynamics of a dissolution paddle might not be sufficient to adequately wet the powder mass. Whilst with an equilibrium solubility experimental setup the powder get wetted more easily. This scenario might also explain the high %RSD of 28.97, which by dissolution testing criteria is unacceptable.

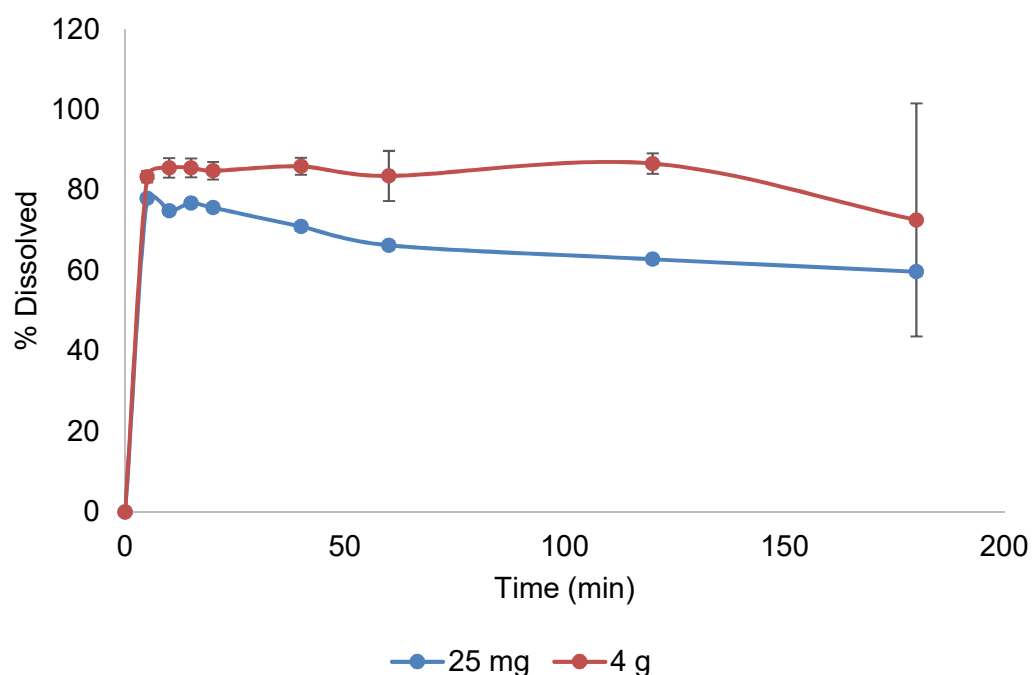


Figure 5.15: The dissolution profile obtained for 4 g and 25 mg baclofen in HCl buffer solution at $37 \pm 0.5^\circ\text{C}$ and 100 rpm paddle stirring speed

5.3.3 Citrate buffer solution (pH 4.6)

Dissolution profiles of baclofen with different weights of 2.5 g in 500 ml and 25 mg in 900 ml in citrate buffer solution are displayed in Figure 5.16. An amount of 2.5 g of baclofen was used to obtain a saturated solution during the dissolution study in accordance with the solubility data reported in section 5.2.3. For 2.5 g amount of baclofen, $98.24 \pm 2.03\%$ dissolution was obtained after 180 min, while for the 25 mg sample, $73.06 \pm 0.10\%$ dissolution was obtained after 180 min with the indication of possible salt formation or complexation with citrate salt, as mentioned in section 5.2.3 at 5 min where $114.77 \pm 19.37\%$ dissolution.

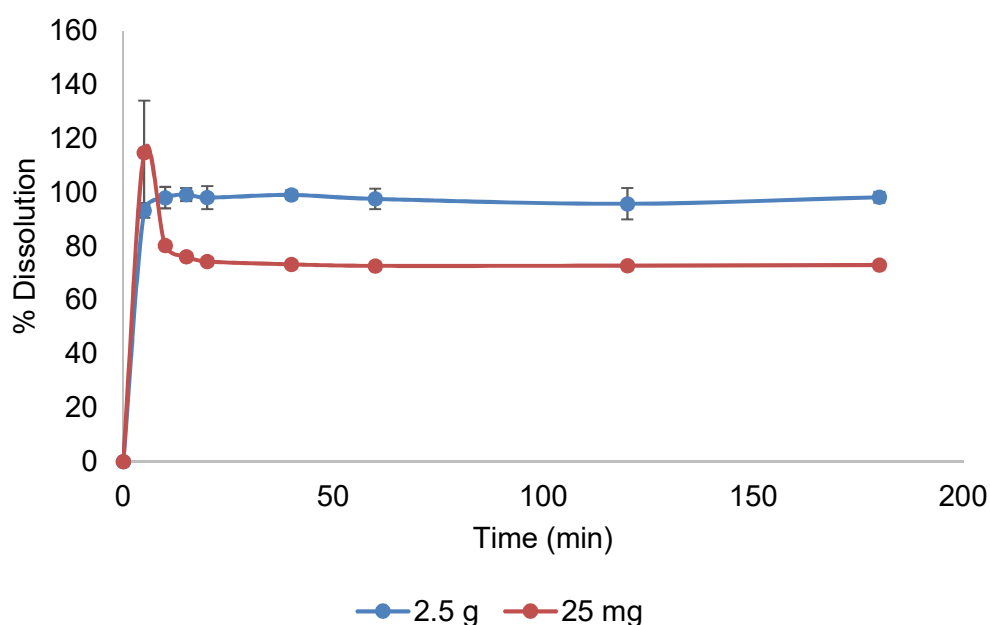


Figure 5.16: The dissolution profile obtained for 2.5 g and 25 mg baclofen in citrate buffer solution at $37 \pm 0.5^\circ\text{C}$ and 100 rpm paddle stirring speed

5.3.4 Phosphate buffer solution (pH 6.8)

Dissolution profiles of baclofen with different weights of 2.3 g in 500 ml and 25 mg in 900 ml in phosphate are displayed in Figure 5.17. An amount of 2.3 g baclofen was used to obtain a saturated solution for the dissolution study in accordance with the solubility data reported in section 5.2.4. This resulted in $83.79 \pm 1.68\%$ dissolution. Whilst the 25 mg baclofen samples achieved a $91.28 \pm 4.58\%$ dissolution after 180 min.

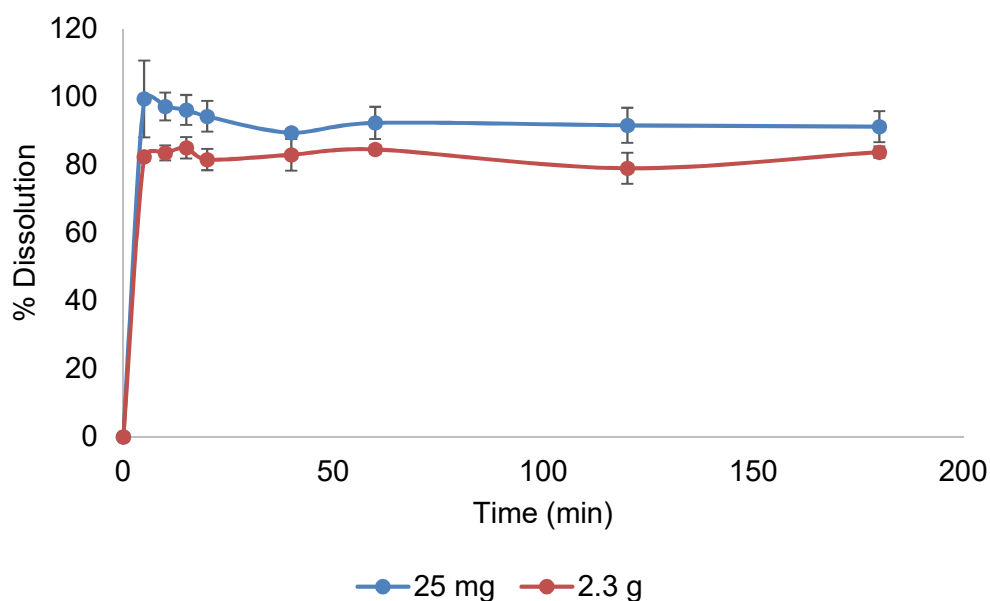


Figure 5.17: The dissolution profile obtained for 2.3 g and 25 mg baclofen in phosphate at $37 \pm 0.5^\circ\text{C}$ and 100 rpm paddle stirring speed

5.3.5 Conclusion

The dissolution profile of baclofen (25 mg and a saturated solution) in various bio-relevant media (water, HCl, citrate and phosphate) shows how the dissolution behaviours of baclofen for 25 mg and the saturated solution in the different bio-relevant media compares in order to determine equilibrium solubility. It is evident that the dissolution profiles differ depending on the bio-relevant media and concentrations used.

5.4 *In vitro* membrane permeation

The *in vitro* permeability of baclofen was determined across Caco-2 cell monolayers grown on filter supports in Transwell® plates in both the apical to basolateral as well as the basolateral to apical direction to determine the BCS classification of baclofen based on the combined data obtained during the course of the study.

5.4.1 Permeability in the apical to basolateral direction

The permeability results (% transported of dose applied) obtained for baclofen (0 - 120 min in triplicate) in the apical to basolateral direction plotted as a function of time are displayed in Figure 5.18.

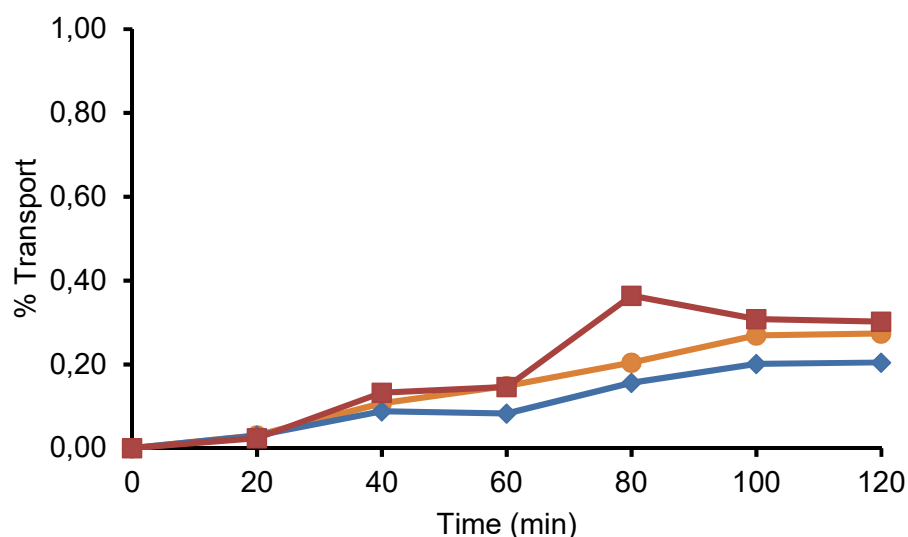


Figure 5.18: Permeability (% transport) in triplicate of baclofen in the apical to basolateral direction across Caco-2 cell monolayers at 37°C

It is clear from Figure 5.18 that the permeation of baclofen is extremely low across the Caco-2 cell monolayers in the apical to basolateral direction since only a cumulative transport of below 0.3% of the applied dose permeated across the epithelial monolayer over a period of 120 min. This is indicative of poor absorption (and potentially low bioavailability), which is also reflected in the relatively low apparent permeability coefficient (P_{app}) value of 0.876×10^{-7} cm/s. Drugs with incomplete absorption has a permeability coefficient of $<1 \times 10^{-7}$ cm/s across Caco-2 monolayers (Artursson *et al.*, 2012).

5.4.2 Permeability in the basolateral to apical direction

The permeability results (% transported of dose applied) obtained for baclofen (0 - 120 min in triplicate) in the basolateral to apical direction plotted as a function of time are displayed in Figure 5.19.

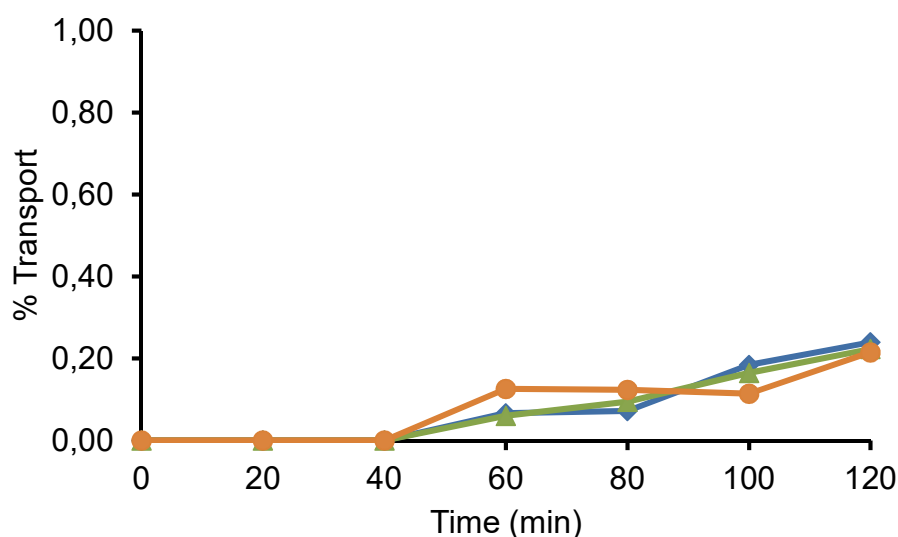


Figure 5.19: Permeability (% transport) in triplicate of baclofen in the basolateral to apical direction across Caco-2 cell monolayers at 37°C.

It is apparent from Figure 5.19 that the permeation of baclofen across the Caco-2 cell monolayers in the basolateral to apical direction exhibited a lag phase of 40 min before any transport occurred. Furthermore, the transport in secretory (or basolateral to apical) direction is lower than in the absorptive (or apical to basolateral) direction. This is also reflected in the apparent permeability coefficient (P_{app}) value of 0.691×10^{-7} cm/s for the basolateral to apical direction. This indicates that no active efflux transport of baclofen is present.

5.4.3 Conclusion

Transport of drugs across the intestinal epithelium can occur by different pathways and mechanisms. Passive diffusion occurs when drug molecules move across the GI epithelium from a region with a high concentration to a region with a lower concentration. *In vivo*, the lower concentration is primarily maintained by blood flow. The rate of absorption is directly proportional to the concentration of the drug at the absorption site. Subsequently, the rate of transport can be determined by the physico-chemical properties of the drug, the nature of the membrane and the concentration gradient of the drug crossing the membrane (Aulton & Taylor, 2013).

In contrast to passive diffusion, active transport may generate gradients across barriers with various energy mechanisms (Sarmiento *et al.*, 2012) and it involves the active participation of the apical cell membrane in the transport process across the membrane, which means the drug has to bind to a carrier or a membrane transporter. Active transport proceeds at a rate that is proportional to the drug concentration only at low concentrations; but at higher concentrations, the carrier mechanism becomes saturated. During active diffusion, the rate of absorption remains constant. Facilitated diffusion, like active transport is a carrier mediated process, but cannot

transport a substance against a concentration gradient therefore it does not require an energy input, but it does require a concentration gradient as driving force like passive diffusion (Aulton & Taylor, 2013).

Based on the membrane permeation of baclofen according to the P_{app} value obtained in this study in the apical to basolateral direction across Caco-2 cell monolayers ($0,876 \times 10^{-7}$ cm/s), it should be classified into Class 3 or 4 of the BCS (i.e. low permeability). The relatively low permeation of baclofen across the Caco-2 epithelial cell membrane may be explained by its relatively low solubility, but potentially also its low membrane permeation ability and absence of uptake by active transporters. The passive diffusion of baclofen was lower in the basolateral to apical direction than in the apical to basolateral direction, probably due to the larger surface area on the apical side of the Caco-2 cell monolayer (presence of villi) compared to the basolateral side (absence of villi). A larger surface area of the membrane across which the permeation takes place favours passive diffusion as described by the Fick's first law (Artursson *et al.*, 2012).

According to the water solubility data 927.50 mg of baclofen will dissolve in 250 ml of water or in other words if one would want to dissolve the maximum daily dose of baclofen (100 mg) one would require 26.95 ml of water. Therefore, the maximum dose of baclofen will dissolve in 250 ml of water, which is the accepted standard as the minimum fluid volume if a drug dose is taken in the fasted state with a glass of water (Aulton, 2013). Using this rule of thumb, baclofen would be classified as highly soluble in 250 ml water, pH 1.2, pH 4.5 and pH 6.8. However, according to Table 1.3 baclofen is slightly soluble in water, pH 4.5, pH 6.8 and sparingly soluble in pH 1.2. Depending on which rule or guideline one uses could allow one to obtain discrepancies in terms of the solubility of the given drug between pH 1 – 8. Following the globally accepted standard on biostudies and the BCS classification of drugs, baclofen was classified as a highly soluble drug since the highest daily dose can be dissolved in much less than 250 ml (Aulton & Taylor, 2013). Looking further into the dissolution studies performed on baclofen during this study it became evident that baclofen can be classified as very rapidly dissolving drug in distilled water, pH 4.5 and pH 6.8, despite the lower equilibrium solubility thereof in these media. The reason being that more than 85% of the drug dissolves within a 15 minute time period. This combined with the relatively low permeability data mentioned above indicates baclofen should be classified into Class 3 of the BCS classification system (i.e. high solubility and low permeability). The dissolution results obtained using 0.1 M HCl buffer solution were, however, contradictory to what was obtained during solubility testing, this can only be ascribed to the proven pH-level sensitivity of baclofen, but significantly impacts the BCS classification of this drug.

Considering the contradictory results obtained, it can help to explain the variation in results found in literature in terms of solubility and bioavailability of baclofen. From a dosage form development perspective, it might be useful to consider the formulation of an extended release dosage form,

which could increase the residence time of the dosage form in the stomach (e.g. gastro-retentive drug delivery system) where the solubility should be higher due to the lower pH level.

References

- Abdelkader, H., Youssef Abdalla, O. & Salem, H. 2008. Formulation of controlled-release baclofen matrix tablets II: Influence of some hydrophobic excipients on the release rate and in vitro evaluation. *AAPS PharmSciTech*, 9(2):675-683.
- Artursson, P., Palm, K. & Luthman, K. 2012. Caco-2 monolayers in experimental and theoretical predictions of drug transport. *Advanced drug delivery reviews*, 64:280-289.
- Aulton, M.E. & Taylor, K.M.G. 2013. Aulton's pharmaceuticals: the design and manufacture of medicines, 4th Edition. Spain: Harcourt Publishers Limited.
- Cruaud, O., Benita, S. & Benoit, J.P. 1998. The characterization and release kinetics evaluation of baclofen microspheres designed for intrathecal injection. *International journal of pharmaceuticals*, 177:247–257.
- Ranpise, N.S., Kolhe, S.R. & Ranade, A.N. 2013. Development and evaluation of bilayer gastroretentive floating drug delivery system for baclofen. *Indian journal of pharmaceutical education and research*, 47(1):41-46.
- Sarmiento, B., Andrade, F., da Silva, S.B., Rodrigues, F., das Neves, J. & Ferreira, D. 2012. Cell-based in vitro models for predicting drug permeability. *Expert opinion on drug metabolism and toxicology*, 8(5):607-621.
- Vekariya, S.L., Patel, P.K., Solanki, S.T., Vasava, N. & Jivani, R. 2012. Influence of hydrophilic polymers on release profile of baclofen from bilayer tablet. *International journal of pharmacy and pharmaceutical sciences*, 4(3):454-458.

CHAPTER 6

CONCLUSION

Baclofen is a central acting muscle relaxant that acts as an agonist of the inhibitory neurotransmitter GABA. Baclofen is currently the drug of choice for the treatment of long-term spasticity and it can be prescribed for the relief of flexor. Baclofen contains a chiral centre and it is marketed as a racemic mixture that consists of equal amounts of R- and S-enantiomers. Some literature sources mention the solubility characteristics of baclofen, however; they do not provide sufficient solubility information on baclofen in different organic solvents (BP, 2016; Moffat *et al.*, 2011; USP, 2016). The solubility shows pH dependence that dissolves freely in very high pH (0.1 N NaOH) and very low pH (0.1 N HCl) solutions, however, the solubility will drop rapidly as the pH increases or decreases to a more neutral pH (Abdelkader *et al.*, 2008; Faisal *et al.*, 2013; Trissel & Zhang, 2013; Ranpise *et al.*, 2013). On the South African market, baclofen is available in a solid pharmaceutical dosage form (tablets) for oral administration (Rossiter, 2012), however, baclofen is available as intrathecal administration on the global market (Ghasemian *et al.*, 2017).

It is well known that pharmaceutical solids can exist in different forms such as polymorphs, hydrates, solvates, co-crystals, salts and amorphous forms. Polymorphs have different crystal structures with the same chemical composition of the crystals (Cui, 2007). Hydrates and solvates are formed when water or organic solvents are trapped within the crystalline structure, respectively (Aulton & Taylor, 2013). Co-crystals contains two different molecules that are made from reactants. Amorphous forms are non-crystalline with only short-range molecular order (Cui, 2007).

The arrangement of molecules in a crystal determines its physico-chemical properties and affects the drugs' performance such as physical and chemical stability, solubility, dissolution rates and in some cases bioavailability (Datta & Grant, 2004; Rodríguez-Spong *et al.*, 2004). Several triggers may lead to solid-state phase transformations of any given drug. Interactions with water can induce phase transitions that can lead to changes in the pharmaceutical and biopharmaceutical performance of the drug (Sandler *et al.*, 2005).

Several methods exist in which the biopharmaceutical performance of a drug may be determined. One such technique is that of using cell cultures. Caco-2 cells are derived from human colon adenocarcinoma and grows in culture to form a polarised monolayer with tight junctions with an apical brush border that differentiate on a semi-permeable membrane and displays similar morphological and functional characteristics as intestinal enterocytes (Alqahtani *et al.*, 2013; Le Ferrec *et al.*, 2001; Sarmiento *et al.*, 2012). For any given drug to be pharmacologically effective, it is important that it reaches the preferred target site at a specified concentration. This requires the critical precondition of sufficient intestinal epithelial permeability. The relationship between

the physico-chemical properties of molecules and their ability to cross the gastro-intestinal (GI) epithelium is rather complex (Gan & Thakker, 1996). Each transport mechanism is depended on certain physico-chemical properties of the absorbed molecules, such as partition coefficient, molecular weight, molecular volume, pKa, solubility, chemical stability, and charge distribution (Le Ferrec *et al.*, 2001).

According to Mirza *et al.*, 2007 baclofen can exist in at least two solid-state state forms namely an anhydrate and a monohydrate. However very little information is available on the physico-chemical properties and different hydration levels of baclofen and how this might influence its solubility, stability, and bioavailability.

The scope of this study was of great importance as different solid-state forms of baclofen could influence the physico-chemical properties thereof. The principal goal was to investigate the impact, and to illustrate the effect, of different solid-state forms of baclofen on its physico-chemical characteristics. A variety of solid-state characterisation methods were used during this study. The methods employed included screening for different solid-state forms of baclofen and investigation of the physico-chemical properties and physical stability of baclofen raw material and any other possible solid-state form thereof. Investigation of the bi-directional *in vitro* permeability of the baclofen anhydrate was described across Caco-2 cell monolayers.

First the physico-chemical properties of baclofen anhydrate were investigated in terms of melting point, loss of moisture upon heating, water content, crystallinity and vapour sorption isotherms. The melting peak temperature of baclofen anhydrate was determined by DSC to be 213.93°C, using a heating rate of 10°C/min. A weight loss of 99% was observed from 200°C to 300°C using TGA confirmed sublimation. HSM micrographs visually correlated with the thermal data.

During the course of this study it was found that the purchased raw material can be characterised as baclofen anhydrate. Literature stated that baclofen may also exist as a monohydrate but through proper physico-chemical studies it became evident that baclofen monohydrate can be characterised as a highly unstable, transient solid-state form of baclofen when out of solution. The monohydrate can only exist in high humidity environments and in conditions where a saturated to supersaturated solution of baclofen is used. The fact that baclofen anhydrate starts to crystallise to the unstable monohydrate at a relative humidity of 35% is something that the pharmaceutical industry that manufactures the raw material or oral dosage forms must be aware of. Furthermore, considering this unstable form of baclofen it is clear that oral dosage formulation processes cannot include steps which involves the use of large quantities of water. The XRPD stability study which investigated the hydration and dehydration of baclofen anhydrate and monohydrate showed that hydration occurs very easily in a moist environment, but that dehydration also occurs just as easily once moisture starts to evaporate from the environment. It

was concluded that baclofen anhydrate has the ability to transform to the unstable monohydrate *via* solvent- and solution-mediated mechanisms, whilst the unstable monohydrate will convert back to the anhydrate *via* a solid-solid phase transformation mechanism. Another well-known method to prepare different solid-state forms of a drug is to quench cool the melt. Initially HSM, FT-IR and XRPD data indicated the possibility of a different solid-state form. However, on further investigation the purity test indicated that it was not baclofen but rather an impurity of baclofen which formed during the heating and melting process.

During the course of this study, equilibrium solubilities of baclofen anhydrate were determined in a variety of solvents that includes acetone, 1-butanol, 2-butanol, ethanol, methanol, 1-propanol and 2-propanol and different biorelevant media that includes water, HCl-, citrate- and phosphate buffer solutions. Baclofen shows to be slightly soluble in acetone, very slightly soluble in 2-butanol, ethanol and methanol and practically insoluble in 1-butanol, 1-propanol and 2-propanol. Baclofen anhydrate showed the highest solubility in the 0.1 M HCl buffer solution but it also became apparent that slight variations of 0.1 in the pH value of the buffer solution affects the solubility significantly. Equilibrium solubility of baclofen anhydrate in distilled water, citrate- and phosphate buffer solutions proved to be very similar. This indicated that highest degree of solubility of baclofen within the gastro-intestinal tract occurs in the stomach.

The dissolution of baclofen raw material was determined in distilled water and in different bio-relevant media using 25 mg and the different saturation concentrations determined from the solubility data. The results were used to ascertain a possibly more accurate BCS classification of baclofen anhydrate. Contradictory results between the solubility and dissolution of baclofen anhydrate in HCl buffer solution allowed us to understand more about the variation in literature reports which also reported on the solubility and bioavailability of baclofen anhydrate. The discrepancies could however be ascribed to the sensitivity of baclofen to different pH-levels, especially lower pH values rather than being influenced by solid-state transformations. Combining the equilibrium solubility and dissolution results in the various bio-relevant media and applying the rule of whether the highest daily dose of the drug will dissolve in 250 ml or less, baclofen anhydrate was classified as a rapidly dissolving drug.

Based on the membrane permeation of baclofen according to the P_{app} value obtained in this study in the apical to basolateral direction across Caco-2 cell monolayers ($0,876 \times 10^{-7}$ cm/s), it should be classified into Class 3 or 4 of the BCS (i.e. low permeability). The relatively low permeation of baclofen across the Caco-2 epithelial cell membrane may be explained by its relatively low solubility, but potentially also its low membrane permeation ability and absence of uptake by active transporters. The passive diffusion of baclofen was lower in the basolateral to apical direction than in the apical to basolateral direction, probably due to the larger surface area on the apical side of the Caco-2 cell monolayer (presence of villi) compared to the basolateral side

(absence of villi). A larger surface area of the membrane across which the permeation takes place favours passive diffusion as described by Fick's first law (Artursson *et al.*, 2012). Based on the high solubility of baclofen anhydrate combined with the proven relatively low permeability data mentioned above indicates that baclofen should be classified into Class 3 of the BCS.

It is worth mentioning that during this study all the research objectives were met and concluded upon. Future prospects or research that emanates from this study would be to investigate the contradictory solubility and dissolution results within HCl buffer solution even more. To investigate the possibility of salt formation of baclofen. Furthermore, to look into the formulation of extended release dosage form options which could allow more baclofen to dissolve in the stomach contents, however this would still not address the low permeation characteristics of this drug molecule.

References

- Alqahtani, S., Mohamed, L.A. & Kaddoumi, A. 2013. Experimental models for predicting drug absorption and metabolism. *Expert opinion on drug metabolism and toxicology*, 9(10):1-14.
- Artursson, P., Palm, K. & Luthman, K. 2012. Caco-2 monolayers in experimental and theoretical predictions of drug transport. *Advanced drug delivery reviews*, 64:280-289.
- Gan, L.L. & Thakker, D.R. 1997. Applications of the Caco-2 model in the design and development of orally active drugs: elucidation of biochemical and physical barriers posed by the intestinal epithelium. *Advanced drug delivery reviews*, 23:77-98.
- Le Ferrec, E., Chesne, C., Artursson, P., Brayden, D., Fabre, G., Gires, P., Guillou, F., Rousset, M., Rubas W. & Scarino, M. 2001. In vitro models of the intestinal barrier. *Alternatives to laboratory animals*, 29:649-668.
- Mirza, S., Miroshnyk, I., Rantanen, J., Aalonen, J., Harjula, P., Kiljunen, E., Heinämäki, J. & Yliruusi, J. 2007. Solid-state properties and relationship between anhydrate and monohydrate of baclofen. *Journal of pharmaceutical sciences*, 96(9):2399-2408.
- Sarmiento, B., Andrade, F., da Silva, S.B., Rodrigues, F., das Neves, J. & Ferreira, D. 2012. Cell-based in vitro models for predicting drug permeability. *Expert opinion on drug metabolism and toxicology*, 8(5):607-621.